Low energy dynamics of non-perturbative structures in high energy and condensed matter systems

A THESIS
SUBMITTED TO THE FACULTY OF THE GRADUATE SCHOOL
OF THE UNIVERSITY OF MINNESOTA
BY

Adam Joseph Peterson

IN PARTIAL FULFILLMENT OF THE REQUIREMENTS
FOR THE DEGREE OF
DOCTOR OF PHILOSOPHY

Mikhail Shifman

August, 2016

Acknowledgements

I would like to express my graditude to my advisor Professor Mikhail Shifman who mentored me for the last five years of my graduate career at the University of Minnesota. His proposals and suggestions provided the basis for my graduate research and this dissertation. Additionally, I am also thankful to my previous advisor Professor Marco Peloso who first took me as his graduate student and provided me the opportunity to participate in theoretical physics research. I am also thankful to Professor Keith Olive, who along with Professor Peloso helped me produce my first published research paper. I would also like to thank the additional members of my preliminary and final dissertation committee, Professors Joe Kapusta and Danial Cronin-Hennessy of the School of Physics, and Professor Alexander Voronov of the Mathematics department at the University of Minnesota. I am also very grateful to all of the professors, staff, and students at the University of Minnesota who participated in my graduate research as well as my teaching assistantships during my graduate career. During my ten year career as both an undergraduate and graduate student I have had the privilage to work with almost every professor and staff member in the University of Minnesota physics department, and unfortunately there are too many to name in this disseration.

I would like to make a special mention to Gianni Tallarita of the Universidad Aldolfo Ibáñez who contributed to many of my graduate research projects and coauthored along with Professor Shifman the last two papers included in this dissertation. His continued patience and support of my career in theoretical physics has not gone unnoticed. I hope to have the pleasure of continuing our research for many years to come.

I would also like to mention the many current and former graduate students at the University of Minnesota physics department, who have all contributed in one way or another to my development as a physics researcher. This list is far too large to include

here, but a few to whom I am especially indebted include Terry Bretz-Sullivan, Dima Spivak, Peter Martin, Xiaoyu Wang, Tobias Gulden, Allison Kennedy, Hannah Rogers, and several more.

Finally, I am forever thankful to my wife Celeste Falcon who has supported my career without fail despite concurrently completing her own doctoral work at the University of Minnesota. I am also thankful to my parents Douglas and Jodi Peterson who constantly encouraged me to go after my academic endeavors throughout my life.

Dedication

This dissertaion is dedicated to my wife Celeste, and my parents Doug and Jodi, for their unwavering support throughout this endeavor.

Abstract

This dissertation presents some results on the application of low energy effective field theory vortex dynamics in condensed matter and materials systems. For the first half of the presentation we discuss the possibility of non-Abelian gapless excitations appearing on $U(1)$ vortices in the B phase of superfluid ^{3}He. Specifically, we focus on superfluid ^{3}He-like systems with an enhanced $SO(3)_L$ rotational symmetry allowing for non-Abelian excitations to exist in the gapless spectrum of vortices. We consider a variety of vortices in the B-phase with different levels of symmetry breaking in the vortex core, and show conditions on the phenomenological parameters for certain vortices to be stable in the bulk. We then proceed to develope the low energy effective field theory of the various vortex types and consider the quantization of excitations. The process of quantization leads to interesting surprises due to non-lorentz symmetry that are not typically encountered in the analogous cases of $U(1) \times SU(N)$ gauge models discussed in high energy theory.

The second half of this dissertation focuses on two types of vortices that appear in a particular model that is a modification of the well known Abelian-Higgs model. The specific modification includes a vector spin field in addition to the $U(1)$ Higgs field and gauge fields of the original model. The particular form of the lagrangian results in a cholesteric vacuum structure, with interesting consequences for the vortices in the model. We observe the effects of such a modification on the well known $U(1)$ vortex appearing in the original model due to the emergent spin field in the vortex core. We also consider a new type of vortex that is most closely related to a spin vortex. This vortex appears due to the topology introduced by the new spin field. The low energy effective field theory is also investigated for this type of vortex.

Contents

List of Tables

List of Figures

Chapter 1

Introduction and Background

1.1 Motivation

This dissertation will be devoted to the topic of low energy dynamics of topological structures in a range of systems related to condensed matter, materials science, and high energy physics. Within the high energy physics community, the application of low energy expansions is an indispensable tool for developing and understanding effective field theories in the strong coupling limit. A particular example is the case of $U(2)_L \times U(2)_R$ axial symmetry breaking leading to the emergent pion dynamics propagating on the QCD background [1, 2]. Although analysis at the fundamental level of quarks and gluons at the energy of pion condensation is highly non-trivial due to the strong coupling of QCD, a simple effective field theory of pions can be written down by knowing the symmetries of the original theory and how they are spontaneously broken in the vacuum at energies below $\Lambda_{\rm QCD}$. The only necessary parameter left unspecified is the pion constant f_π, which is determined by the details of the fundamental theory. The effecitveness of this approach follows from universality, which ensures that the low energy properties of a physical system are determined by the symmetries of the theory and a set of parameters describing the interactions of low energy excitations.

In recent years it has been suggested [3] that universality could play a larger role in the understanding of high energy systems where experimental probes do not exist. In particular, it has been shown that many outstanding problems in high energy physics and cosmology can be modeled within the context of condensed matter systems where

the microscopic physics is understood. Properties such as mass hierarchy, quantum gravity, and the cosmological constant can all be shown to emerge as effective low energy phenomena of certain (sometimes hypothetical) condensed matter systems with the appropriate symmetry structures. Knowing the microscopic behavior of these condensed matter systems can offer insight on how such phenomena emerge in the context of high energy physics. In an age where direct experimental data is increasingly difficult to obtain, this may be a necessary approach to understanding particle physics and cosmology at greater energies.

This process can also be applied in reverse where the techniques of high energy physics can be applied to condensed matter systems and lead to interesting results that may have been overlooked by previous analysis. Most of this dissertation will focus on this second application, and present new viewpoints on certain condensed matter systems from the point of view of high energy theory. Along the way, new results about previously studied systems will be presented that follow from simple applications of high energy theory techniques.

The systems we consider follow from superfluidity and superconductivity applied at the Ginzberg-Landau level of fields, which is particularily suited to systems with spontaneous symmetry breaking below a critical temperature. The first system we will consider is the case of superfluids with a tensorial order parameter and a particular group structure supporting $U(1)$ mass vortices in the bulk. The closest physical system resembling these characteristics is superfluid Helium-3 in the B-phase. In another case, we will consider an Abelian-Higgs model with a spin field developing a cholesteric vacuum structure. Such models are more difficult to justify experimentally, however they are simple to imagine by considering the hypothetical situation of a type II superconductor with a liquid crystal vacuum background. In both cases our goal will be to construct vortex solutions on the bulk and develope the $1+1$ dimensional low energy effective field theory of gapless and quasi-gapless excitations localized on the vortex string. This process will lead to new insights about the behavior of gapless excitations appearing in condensed matter systems, as well as provide specific examples of universality between high energy, cosmological, and condensed matter systems.

The remainder of this first chapter will introduce the necessary formalism and background required to consider the specific systems discussed in the following chapters.

The remainder of this dissertation will study specific examples where these methods are applied. Each chapter presents the contents of published papers written by the author along with several collaborators. Chapters 2 and 3 present and exploration of non-Abelian vortices appearing in systems closely related to superfluid ^{3}He in the B phase. We will explore the possibility of non-Abelian gapless excitations appearing in the vortex core and the conditions required for their exsitence. Chapters 4 and 5 will introduce a variant of the Abelian-Higgs model with a spin field presenting a cholesteric structure in the vacuum. We will discuss two types of topological vortices in this model. The first type is the well known mass vortex, modified due to its back reaction with the added spin field. The second vortex appears only due to the broken symmetries of the spin field, and is thus a new type of vortex not previously discussed (at least in this context) in the literature. In chapter 6 we will discuss general conclusions that can be drawn from the models presented. Additionally, we will include a discussion of potential extensions of these studies for future projects.

1.2 Abelian Vortices and effective field theories

We begin with a general discussion of topological vortices. In every context considered in the following chapters our interest will be related to topological vortices appearing in a higher dimensional bulk field theory. The vortices appear due to a symmetry structure admitting a non-trivial mapping of a closed loop γ in coordinate space to a target space S^1 of a unit circle in the complex plane, which is part of the manifold of vacuum solutions as shown in Figure 1. We can illustrate this with an example from the four dimensional model of a complex scalar field with Lagragian:

$$\mathcal{L} = |\partial_\mu \phi|^2 - \lambda(|\phi|^2 - v^2)^2. \tag{1.1}$$

This model presents a $U(1)$ symmetry of phase rotations of the field $\phi(x)$

$$\phi(x) \to \phi(x)\mathrm{e}^{\mathrm{i}\alpha}, \tag{1.2}$$

where α is a constant phase angle representing translations along the internal $U(1)$ space. We wish to consider static vortex string solutions within this model with axis oriented along a chosen spatial direction. We are obviously free to choose this direction to be the z-direction.

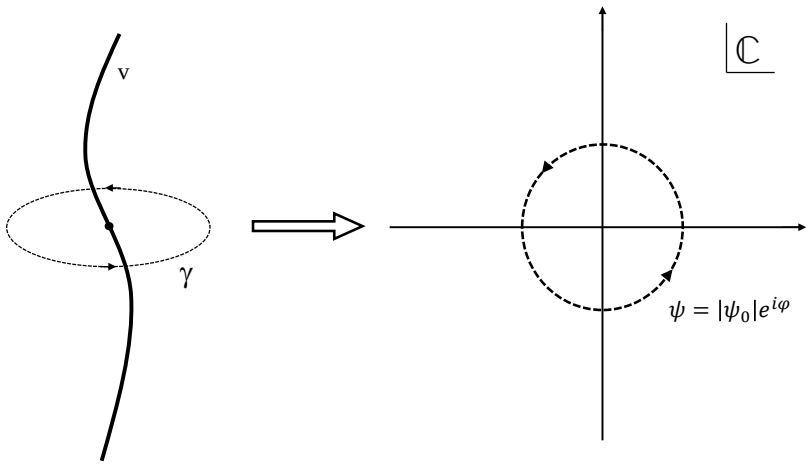

Figure 1.1: A non-trivial mapping of the closed curve γ in coordinate space, to the unit circle of the target space $\mathbb{C}$.

To determine the vortex solution in detail we consider the energy functional of our static field:

$$E = \int d^2x \left\{ \partial_i \bar{\phi} \partial_i \phi + \lambda (\bar{\phi}\phi - v^2)^2 \right\}, \tag{1.3}$$

where integration only over the coordinates perpendicular to the z direction are required, since ϕ is assumed to be independent of z. We determine the static solution by minimizing this energy functional under variations of $\phi(x)$. For a vortex solution we want the field $\phi(x)$ to map a spatial loop far from the vortex core to the $U(1)$ target space given by the phase of ϕ. We therefore choose an ansatz

$$\phi(r, \varphi) = v f(r) \mathrm{e}^{\mathrm{i}n\varphi}, \tag{1.4}$$

where n is an integer and φ is the polar angle in cylindrical coordinates. Clearly, a finite energy in the limit far from the vortex core requires

$$f(r \to \infty) \to 1. \tag{1.5}$$

Additionally, in the limit $r \to 0$, we must have vanishing $f(r)$ for $n \neq 0$ so that $\phi(x)$ is well defined at the origin:

$$f(r \to 0) \to 0. \tag{1.6}$$

The integer n is known as the winding number of the maping $\mathrm{e}^{\mathrm{i}n\varphi}$. In general, any mapping $U(\varphi)$ from the coordinate space $S^1 \ni \varphi$ to the target phase space $U(1)$ can be characterized by the winding number:

$$n = \frac{\mathrm{i}}{2\pi} \int d\varphi U \partial_\varphi U^\star. \tag{1.7}$$

It can be shown that the winding number is invariant under any continuous deformation of the maping $U(\varphi)$ and is thus a topological property of the mapping. This implies that the ansatz (1.4) representing a vortex of winding n is topologically stable, and cannot transition to a solution of different winding without overcoming a vary large energy barrier. In particular, the vortex solution $n = 1$ is stable and cannot decay to the vacuum state $\phi(x) = v$ (see Figures 2 and 3).

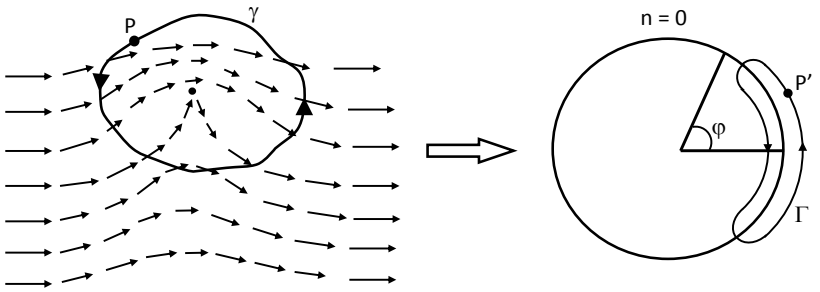

Figure 1.2: A view of the xy plane of a particular field configuration with zero winding is shown. The complex phases of the field are indicated as two dimensional vectors. A mapping of a closed curve γ to the curve Γ in the target space is shown. The mapping is topologically trivial because Γ can be continuously deformed to a point.

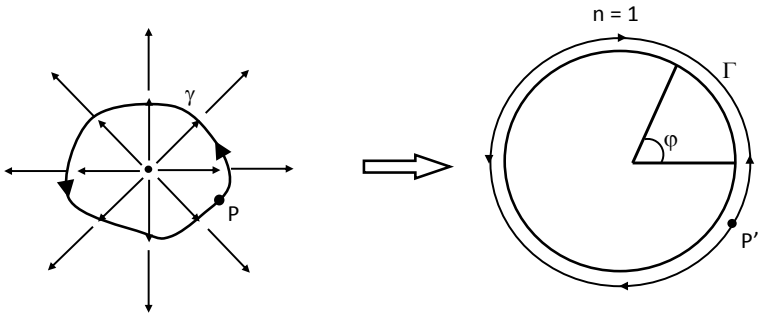

Figure 1.3: Here a non-trivial field configuration with winding $n = 1$ is shown along with the mapping from the closed curve γ to the unit circle in $\mathbb{C}$. In this case, the curve Γ cannot be continuously deformed to a point indicating a topologically non-trivial configuration.

To put this discussion in mathematical terms, we are characterizing the target space by the behavior of closed curves withing the space. An equivalence class of closed curves that can be continuously deformed into each other can be formulated on this space. For the $U(1)$ phase space, equivalence classes are labeled by the winding number $n \in \mathbb{Z}$. This is known as the fundamental group of the space $U(1)$ and is denoted:

$$\pi_1(U(1)) = \mathbb{Z}. \tag{1.8}$$

Returning to the physical system above, the details of the vortex solution at finite distances from the center now depend on a calculation of the solution from the equations of motion subject to the boundary conditions (1.5) and (1.6). There is however one more important detail to consider before proceeding further. If one considers the limit far from the vortex core we find

$$\partial_i \phi \to \mathrm{i}nv\partial_i\varphi = \mathrm{i}nv\epsilon_{ij}\frac{x_j}{r^2}, \text{ as } r \to \infty, \tag{1.9}$$

where ϵ_{ij} is the two index Levi-Cevita symbol. This would imply a logarithmic divergence of the energy functional (1.3) at large r, making our solution inconsistent. Two approaches to this problem often appear in the literature. For the case of systems where the $U(1)$ phase represents a gauge degree of freedom, we may replace our original Lagrangian with the Abelian-Higgs model

$$\mathcal{L} = |D_\mu \phi|^2 - \lambda(|\phi|^2 - v^2)^2 - \frac{1}{4e^2} F_{\mu\nu} F^{\mu\nu}, \tag{1.10}$$

where

$$D_\mu \phi = (\partial_\mu - \mathrm{i} A_\mu)\phi, \text{ and } F_{\mu\nu} = \partial_\mu A_\nu - \partial_\nu A_\mu. \tag{1.11}$$

For high energy systems this is the only modification consistent with Lorentz invariance allowing for finite energy vortex strings. This is also the case for superconductors where the order parameter representing Cooper pairs of electrons which are charged under the gauge $U(1)$.

The other possibility encountered is the case of a system in a finite container. This would be the case for superfluids where the order parameter has a global $U(1)$ phase. For this case one would have to consider finite edge effects that essentially follow from the broken translational symmetry from the container walls. Both cases of a gauged $U(1)$ and a global $U(1)$ phase will appear in our examples below, and we will consider the effects that follow for each particular case.

With these cases in mind the vortex solution for winding n can be determined by solving for the profile $f(r)$ (and $A^\mu(x)$ for the gauged case) using the equations of motion. The solution

$$\phi_0(x_\perp) = v f(r) \mathrm{e}^{\mathrm{i}n\varphi}, \tag{1.12}$$

represents a vortex centered at the origin in the xy plane with axis pointing along the z direction. The subscript 0 will be used to denote the $(n = 1)$ vortex solution centered at the origin. Here $x_\perp$ denotes the coordinates x, y perpendicular to z.

In the problems considered in this dissertation our goal will be to study the low energy excitations of the vortex string. The topological stability of the vortex allows us to consider small perturbations of the vortex solution generated from the broken symmetry transformations. In this particular case, the translations in the xy plane are broken by the vortex line. We consider a field configuration of the following form:

$$\phi(x_\perp, z, t) = \phi_0(x_\perp - \xi_\perp(z, t)), \tag{1.13}$$

where $\xi_\perp(z,t)$ is a translation of the coordinates $x_\perp$ that is dependent on the time t and the z direction (see Figure 4). For small amplitudes of $\xi_\perp$ that are slowly dependent on t and z we may expand (1.1) to second order in $\xi_\perp$. The terms linear in the field perturbation are always shown to vanish due to the equations of mortion. Variables such as $\xi_\perp(z,t)$ that are generated from broken symmetries, are referred to as modulus fields in the high energy community, and collective coordinates in condensed matter. Performing the expansion we can write the action:

$$S = S^{(0)} + \int d^4x \left\{ \partial^\alpha \xi_I \partial_\alpha \xi_J \partial_I \bar{\phi}_0 \partial_J \phi_0 \right\}, \tag{1.14}$$

where $S^{(0)}$ is the unperturbed action for the vortex ϕ_0. The index $\alpha = 0, 3$ represents the t and z coordinates, while $I = 1, 2$ is used for $x_\perp = (x, y)$. We now perform the integration over $x_\perp$ in (1.14) resulting in the effective lagrangian in $1+1$-dimensions for the fields $\xi_\perp$:

$$\mathcal{L}_\xi = \frac{T_{IJ}}{2} \partial^\alpha \xi_I \partial_\alpha \xi_J, \tag{1.15}$$

where

$$\frac{T_{IJ}}{2} = \int d^2x_\perp \partial_I \bar{\phi}_0 \partial_J \phi_0. \tag{1.16}$$

The constant matrix T_{IJ} may be interpreted as the tension in the string. In this particular case the axial symmetry of the vortex solution $\phi_0(x_\perp)$ under rotations about the z axis implies that $T_{IJ} \propto \delta_{IJ}$.

We have thus written down an effective field theory in $1 + 1$ dimensions for low energy excitations of a vortex in the Abelian-Higgs model. These general methods will be applied to the vortices appearing in the models below. These effective field theories may then be used to make predictions about the behavior vortex excitations and how they may be studied in experiments.

1.3 Non-Abelian vortices

Part of the motivation for studying the specific models in this dissertation will be to characterize the low energy dynamics of vortices when the internal symmetry group is non-Abelian. In the Abelian-Higgs model in the previous section, the internal symmetry group consisted of only the single $U(1)$ factor for phase rotations. Only the broken

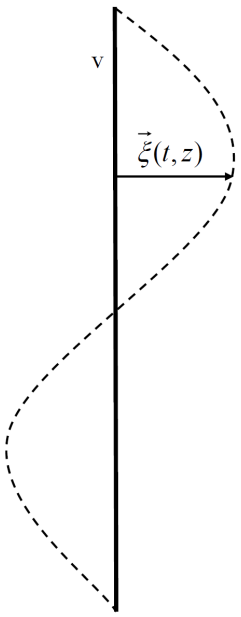

Figure 1.4: The effect of the z and t dependent translation $\vec{\xi}(z,t)$ on the vortex solution is shown.

translational symmetries in the x and y directions could produce excitations living on the vortex axis. However, for a model with a non-Abelian internal symmetry group G, it may be possible to construct vortices that spontaneously break some of the group factors in G. The broken generators of the non-Abelian subgroups of G will produce additional moduli in the effective $1+1$ dimensional field theory, leading to additional gapless excitations of the vortex string. We follow the discussion given in [2].

We briefly illustrate this process with an example from high energy physics, which will turn out to be similar to the superfluid systems we consider in the following chapters. The model is given by:

$$\begin{aligned}\mathcal{L} = &-\frac{1}{4g_1^2}(F_{\mu\nu})^2 - \frac{1}{4g_2^2}(F^a_{\mu\nu})^2 + (D_\mu\phi^A)^\star(D^\mu\phi^A) \\ &+ \frac{\lambda_1^2}{8}\left(\phi^\star_A\phi_A - 2v^2\right)^2 + \frac{\lambda_2^2}{2}\left(\phi^\star_A\frac{\tau_a}{2}\phi_A\right),\end{aligned} \tag{1.17}$$

where $g^2_{1,2}$ and $\lambda^2_{1,2}$ are constants. The theory describes the fields ϕ^A that transform as spinors under the $U(1)\times SU(2)_C$ gauge groups. The subscript C remindes us that

$SU(2)_C$ is the gauge group for fields with a color charge as in QCD. The symbols τ_a are the Pauli matrices. The index $A = \{1, 2\}$ is a flavor index (not the color index for the spinor representation). In fact it can be shown that this theory has a separate $SU(2)_F$ flavor symmetry in addition to the gauge symmetries. Sometimes the field ϕ is written as Φ^{iA}, where i is the color index and A is the flavor index. The complete internal symmetry group for the model (1.17) is

$$G = U(1) \times SU(2)_C \times SU(2)_F. \tag{1.18}$$

A general transformation of the field Φ can be written in matrix notation:

$$\Phi \to \mathrm{e}^{\mathrm{i}\alpha} U \Phi V, \tag{1.19}$$

where U and V are 2×2 unitary matrices from $SU(2)_C$ and $SU(2)_F$ respectively.

It is easy to show that a particular vacuum for this model is given by the solution:

$$\Phi^{iA}_{\mathrm{vac}} = v\delta^{iA}. \tag{1.20}$$

This vacuum configuration is invariant to the particular subset of transformations in G given by:

$$\Phi \to U \Phi U^{\dagger}. \tag{1.21}$$

In otherwords, the vacuum preserves a color-flavor locked symmetry, which is denoted as $SU(2)_{C+F}$. This means that the space of degenerate vacua can be written as:

$$G/H = U(1) \times \frac{SU(2)_C \times SU(2)_F}{SU(2)_{C+F}} = U(1) \times SU(2). \tag{1.22}$$

Topological vortices exist in this model due to the $U(1)$ factor in degeneracy space G/H. They are determined from the boundary condition of the field Φ far from the origin given by:

$$\Phi \to \mathrm{e}^{\mathrm{i}n\varphi} \begin{pmatrix} 1 & 0 \\ 0 & 1 \end{pmatrix}. \tag{1.23}$$

However, if we were to determine the complete vortex configuration for Φ and expand the lagrangian in terms of the collective coordinates from broken symmetry generators, we would find that no collective coordinates in addition to the translational coordinates $\xi_\perp$ appear. This is because this particular vortex solution for Φ preserves the locked $SU(2)_{C+F}$ symmetry.

However, there are additional topological vortices that break the SU_{C+F} symmetry by winding not only in the $U(1)$ part of G/H, but also the $SU(2)$ factor. In the asymptotic $r \to \infty$ limit, the field Φ assumes the form

$$\Phi = v \exp\left[\mathrm{i}\varphi \frac{1 \pm \tau^3}{2}\right]. \tag{1.24}$$

This vortex maps a closed curve γ in coordinate space to a closed loop in the $U(1) \times SU(2)$ degeneracy space, that is not contractable to a point, and is distinct from the Abelian vortex previously considered. We now consider a $SU(2)_{C+F}$ transformation that is dependent on t and z given by:

$$\Phi(x_\perp, z, t) = \exp\left(\mathrm{i}\vec{\omega} \cdot \frac{\vec{\tau}}{2}\right) \Phi_0 \exp\left(-\mathrm{i}\vec{\omega} \cdot \frac{\vec{\tau}}{2}\right), \tag{1.25}$$

where the fields $\vec{\omega}(t, z)$ are non-Abelian collective coordinates defining the $SU(2)_{C+F}$ transformations. In fact, the vortex solution (1.24) is invariant to the $U(1)$ subgroup of $SU(2)_{C+F}$ generated by rotations about the third direction with $\omega^a = \omega\delta^{a3}$. Thus, the non-Abelian moduli of the vortex solution (1.24) live on the coset space

$$SU(2)_{C+F}/U(1) = S^2, \tag{1.26}$$

where S^2 denotes the two dimensional sphere. In the $1+1$ dimensional effective field theory following from an expansion in the moduli fields $\omega_{1,2}$, would have two modes appearing in addition to the translational modes from the fields $\xi_\perp(z, t)$. We could represent the two non-Abelian modes as a unit vector living on S^2 as shown in Figure 5.

This example shows that in general we may find non-Abelian collective coordinates on vortices whose solutions break a non-Abelian symmetry of the vacuum manifold. In this case the vacuum symmetry $SU(2)_{C+F}$ was broken by the vortex solution. A similar mechanism will apply to the systems considered in the following chapters.

1.4 Microscopic description of superfluids and superconductors

In the condensed matter systems we discuss below the continuous field variables will emerge from the collective dynamics of systems with a large number of individual particles (known as the thermodynamic limit). This continuous approximation to the

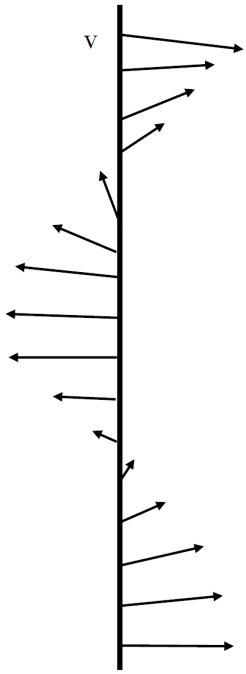

Figure 1.5: A non-Abelian excitation is illustrated as a z and t dependent rotation of a unit vector. We have represented the vector in the coordinate space for clarity, however it is emphasized that the vector transforms in the internal space S^2.

discrete many body theory appearing at the macroscopic level is known as Ginzburg-Landau theory. To give some context for the macroscopic Ginzburg-Landau descriptions of the systems to be discussed we will begin with an introduction to the microscopic behavior of the relevant systems. In principle, from the point of view of high energy physics, this step could be considered unnecessary. Our interest for this thesis will be almost completely devoted to the emerging macroscopic behavior as a semi-classical field theory, and all the results will follow from the Ginzburg-Landau free energy. However, for completeness it is important to discuss the microscopic behavior that must be understood to justify the Ginzburg-Landau description. Doing so will also illustrate how the principles of condensed matter physics can be used to gain insight on the behavior of the vacuum at the Planck scale.

The case of superfluid ^{3}He will be our most referenced system below, and therefore is a natural model system for discussing the microscopic physics. We will develope the BCS

theory of superfluid ^{3}He as discussed in [4, 5] in some detail here. Our starting point is to consider pair correlations in a system of weakly interacting fermions leading to an order parameter describing the symmetry breaking behavior below a critical temperature. Specifically, pairs of ^{3}He atoms experience an attractive interaction with a hard repulsive core much like a Lennard-Jones potential for interactions of neutral atoms and molecules. The repulsive core for the interaction potential can be attributed to large number of particles in the fermi sphere. The specific form of the potential between ^{3}He atoms will not concern us here. We only wish to show that any arbitrary attractive interaction between ^{3}He atoms will favor the pairing state over the Fermi sea of uncorrelated single particle states.

We begin by discussing the pairing wave function between two helium-3 atoms assuming nothing about the potential interaction between them other than the weak attractive coupling and the hard repulsive core. The complete pairing wavefunction may be written as:

$$\Phi(\vec{r}_1, \vec{r}_2, \alpha, \beta) = \exp\left[\frac{1}{2}\mathrm{i}\vec{P}\cdot(\vec{r}_1 + \vec{r}_2)\right]\psi(\vec{r}_1 - \vec{r}_2)\chi(\alpha, \beta). \tag{1.27}$$

We have chosen to use relative coordinates where $\vec{P}$ is the center of mass momentum, $\psi(\vec{r}_1 - \vec{r}_2) \equiv \psi(\vec{r})$ represents the spatial separation between the atoms, and $\chi(\alpha, \beta)$ is the spin function. For the moment we will consider the function $\psi(\vec{r})$ in (1.27) as a single particle wavefunction of the spatial separation $\vec{r}$. Later, we will adapt our discussion to manybody theory in a mean field approximation.

The Schrodinger equation is applied to the spatial part of the wave function (1.27) to determine the eigenstates and energies where we will ignore spin interactions. In this case, we assume the interaction potential $V(r)$ is a function only of the spatial separation $r \equiv |\vec{r}_1 - \vec{r}_2|$. In terms of momentum eigenstates:

$$\begin{aligned}\psi(\vec{r}) &= \frac{1}{(2\pi)^3}\int d^3k \mathrm{e}^{\mathrm{i}\vec{k}\cdot\vec{r}}\psi_{\vec{k}}, \\ V_{\vec{k}} &= \int d^3r \mathrm{e}^{-\mathrm{i}\vec{k}\cdot\vec{r}}V(r).\end{aligned} \tag{1.28}$$

This gives the Schrodinger equation:

$$\left(\xi_{\vec{k}+\vec{P}/2} + \xi_{\vec{k}-\vec{P}/2} - E\right)\psi_{\vec{k}} = -\frac{1}{(2\pi)^3}\int_{q>k_F} d^3q V_{\vec{k}-\vec{q}}\psi_{\vec{q}}, \tag{1.29}$$

where k_F is the fermi momentum. Here we have defined $\xi_{\vec{q}}$ as the quasi-particle energy measured relative to the fermi energy:

$$\xi_{\vec{q}} = \frac{\hbar^2 q^2}{2m} - \mu, \tag{1.30}$$

and μ is the chemical potential, which is equal to the Fermi energy ϵ_F at zero temperature.

The momentum $\vec{P}$ is the center of mass momentum of the ^{3}He pair. Thus, the energy will be minimized for the case $\vec{P} = 0$. We will consider small spatial variations of the center of mass wave function in the later sections when we consider spatially varying order parameters. For establishing the favorability of pairing states we will set $\vec{P} = 0$.

For a spherically symmetric potential we may decompose $V_{\vec{k}-\vec{q}}$ and $\psi_{\vec{k}}$ into spherical harmonics

$$\begin{aligned} V_{\vec{k}-\vec{q}} &= \sum_{l=0} (2l+1) V_l(k,q) P_l(\hat{k}\cdot\hat{q}), \\ \psi_{\vec{k}} &= \sum_{lm} a_{lm} \psi_l(k) Y_{lm}(\hat{k}). \end{aligned} \tag{1.31}$$

Additionally, we make the reasonable approximation that only single particle momentum states near the Fermi surface should participate in the pair interaction and therefore we may assume

$$V_l(k,q) = \begin{cases} V_l \ \ (|\xi_k|,\ |\xi_q| \leq \epsilon_c \\ 0 \ \ \text{otherwise} \end{cases}, \tag{1.32}$$

where $\epsilon_c << \epsilon_F$, defines a thin shell of states around the Fermi surface. For superconductors, ϵ_c represents the limiting Debye frequency of phonon excitations, determined from the lattice spacing. For superfluid ^{3}He it is simply a phenomenological parameter that is measured experimentally.

With these assumptions the Schrodinger equations for the pairing amplitude reduces to

$$\psi_l(k) = -\frac{V_l N(0)}{2\xi_k - E} \int_0^{\epsilon_c} \psi_l(q) d\xi_q, \tag{1.33}$$

where $N(\xi)$ is the density of states. We are assuming $N(\xi)$ is a slowly varying function on the scale of ϵ_c. Finally, by integrating ξ_k over the thin shell defined by $0 \leq \xi_k \leq \epsilon_c$ we find:

$$-\frac{1}{V_l} = N(0) \int \frac{d\xi}{2\xi - E} = \frac{N(0)}{2} \log \frac{E - 2\epsilon_c}{E}. \tag{1.34}$$

For an attractive interaction in the lth partial wave where $V_l < 0$, we must have $E < 0$. Thus, any attractive interaction for any orbital state will lead to a bound pair of single particle states near the Fermi surface.

We wish to promote this analysis of two particle correlations to many body theory of a large number of interacting fermions. This is accomplished by promoting the single particle wavefunctions to dynamical field operators constructed from particle creation (annihiation) operators $a^\dagger_{k\alpha}$ ($a_{k\alpha}$), which create (destroy) fermions with momentum $\vec{k}$ and spin projection $\alpha = (\uparrow, \downarrow)$. They must of course satisfy appropriate anti-commutation relations to be interpreted as fermi operators:

$$\begin{aligned} \left\{ a_{\vec{k}\alpha}, a_{\vec{k'}\beta} \right\} &= \left\{ a^\dagger_{\vec{k}\alpha}, a^\dagger_{\vec{k'}\beta} \right\} = 0, \\ \left\{ a_{\vec{k}\alpha}, a^\dagger_{\vec{k'}\beta} \right\} &= \delta_{\vec{k}\vec{k'}} \delta_{\alpha\beta}. \end{aligned} \tag{1.35}$$

Using these operators we may write the Hamiltonian of the interacting fermion system as

$$\begin{aligned} H - \mu N = & \sum_{\vec{k}\alpha} \left(\frac{\hbar^2 \vec{k}^2}{2m} - \mu \right) a^\dagger_{k\alpha} a_{k\alpha} \\ & + \frac{1}{2} \sum_{\vec{k}\vec{k'}\vec{q}} \sum_{\alpha\beta\alpha'\beta'} \langle -\vec{k}\alpha,\ \vec{k} + \vec{q}\beta |\, V \,| \vec{k'}\alpha',\ -\vec{k'} + \vec{q}\beta' \rangle\, a^\dagger_{\vec{k'}\alpha'} a^\dagger_{-\vec{k'}+\vec{q}\beta} a_{-\vec{k}\alpha} a_{\vec{k}+\vec{q}\beta}, \end{aligned} \tag{1.36}$$

where the chemical potential μ fixes the average particle number to $\bar{N}$. The first term in (1.36) is the kinetic energy of the individual particles measured relative the the fermi surface. The second term is the two fermion interaction. This term is written as a momentum transfer that is interpreted as the annihilation of two fermions in particular momentum (and spin) states and replacing them with two fermions of different momentum states. The coefficient $\langle -\vec{k}\alpha,\ \vec{k} + \vec{q}\beta |\, V \,| \vec{k'}\alpha',\ -\vec{k'} + \vec{q}\beta' \rangle$ is the transition amplitude that can be determined from the single particle analysis above.

The goal is to diagonalize the Hamiltonian (1.36) and determine the eigenvalues and eigenvectors. Clearly, this cannot be done analytically due to the interaction term involving four field operators. In the BCS approximation it is instead assumed that at low temperatures a macroscopic number of fermions will be in a pair correlated state. It is thus assumed that in the thermodynamic limit the expectation value $\langle a_{-\vec{k}\beta} a_{\vec{k'}\alpha} \rangle$ and it's hermitian conjugate will be nonvanishing. We may thus approximate the Hamiltonian

using a mean field approach where the two fermion annihilation/creation operators are written as a deviation from the ground state expectation value:

$$a_{-\vec{k}\beta}a_{\vec{k}'\alpha} = \langle a_{-\vec{k}\beta}a_{\vec{k}'\alpha}\rangle + \left(a_{-\vec{k}\beta}a_{\vec{k}'\alpha} - \langle a_{-\vec{k}\beta}a_{\vec{k}'\alpha}\rangle\right), \tag{1.37}$$

where for the BCS ground state expectation value is written as

$$\langle a_{-\vec{k}\beta}a_{\vec{k}'\alpha}\rangle = \delta_{\vec{k}\vec{k}'}F_{\vec{k}\alpha\beta}. \tag{1.38}$$

Expanding the free energy (1.36) and dropping terms of second order in the deviation from (1.37) we find

$$\begin{aligned} H - \mu N &= \sum_{\vec{k}\alpha}\xi_{\vec{k}\alpha}a^{\dagger}_{k\alpha}a_{k\alpha} \\ &+ \frac{1}{2}\sum_{\vec{k}\alpha\beta}\left(\Delta^{\star}_{\vec{k}\alpha\beta}a_{-\vec{k}\beta}a_{\vec{k}\alpha} + a^{\dagger}_{\vec{k}\alpha}a^{\dagger}_{-\vec{k}\beta}\Delta_{\vec{k}\beta\alpha}\right) - \frac{1}{2}\sum_{\vec{k}\alpha\beta}\Delta^{\star}_{\vec{k}\alpha\beta}F_{\vec{k}\alpha\beta}, \end{aligned} \tag{1.39}$$

where we have defined the two index gap parameter

$$\Delta_{\vec{k}\alpha\beta} = \sum_{\vec{k}'\alpha'\beta'}\langle -\vec{k}\alpha,\ \vec{k}\beta|\, V\, |\vec{k}'\alpha',\ -\vec{k}'\beta'\rangle\, F_{\vec{k}'\alpha'\beta'}. \tag{1.40}$$

We will later interpret $\Delta_{\vec{k}\alpha\beta}$ as the order parameter of the superfluid phase.

To achieve diagonalization we make a canonical transformation of the field operators to remove the off-diagonal $a_{-\vec{k}\beta}a_{\vec{k}\alpha}$ and the hermitian conjugates. This is done by writing the canonical quasi-particle field operators:

$$\begin{aligned} b_{\vec{k}\alpha} &= \sum_{\beta}\left(u_{\vec{k}\alpha\beta}a_{\vec{k}\beta} - v_{\vec{k}\alpha\beta}a^{\dagger}_{-\vec{k}\beta}\right), \\ b^{\dagger}_{\vec{k}\alpha} &= \sum_{\beta}\left(u^{\star}_{\vec{k}\alpha\beta}a^{\dagger}_{\vec{k}\beta} - v^{\star}_{\vec{k}\alpha\beta}a_{-\vec{k}\beta}\right), \end{aligned} \tag{1.41}$$

where $u_{\vec{k}\alpha\beta}$ and $v_{\vec{k}\alpha\beta}$ are variational parameters that are chosen to minimize the ground state free energy. Later it will be shown that $u_{\vec{k}\alpha\beta}$ ($v_{\vec{k}\alpha\beta}$) will represent the amplitude that the pair state $|\vec{k}\alpha\beta\rangle$ is unoccupied (occupied) respectively. Thus, Fermi-Dirac statistics requires:

$$u_{-k\alpha\beta} = u_{k\beta\alpha}, \quad v_{-k\alpha\beta} = -v_{k\beta\alpha}. \tag{1.42}$$

For the operator $b^\dagger_{k\alpha\beta}$ ($b_{k\alpha\beta}$) to be interpreted as canonical fermi creation (annihilation) operators we must require:

$$\begin{aligned}\left\{b_{\vec{k}\alpha}, b_{\vec{k'}\beta}\right\} &= \left\{b^\dagger_{\vec{k}\alpha}, b^\dagger_{\vec{k'}\beta}\right\} = 0,\\ \left\{b_{\vec{k}\alpha}, b^\dagger_{\vec{k'}\beta}\right\} &= \delta_{\vec{k}\vec{k'}}\delta_{\alpha\beta}.\end{aligned} \tag{1.43}$$

This is achieved if $u_{\vec{k}\alpha\beta}$ and $v_{\vec{k}\alpha\beta}$ satisfy the additional constraints

$$\begin{aligned}\mathbf{u}_k\mathbf{v}_k - \mathbf{v}_k\mathbf{u}_k &= 0\\ \mathbf{u}_k\mathbf{u}_k^\dagger + \mathbf{v}_k\mathbf{v}_k^\dagger &= \mathbf{1},\end{aligned} \tag{1.44}$$

where $\mathbf{u}_k$ and $\mathbf{v}_k$ are the 2×2 matrices $u_{k\alpha\beta}$ and $v_{k\alpha\beta}$.

The relations (1.41) can be inverted to give

$$a_{\vec{k}\alpha} = \sum_\beta \left(u_{\vec{k}\alpha\beta} b_{\vec{k}\beta} + v_{\vec{k}\alpha\beta} b^\dagger{}_{-\vec{k}\beta}\right). \tag{1.45}$$

We may now insert (1.45) into the mean field hamiltonian (1.39) and choose the parameters $u_{\vec{k}\alpha\beta}$ and $v_{\vec{k}\alpha\beta}$ to eliminate the off-diagonal terms $b_{\vec{k}}b_{-\vec{k}}$ and $b^\dagger_{\vec{k}}b^\dagger{}_{-\vec{k}}$. This yeilds the relation

$$2\xi_k\mathbf{u}_k\mathbf{v}_k - \mathbf{v}_k\mathbf{\Delta}_k^\dagger\mathbf{v}_k + \mathbf{u}_k\mathbf{\Delta}_k\mathbf{u}_k = 0. \tag{1.46}$$

This equation along with the constraints defined above can be solved for the following form of the variational parameters that will be of interest to the subsequent discussion:

$$\begin{aligned}u_{k\alpha\beta} &= \delta_{\alpha\beta}\frac{\xi_k + E_k}{D_k}\\ v_{k\alpha\beta} &= -\frac{\Delta_{k\alpha\beta}}{D_k},\end{aligned} \tag{1.47}$$

where we have defined

$$\begin{aligned}E_k &= \sqrt{\xi_k^2 + \mathrm{Tr}(\mathbf{\Delta}_k\mathbf{\Delta}_k^\dagger)}\\ D_k &= \sqrt{2E_k(\xi_k + E_k)}\end{aligned} \tag{1.48}$$

By substituting these forms of $\mathbf{u}_k$ and $\mathbf{v}_k$ into the mean field Hamiltonian (1.39) we arrive at

$$H_{\mathrm{MF}} - \mu N = \sum_{\vec{k}\alpha}\left[\frac{1}{2}\mathrm{Tr}\left(\mathbf{\Delta}_k\mathbf{\Delta}_k^\dagger\right)\left(\frac{1}{2E_k} - \frac{1}{\xi_k + E_k}\right) + E_k b^\dagger_{k\alpha}b_{k\alpha}\right]. \tag{1.49}$$

The ground state for this Hamiltonian is determined finding the eigenvector $|\psi_{\rm BCS}\rangle$ that is annihilated by the operators $b_{k\alpha}$:

$$b_{k\alpha}\,|\psi_{\rm BCS}\rangle = 0. \tag{1.50}$$

It can be shown that this condition is satisfied by the following form of the BCS ground state:

$$|\psi_{\rm BCS}\rangle = \prod_{\vec{k}}\prod_{\alpha}\left(u_{\vec{k}\alpha\alpha} + \sum_{\beta} v_{\vec{k}\alpha\beta} a^{\dagger}_{\vec{k}\alpha} a^{\dagger}_{-\vec{k}\beta}\right)|0\rangle\,. \tag{1.51}$$

The original variational parameters $v_{k\alpha\beta}$ and $u_{k\alpha\beta}$ are thus appropriately interpreted as amplitudes for occupied and empty states.

It remains to determine the gap parameter $\Delta_{k\alpha\beta}$. This is done by applying a self consistency condition. At zero temperature the ground state expectation value for $F_{k\alpha\beta}$ can be determined:

$$F_{k\alpha\beta} = \langle a_{-\vec{k}\beta} a_{\vec{k}'\alpha}\rangle_{\rm BCS} = -\frac{\Delta_{k\alpha\beta}}{2E_k}. \tag{1.52}$$

Using the original definition of the gap parameter (1.40) in terms of $F_{k\alpha\beta}$ we have:

$$\Delta_{k\alpha\beta} = -\sum_{k'\alpha'\beta'} \langle -\vec{k}\alpha,\ \vec{k}\beta|\, V\,|\vec{k}'\alpha',\ -\vec{k}'\beta'\rangle\, \frac{\Delta_{k'\alpha'\beta'}}{2E_{k'}} \tag{1.53}$$

To simplify matters further we consider an interaction that is independent of spin:

$$\langle -\vec{k}\alpha,\ \vec{k}\beta|\, V\,|\vec{k}'\alpha',\ -\vec{k}'\beta'\rangle = V_{\vec{k}-\vec{k}'}\delta_{\alpha\alpha'}\delta_{\beta\beta'}, \tag{1.54}$$

This requires the Cooper pairs to form in either the pure spin triplet or spin singlet. With this assumption we may write the zero temperature self consistency condition:

$$\Delta_{k\alpha\beta} = -\sum_{k'\alpha'\beta'} V_{k-k'}\frac{\Delta_{k'\alpha\beta}}{2E_{k'}}. \tag{1.55}$$

The mean field self consistent method is also applicable to the case of finite temperature. In this case the expectation value

$$\langle a_{-\vec{k}\beta} a_{\vec{k}'\alpha}\rangle = \delta_{kk'} F_{k\alpha\beta}, \tag{1.56}$$

is interpreted as a thermal average of the operator in the grand canonical ensemble. The density matrix is written as:

$$\hat{\rho} = \exp -\left(\frac{\hat{H}_{MF} - \mu\hat{N}}{k_B T}\right), \tag{1.57}$$

where the mean field hamiltonian H_{MF} is now approximated using the thermal averages for $F_{k\alpha\beta}$ and $\Delta_{k\alpha\beta}$. For finite temperatures the diagonalization procedure leads to:

$$H_{MF} - \mu N = \sum_{k\alpha} \left[-\frac{1}{2(\xi_k + E_k)} \mathrm{Tr}(\mathbf{\Delta}_k \mathbf{\Delta}_k^\dagger) - \frac{1}{2} \mathrm{Tr}(\mathbf{\Delta}_k^\dagger \mathbf{F}_k) + E_k b_{k\alpha}^\dagger b_{k\alpha} \right], \tag{1.58}$$

where E_k is defined in terms of a temperature dependent gap paramter $\Delta_{k\alpha\beta}$. We may now use this diagonalized hamiltonian to write the occupation probability for the quasi-particle in the state $|k\alpha\rangle$:

$$\langle b_{k\alpha}^\dagger b_{k'\beta} \rangle = \delta_{kk'} \delta_{\alpha\beta} f_k, \tag{1.59}$$

where we have denoted the occupation probability factor

$$f_k = \frac{1}{\exp\left(\frac{E_k}{k_B T}\right) + 1}. \tag{1.60}$$

The other operator averages $\langle b_{k\alpha} b_{k'\beta} \rangle$ and its complex conjugate are identically zero. The factor f_k may now be used to determine the thermal average value for $F_{k\alpha\beta}$ in (1.56). Using the definition of the gap parameter in terms of $F_{k\alpha\beta}$ we find the self consistency condition at finite temperature:

$$\Delta_{k\alpha\beta} = -\sum_{k'} V_{k-k'} \frac{\Delta_{k'\alpha\beta}}{2E_{k'}} \tanh\left(\frac{E_k}{2k_B T}\right) \tag{1.61}$$

This form of the consistency equation can be used to determine the critical temperature T_c for specific functional forms of $\Delta_{k\alpha\beta}$.

The following discussion proceeds in the same fashion where the gap parameter is determined either by (1.55) or (1.61).

Returning to the originial discussion, from the single particle wave function analysis above we assume that the potential $V_{\vec{k}-\vec{k}'}$ is dependent only on the angle between $\vec{k}$ and $\vec{k}'$. This arises from the requirement that the only momenta $|\vec{k}|$ relevant for pair correlations varies on a scale much less than the fermi momentum k_F. We further assume that only a single angular momentum component of $V_{k-k'}$ has a significant contribution to the pair interaction. We may therefore write the potential as

$$V_{\vec{k}-\vec{k}'} = \begin{cases} (2L+1) V_L P_L(\cos\theta_k) & (|\xi_k|, |\xi_{k'}| < \epsilon_c) \\ 0 & \text{otherwise.} \end{cases} \tag{1.62}$$

With these final assumptions in mind we may assume that the Cooper pairs form in the orbital state $l = L$. Therefore, only the L spherical harmonics need to be included in the expansion of the gap parameter $\Delta_{\vec{k}\alpha\beta}$, which is additionally independent of $|\vec{k}|$ to a reasonable approximation.

For the case of superfluid ^{3}He it is experimentally shown that the hard repulsive core of the pair interaction requires the leading component of the potential to be the orbital $L = 1$ term, with small contributions from $l \neq L$ components. To satisfy the symmetry requirements for identical fermi pairs this forces the order parameter $\Delta_{\alpha\beta}$ to be symmetric in its indices. Thus, the dominating contribution to the order parameter for superfluid ^{3}He below the critical temperature is the orbital $L = 1$ spin $S = 1$ pairing amplitude. It is standard to expand the gap parameter in terms of a vector $\vec{e}(\hat{k})$ transforming in spin space:

$$\Delta_{\vec{k}\alpha\beta} = \sum_{\mu} e_{\mu}(\hat{k})(\sigma_{\mu}\mathrm{i}\sigma_2)_{\alpha\beta}. \tag{1.63}$$

Additionally, we expand $e_{\mu}(\hat{k})$ in terms of the $\hat{k}$ components in the orbital basis:

$$e_{\mu}(\hat{k}) = \sum_{i} e_{\mu i}\hat{k}_i. \tag{1.64}$$

The coefficients $e_{\mu i}$ are referred to as the order parameter for a non-conventional superfluid. It is interpreted as a complex 3×3 tensorial order parameter transforming as a vector in the orbital $SO(3)_L$ and spin $SO(3)_S$ rotation groups.

Once we have the order parameter $e_{\mu i}$ in hand we would like to consider its dynamics on a macroscopic level. In particular, we would now like to consider an order parameter that varies in time and space as a field. Loosely speaking, this large scale variation of the order parameter follows from the consideration of finite center of mass momentum $\vec{P}$ of the Cooper pairs. This will be done in the following section.

1.5 Macroscopic description of superfluids

To discuss superfluids on a macroscopic scale with a spatially varying order parameter the approach is to consider the Ginzburg-Landau free energy, which can be derived from the BCS theory. The approach to writing down the Ginzburg-Landau free energy is to

consider the symmetries required to be satisfied by the microscopic BCS Hamiltonian and assume that the macroscopic theory retains these symmetries. If we also consider temperatures just below the critical temperature, then it is only necessary to consider the first few terms in the potential energy of the Ginzburg-Landau free energy. If additionally, we consider only slowly varying spatial dependence of the order parameter, then the kinetic terms appearing in the macroscopic theory can be considered only to lowest non-trivial order.

These points are made concrete by considering the case of the simplest model of superconductivity originally introduced by Bardeen, Cooper, and Schaffer. In that case the order parameter appears as a condensation of Cooper pairs of electrons. The gap parameter $\Delta_{\vec{k}}$ is related to the expectation value of annihilation operators of electrons:

$$\Delta_{\vec{k}} = -\sum_{\vec{q}} V_{\vec{k}-\vec{q}} \langle c_{-\vec{q}\downarrow} c_{\vec{q}\uparrow} \rangle. \tag{1.65}$$

Under the $U(1)$ gauge transformation of electron field operators the order parameter transforms as

$$\Delta \to \mathrm{e}^{2\mathrm{i}\varphi}\Delta. \tag{1.66}$$

Thus, the non-zero gap parameter below the critical termperature indicates the spontaneous breaking of the $U(1)$ gauge symmetry and a macroscopic rigidity of the phase in the superconductor.

To pass to the G-L theory we consider slow spatial variations of the gap parameter $\Delta(\vec{r})$ representing small momentum boosts of the Cooper pairs. In this sense, we define the order parameter $\psi(\vec{r})$ proportinal to the spatially varying gap parameter $\Delta(\vec{r})$ and interpret it as a complex boson field at low momentum. We may then write down a Ginzburg-Landau free energy density near $T = T_c$ consistent with the $U(1)$ phase symmetry required by the microscopic theory:

$$F_{GL} = \frac{\hbar^2}{2m^\star} \left| \left(\nabla - \frac{\mathrm{i}e^\star}{\hbar c} \vec{A} \right) \psi(\vec{r}) \right|^2 - \alpha|\psi|^2 + \frac{\beta}{2}|\psi|^4 + \frac{h^2}{8\pi}, \tag{1.67}$$

where the parameters α and β are dependent on the temperature of the superconductor, and $m^\star$ is the effective mass of the Cooper pair, which for weak coupling can be considered twice the electron mass. The charge $e^\star$ is the charge of the pairing field $\psi(\vec{r})$ and is twice the electron charge in this case. Since the $U(1)$ phase symmetry for

a superconductor is a gauge symmetry, we have included the vector potential $\vec{A}$ in the free energy as well as the contribution from the microscopic magnetic flux density $h(\vec{r})$.

For a spatially homogenous order parameter the minimization of the free energy gives

$$|\psi|^2 = -\frac{\alpha}{\beta} \equiv \Delta(T)^2. \tag{1.68}$$

In fact, by comparison with the BCS microscopic theory, all parameters of the G-L free energy can be determined unambiguously.

The same method applies to the Ginzburg-Landau free energy of a superfluid or superconductor with a tensorial order parameter such as the case with superfluid ^{3}He. We simply write down the most general free energy expression near the critical temperature with the symmetry group structure imposed by the microcsopic BCS model. By comparision with the BCS expression for the free energy we may determine the phenomenalogical parameters appearing in the free energy.

It was determined in the previous section that the order parameter for superfluid ^{3}He was a complex 3×3 tensorial order parameter $e_{\mu i}(\vec{r})$ transforming under the symmetry group

$$G = U(1) \times SO(3)_S \times SO(3)_L, \tag{1.69}$$

where the $U(1)$ group represents the phase of the field operator for ^{3}He Cooper pairs, and the subscripts S and L refer to the spin and orbital rotation groups respectively. We remember of course that in the superfluid ^{3}He case, the $U(1)$ phase is a global symmetry as opposed to the gauge symmetry appearing in the BCS superconductor. With this information in mind the most general Ginzburg-Landau free energy at temperatures near T_c can be written as:

$$\begin{aligned}
&F_{\rm GL} = F_{\rm grad} + V, \\
&F_{\rm grad} = \gamma_1 \partial_i e_{\mu j} \partial_i e^\star_{\mu j} + \gamma_2 \partial_i e_{\mu i} \partial_j e^\star_{\mu j} + \gamma_3 \partial_i e_{\mu j} \partial_j e^\star_{\mu i}, \\
&V = -\alpha e_{\mu i} e^\star_{\mu i} + \beta_1 e^\star_{\mu i} e^\star_{\mu i} e_{\nu j} e_{\nu j} + \beta_2 e^\star_{\mu i} e_{\mu i} e^\star_{\nu j} e_{\nu j} + \beta_3 e^\star_{\mu i} e^\star_{\nu i} e_{\mu j} e_{\nu j} \\
&+ \beta_4 e^\star_{\mu i} e_{\nu i} e^\star_{\nu j} e_{\mu j} + \beta_5 e^\star_{\mu i} e_{\nu i} e_{\nu j} e^\star_{\mu j},
\end{aligned} \tag{1.70}$$

where again the parameters γ_i, α, and β_i are phenomenological parameters dependent on the temperature and pressure. For the weak coupling case at zero pressure they can

be derived from the BCS model

$$\begin{aligned}
\alpha &= \frac{N(0)}{3}\left(1-\frac{T}{T_c}\right), \\
-2\beta_1 &= \beta_2 = \beta_3 = \beta_4 = -\beta_5 = \frac{7N(0)\zeta(3)}{120(\pi T)^2}, \\
\gamma_1 &= \gamma_2 = \gamma_3 = 7\zeta(3)N(0)\frac{v_F^2}{240(\pi T)^2},
\end{aligned} \tag{1.71}$$

where $N(0) = m^\star k_F/2\pi^2\hbar^2$ is the density of states for single particle fermion excitations near the fermi surface.

The Ginzburg-Landau model may also be applied to strong coupling as would be the case for a fermi liquid. However, expressions for the phenomenological parameters are considerably more difficult to determine from the microscopic theory and typically require results from experiments to determine their dependence on temperature and pressure. In the chapters below we will not concern ourselves with the specific microscopic models leading to the parameter values appearing in the free energy expression. For our purposes we will simply vary the phenomenological parameters as we see fit to achieve the macroscopic behavior we wish to study. Whenever it is possible we will give some experimental or theoretical evidence that certain condensed matter systems exist with the chosen parameter values.

1.6 Time dependence in superfluid ^{3}He Models

In the models of superfluid ^{3}He we consider below the specific time dependence will be crucial for determining the dynamics of the Goldstone excitations we wish to study. In standard applications to many body systems, the dispersion relations for the Goldstone excitations are derived from the BCS hamiltonian. By making use of a Bogoliubov transformation of particle creation and annihilation operators and searching for the eigenmodes with vanishing frequency ω in the limit of vanishing wave vector k. For the collective excitations appearing on vortices in superfluid ^{3}He, we will find it more convenient to work with a time dependent Ginzburg-Landau model describing the boson field of Cooper pairs of ^{3}He atoms, rather than the microscopic BCS model of single particle excitations from the fermi surface.

We choose to include time dependence in the Ginzburg-Landau theory by modifying the model (1.70):

$$\begin{aligned} F_{\mathrm{GL}} &= F_{\mathrm{time}} + F_{\mathrm{grad}} + V, \\ F_{\mathrm{time}} &= \mathrm{i} e_{\mu i} \partial_t e^{\star}_{\mu i}. \end{aligned} \tag{1.72}$$

This form of the time dependent term allows us to interpret the order parameter $e_{\mu i}$ as the wavefunction for a non-relativistic boson with two spin degrees of freedom transforming as vectors in their respective spaces. By varying (1.72) with respect to $e^{\star}_{\mu i}$ we can see that the order parameter obeys a Schrodinger equations whose potential energy depends on the local boson density functions:

$$\mathrm{i}\partial_t e_{\mu i} = -\gamma_1 \nabla^2 e_{\mu i} - (\gamma_2 + \gamma_3)\partial_i \partial_j e_{\mu j} + \frac{\partial V}{\partial e^{\star}_{\mu i}}. \tag{1.73}$$

The dispersion relations will follow from diagonalization of this equation of motion in the momentum basis.

Chapter 2

Non-Abelian Vortices in Condensed Matter Systems

In this chapter, which was originally presented in [6], we will discuss the topic of topological vortices with non-Abelian gapless and quasi-gapless modes in condensed matter systems with tensorial order parameter. The model we will consider here is most closely related to superfluid ^{3}He in the B phase. However, in order to make contact with the concept of non-Abelian gapless modes we will consider a Ginzburg-Landau theory with certain simplifications to the superfluid ^{3}He-B model. As we will see below, these modifications lead to enhancements of the symmetry structure that allow non-Abelian subgroups to survive condensation and vortex formation. These are the necessary ingredients for non-Abelian collective coordinates to appear. Strictly speaking, these modifications do not exist in any experimentally observed model in condensed matter. However, our model illustrates the emergence of non-Abelian modes on mass vortices and may provide an avenue for their experimental search should similar systems be constructed. In the next chapter we will extend this analysis to a more experimentally reasonable version of the model and discuss the specific types of vortices appearing in superfluid ^{3}He.

2.1 Introduction

In recent years there has been a growing interest among high energy theorists in condensed matter systems with non-Abelian group structure. Such condensed matter systems share a deep connection with many models of high energy physics due to the universality of effective field theories describing the low energy dynamics of the underlying microscopic physics [3, 7]. Because of this universality, studying condensed matter systems can offer insight on many of the unsolved problems in high energy particle physics and cosmology, and vice versa.

In particular condensed matter systems such as superfluid helium-3 as well as other systems with similar symmetry structure have attracted much attention from the high energy community. The non-Abelian group structure and the tensorial nature of the order parameter results in a wealth of phenomena that share close similarities with high energy theories, specifically Yang-Mills theories [3]. The degeneracy of the order parameter in the B-phase ground state allows for the existence of topologically stable mass vortices of the $\mathbb{Z}$-type similar to flux tubes presenting string-like solitons in four-dimensional Yang-Mills theories [8, 9, 10, 11, 12, 13]. The Nambu-Goldstone excitations of these vortices in ^{3}He-B can be described by a low energy effective field theory using the same methods as those used to determine the low energy dynamics of the flux tubes in Yang-Mills theories [14]. The Kelvin modes and $U(1)$ axial rotational modes of ^{3}He-B vortices have been thoroughly investigated both theoretically and experimentally [15, 16, 17, 18, 19, 20, 21]; however it has been recently shown that additional non-Abelian orientational modes may emerge in certain cases [14]. Specifically, the cases we are referring to are those systems with a Ginzburg-Landau free energy of the form of superfluid ^{3}He with small parameters γ_2 and γ_3 (see (2.6) below). This requirement is imposed to ensure that the non-Abelian modes from $SO(3)_{S+L}$ are independent or nearly independent of the modes associated with coordinate rotations from $SO(3)_{\text{coord}}$. An analogous case can be discussed in the context of elasticity in two dimensions where the unphysical case of vanishing bulk modulus leads to an enhanced symmetry under rotations $O(2) \to O(2) \times O(2)$. Such an enhanced symmetry plays a role in the equivalence of scale and conformal symmetry in the theory of elasticity [22]. If we were to consider $\gamma_2, \gamma_3 \sim \gamma_1$ the non-Abelian modes would no longer be quasi-gapless as we will

show below.

The case of $\gamma_2, \gamma_3 \to 0$ could be approximately achieved in an ultra-cold fermi gas with p-wave pairing, but strictly speaking, superfluid ^{3}He does not satisfy this condition. All of our assertions below as well as any mention of Ginzburg-Landau description of superfluid ^{3}He will refer to the case where γ_2, γ_3 are either vanishing or small relative to γ_1. In these cases the non-Abelian modes are either gapless or quasi-gapless respectively.

Non-Abelian orientational modes localized on mass vortices also appear in Yang-Mills theories admitting a $U(1) \times SU(N)$ gauge symmetry [8, 9, 10, 11, 12, 13]. Typically the moduli fields associated with the orientational modes are described by a sigma model at low energy [2, 23], and it is expected that a similar situation should occur for the non-Abelian modes of ^{3}He-B [14]. The appearance of these additional modes is of course due to the tensor type order parameter and the symmetry structure of the Ginzburg-Landau free energy.

The tensorial nature of the order parameter results from the behavior of the ^{3}He atoms at low temperatures. At the critical temperature, the helium atoms condense to form pairs similar to Cooper pairing in the BCS description of superconductivity [24]. However, unlike conventional superfluids and superconductors, which are described by a wave function with a single complex component, the pairing in superfluid ^{3}He occurs in p-wave $L = 1$ orbitals due to the short range repulsive core behavior of the interaction between helium-atoms. Due to Fermi-Dirac statistics the spin degree of freedom is required to from a symmetric $S = 1$ pairing, and thus the complete order parameter is given by a 3×3 matrix with complex components [25, 26, 27]. Thus, in the absence of spin-orbit and magnetic interactions, the superfluid ^{3}He system is described by a Ginzburg-Landau free energy possessing a symmetry group

$$G = U(1)_P \times SO(3)_S \times SO(3)_L, \tag{2.1}$$

where $U(1)_P$ is the group of global phase rotations of the order parameter. In the B-phase ground state the symmetry group G is spontaneously broken down by the order parameter retaining a spin-orbit locked symmetry

$$G \to H_B = SO(3)_{S+L}. \tag{2.2}$$

This type symmetry breaking also occurs in the theory of color superconductivity observed in quark matter at high density where the color $SU(3)_C$ and flavor $SU(3)_F$

symmetries are spontaneously broken to a diagonal color-flavor locked $SU(3)_{C+F}$ symmetry [28].

The existence of topologically stable mass vortices in ^{3}He-B results from the $U(1)_P$ phase degeneracy of the order parameter in the B-phase ground state. This is indeed the result of a general mechanism of vortex generation by symmetry breaking, which was outlined for gauge theories in [29]. The gapless excitations of the vortices are determined by the moduli fields that are generated from symmetry transformations acting nontrivially on a given vortex solution. The goal of the present chapter is to explore such vortex excitations using techniques that are standard to high energy theory. Particularly, we are interested in exploring the non-Abelian gapless and quasi-gapless modes localized on the vortex axis and their interactions with the well known Kelvin modes and $U(1)$ axial modes. The general framework for determining the low energy dynamics of vortices in systems like superfluid ^{3}He-B was outlined in [14], and we will follow the same procedure in our analysis. Here we will consider specific forms of the order parameter describing vortex solutions, and carry out the calculation of the effective free energy of the gapless and quasi-gapless modes. In general the order parameter $e_{\mu i}$ is a complex 3×3 matrix function of the coordinates $\vec{x}_\perp = (x, y)$ perpendicular to the vortex axis, which is convenient to decompose into its trace, symmetric, and anti-symmetric components

$$\begin{aligned} e_{\mu i} &= \frac{1}{3} e_{\sigma\sigma}\, \delta_{\mu i} + e^S_{\mu i} + e^A_{\mu i}, \\ e^S_{\mu i} &= e_{\{\mu i\}} - \frac{1}{3} e_{\sigma\sigma} \delta_{\mu i}, \\ e^A_{\mu i} &= e_{[\mu i]} \equiv \varepsilon_{\mu i k} \chi^k. \end{aligned} \tag{2.3}$$

As was suggested in [14] we will restrict the order parameter to the trace and anti-symmetric parts

$$e_{\mu i} = e^{i\phi} f(\vec{x}_\perp) \delta_{\mu i} + \varepsilon_{\mu i k} \chi^k(\vec{x}_\perp). \tag{2.4}$$

This restriction is imposed to both simplify the analysis, and contain enough complexity to illustrate the dynamics of the non-Abelian orientational modes of the vortex solution. However, we hasten to emphasize that this ansatz is an oversimplification from both experimental [19, 20, 21] and theoretical standpoints [30, 31]. More general forms of the order parameter will be considered in the next chapter.

The number of low energy non-Abelian modes will be dependent on the symmetry of the order parameter (2.4). When $\gamma_2, \gamma_3 = 0$ we will find either two or three additional non-Abelian modes depending on whether the solution retains a $U(1)_z$ axial symmetry or not. In the case of an axially symmetric solution we will show that there are two moduli living on the degeneracy space given by $SO(3)_{S+L}/U(1) \simeq S^2$. An axially asymmetric solution has three moduli on the degeneracy space $SO(3)_{S+L}/1 \simeq S^3/\mathbb{Z}_2$. Here we are referring to an axial transformation from the group $SO(2)_{S+L}$ about the z-axis.

We mention that we are considering the $U(1)_P$ phase symmetry of G as a global symmetry and thus we may find an additional axial mode generated from this group. It is immediately emphasized that this situation is distinct from a $U(1)$ gauge symmetry considered in Yang-Mills theories where the additional mode can be removed by a gauge transformation.

For $\gamma_2, \gamma_3 \neq 0$ but small, some of these modes will acquire small mass gaps, and will be considered as quasi-gapless. The number of physical excitations may further be reduced after quantization due to the nature of gapless modes in the case of non-relativistic systems where the Goldstone Theorem [32, 33] is more subtle [34, 35, 36]. We will not discuss this issue in detail here. The discussion of quantization will be left for the next chapter.

We will begin in section II with a review of the Ginzburg-Landau description of the superfluid ^{3}He B phase and discuss the topological arguments leading to the existence of stable vortices in the bulk. The specific form of the ansatz (2.4) will be determined and the conditions required on the phenomenological parameters of the free energy to allow the formation of an anti-symmetric component will be calculated in section III. In section IV, we will discuss the symmetries broken by the vortex solutions and determine the number and type of emerging moduli fields due to the broken symmetries. In section V, we will formulate the emerging effective free energy describing the dynamics of the non-Abelian modes and their interactions with the Kelvin and axial modes. We will conclude in section VI with a discussion of our results and their relations to similar phenomena in high energy theory.

2.2 The Ginzburg-Landau description of superfluid ^{3}He-B

In this section we will briefly review the Ginzburg-Landau theory describing the superfluid phases of ^{3}He. We will follow the description as given by [3] and [37, 40] where more detailed discussions can be found. As discussed above the order parameter $e_{\mu i}$ is a complex 3×3 matrix that transforms under the vector representations of $SO(3)_L$ and $SO(3)_S$

$$e_{\mu i} \to e^{i\psi} S_{\mu\nu} L_{ij} e_{\nu j}, \tag{2.5}$$

where $e^{i\psi}$ is an element of the global $U(1)_P$ phase rotations. We write the most general free energy possessing the complete symmetry $G = U(1)_P \times SO(3)_S \times SO(3)_L$ [26, 31, 38, 39]

$$\begin{aligned}
&F_{\rm GL} = F_{\rm time} + F_{\rm grad} + V, \\
&F_{\rm time} = i e_{\mu i} \partial_t e^\star_{\mu i}, \\
&F_{\rm grad} = \gamma_1 \partial_i e_{\mu j} \partial_i e^\star_{\mu j} + \gamma_2 \partial_i e_{\mu i} \partial_j e^\star_{\mu j} + \gamma_3 \partial_i e_{\mu j} \partial_j e^\star_{\mu i}, \\
&V = -\alpha e_{\mu i} e^\star_{\mu i} + \beta_1 e^\star_{\mu i} e^\star_{\mu i} e_{\nu j} e_{\nu j} + \beta_2 e^\star_{\mu i} e_{\mu i} e^\star_{\nu j} e_{\nu j} + \beta_3 e^\star_{\mu i} e^\star_{\nu i} e_{\mu j} e_{\nu j}, \\
&+ \beta_4 e^\star_{\mu i} e_{\nu i} e^\star_{\nu j} e_{\mu j} + \beta_5 e^\star_{\mu i} e_{\nu i} e_{\nu j} e^\star_{\mu j},
\end{aligned} \tag{2.6}$$

where the parameters γ_i, α, and β_i are phenomenological parameters depending on temperature and pressure that can be determined from BCS-like calculations from the underlying microscopic theory [27] and may include corrections from strong coupling considerations [41]. In the weak coupling limit at zero pressure the BCS calculations give [26, 31]

$$\begin{aligned}
&\alpha = \frac{N(0)}{3}\left(1 - \frac{T}{T_c}\right), \\
&-2\beta_1 = \beta_2 = \beta_3 = \beta_4 = -\beta_5 = \frac{7N(0)\zeta(3)}{120(\pi T)^2}, \\
&\gamma_1 = \gamma_2 = \gamma_3 = 7\zeta(3)N(0)\frac{v_F^2}{240(\pi T)^2},
\end{aligned} \tag{2.7}$$

where $N(0) = m^\star k_F / 2\pi^2\hbar^2$. However, we quickly point out that in the present chapter we will adjust the constants at our will depending on the particular features we wish to illustrate. The time-dependent part $F_{\rm time}$ of (2.6) is typically discussed for non-equilibrium dynamics where quasi-static approximations are not valid (see for example [42] and [43]).

The free energy can be minimized by considering the subgroups of the group G. Two of these subgroups can be realized physically, which are characterized by the A phase $H_A = U(1) \times U(1)$, and the B phase $H_B = SO(3)_{S+L}$. In the bulk A phase the order parameter takes the form

$$(e_0^A)_{\mu i} = \frac{\Delta}{\sqrt{2}} V_\mu (\Delta_i' + i\Delta_i''), \tag{2.8}$$

where $\vec{V}$ is a unit vector in the direction of the spin, and $\vec{\Delta}'$ and $\vec{\Delta}''$ are mutually orthogonal unit vectors whose cross product $\vec{\Delta}' \times \vec{\Delta}''$ is in the direction of the orbital angular momentum [25]. In this chapter we will consider only the bulk B phase characterized by the order parameter

$$(e_0)_{\mu i} = e^{i\psi} \Delta (R_0)_{\mu i}, \tag{2.9}$$

where $(R_0)_{\mu i}$ is a generic element of $SO(3)$. The gap parameter Δ can be found by inserting (2.9) into the potential V in (2.6) and minimizing the expression. The result is

$$\Delta = \frac{\alpha}{6\beta_{12} + 2\beta_{345}}, \tag{2.10}$$

where we are employing a shorthand notation

$$\begin{aligned} \gamma_{abc...} &= \gamma_a + \gamma_b + \gamma_c + ..., \\ \beta_{abc...} &= \beta_a + \beta_b + \beta_c + ... \end{aligned} \tag{2.11}$$

We recognize that the order parameter (2.9) is invariant under the simultaneous spin and orbital rotations

$$S_{\mu\nu} L_{ij} (R_0)_{\nu j} = (R_0)_{\mu i}, \tag{2.12}$$

when $S = R_0 L R_0^T$. Thus we observe the bulk B phase preserves a locked spin-orbit rotational symmetry $H_B = SO(3)_{S+L}$ [3, 37, 40]. The degeneracy of the ground state allows us to choose $(R_0)_{\mu i} = \delta_{\mu i}$.

For our purposes we will restrict our analysis to the case that γ_2, γ_3 are small compared to γ_1. In the case that $\gamma_2, \gamma_3 = 0$ the free energy (2.6) is invariant under the separate orbital $SO(3)_L$ and coordinate $SO(3)_{\text{coord}}$ rotations. Thus the complete symmetry group G is enhanced by an additional set of rotational generators from $SO(3)_{\text{coord}}$ and we can treat the orbital and spin degrees of freedom as internal symmetries. As

γ_2, γ_3 are increased to small but non-zero values the symmetry group G is explicitly broken so that orbital rotations from $SO(3)_L$ must be performed with the corresponding coordinate rotations from $SO(3)_{\text{coord}}$. We will show below how this explicit breaking affects the gapless modes of the vortex solutions below.

To discuss topological vortices in the bulk B phase we consider the degeneracy space

$$G/H_B = U(1)_P \times SO(3). \tag{2.13}$$

The topologically stable solutions are determined by the first fundamental group

$$\pi_1(U(1) \times SO(3)) = \mathbb{Z} + \mathbb{Z}_2. \tag{2.14}$$

The $\mathbb{Z}$-sector describes the mass vortices, which are characterized by an integer topological winding n of the phase $e^{i\psi} \sim e^{in\phi}$. The $\mathbb{Z}_2$-sector describes the spin vortices with winding $\nu \in \{0, 1\}$. We will consider the case $n = 1,\ \nu = 0$ below.

Once the existence of stable topological mass vortices is established, the specific form of the order parameter $e_{\mu i}$ describing the vortex solution must be determined by minimizing the free energy (2.6) with the requirement that the solution have a non-trivial winding n. In principle it is necessary to consider the full form of the order parameter, however to simplify the analysis we will assume the form of the order parameter given by [14]

$$e_{\mu i} = e^{i\phi} f(\vec{x}_\perp)\delta_{\mu i} + \varepsilon_{\mu ik}\chi^k(\vec{x}_\perp), \tag{2.15}$$

where $\vec{x}_\perp = (x, y)$ is the coordinate vector perpendicular to the vortex axis, and f and χ^k are to be determined by minimizing (2.6). We will require that $f(\vec{x}_\perp)$ be real, however we will not necessarily consider $\chi^k(\vec{x}_\perp)$ to be real. The boundary conditions required by f and χ^k due to the winding and B phase vacuum are given by

$$\begin{aligned} f(r_\perp \to 0) = 0, \quad f(r_\perp \to \infty) = \Delta \\ \chi^k(r_\perp \to \infty) = 0. \end{aligned} \tag{2.16}$$

Since χ^k is not restricted by any winding we do not assume any value for χ^k as $r_\perp \to 0$. We will establish in the next section the conditions for which a non-trivial χ^k field develops in the vortex core.

A more complete ansatz, including symmetric components, as well as solutions more closely related to cases encountered experimentally, will be considered in the next chapter.

2.3 Anti-symmetric tensor structure in the vortex core

Having restricted our ansatz for the order parameter to the form (2.15) we can determine the requirements on the β_i coefficients such that a non-trivial vector field χ^k develops. We will proceed in similar fashion as discussed in [44] in the context of superconducting strings. An analogous calculation has been recently considered in [45] for the Abrikosov-Nielsen-Olesen (ANO) string [46, 47]. We begin with the case that $\chi^k = 0$ everywhere

$$(e_0)_{\mu i} = e^{i\phi} f(r_\perp)\delta_{\mu i}. \tag{2.17}$$

Here we are assuming the function f is a real function of $r_\perp = |\vec{x}_\perp|$. We proceed by considering the stability of the solution (2.17) under small perturbations of the χ^k field. We will assume for the moment that the small χ^k field is also a function of $r_\perp$ only and consider the case $\gamma_2, \gamma_3 = 0$. Thus we are free to set

$$\vec{\chi} = (0, 0, \chi(r_\perp)), \tag{2.18}$$

due to the independence of orbital and coordinate rotations. We determine the form of $f(r_\perp)$ by inserting the ansatz (2.17) into the free energy (2.6) and minimizing. The numerical solution of $f(r_\perp)$ is shown in Figure 2.1.

After determining $f(r_\perp)$ we now assume a small perturbation $\chi(r_\perp)$ leaving the form of $f(r_\perp)$ fixed. Looking at the χ dependent part of the free energy (2.6) we find

$$F_\chi = \int r_\perp dr_\perp \left\{ i\chi \frac{\partial \chi}{\partial t} + \chi L_2 \chi + \mathcal{O}(\chi^4) \right\}, \tag{2.19}$$

where L_2 is given given by:

$$\begin{aligned} L_2 &= -2\gamma_1 \tfrac{1}{r_\perp} \tfrac{\partial}{\partial r_\perp} \left(r_\perp \tfrac{\partial}{\partial r_\perp} \right) + V(r_\perp), \\ V(r_\perp) &= 4(3\beta_2 + 2\beta_4) f^2(r_\perp) - 2\alpha. \end{aligned} \tag{2.20}$$

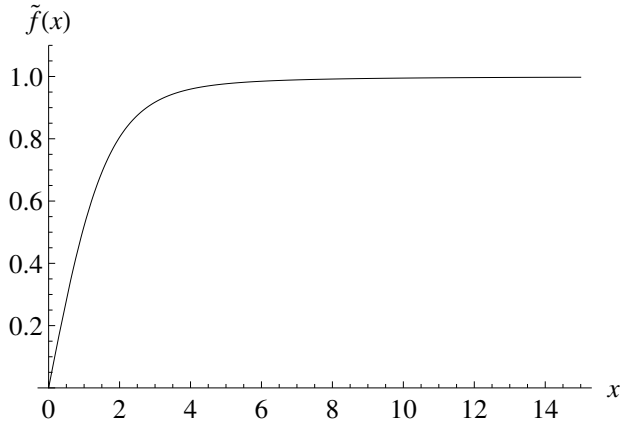

Figure 2.1: The numerical solution $\tilde{f}(x) = f(x)/\Delta$ is plotted. Here we have defined $x \equiv r_\perp \sqrt{\alpha/\gamma_1}$. For $x \ll 1$ the solution follows the form $\tilde{f}(x) \sim 0.583x$. In the opposite limit $x \gg 1$ the function $\tilde{f}(x) \to 1 - 1/2x^2 + \mathcal{O}(x^{-4})$.

In this form L_2 represents a Schrodinger operator, whose eigenvalues and eigenfunctions can be determined from

$$L_2\chi_n = \omega_n\chi_n, \text{where } \chi = \sum_n a_n\chi_n(r). \tag{2.21}$$

A negative eigenvalue ω_0 of L_2 would imply the existence of a solution $\chi_0(r)$ such that $F_\chi < 0$, and thus would represent an instability of the ansatz (2.17).

Solving numerically (2.21) we find that $\omega_0 < 0$ if

$$\frac{1}{2} \leq \frac{3\beta_2 + 2\beta_4}{6\beta_{12} + 2\beta_{345}} \lesssim 0.76, \tag{2.22}$$

where the lower bound is required to satisfy the boundary condition $\chi(r_\perp \to \infty) \to 0$. A numerical solution for $\chi(r_\perp)$ when this condition is satisfied is shown in Figure 2.2.

We immediately point out that this condition (2.22) is not absolute, and represents only the case in which a diagonal ansatz (2.17) is locally unstable. If the condition is not satisfied the diagonal ansatz may only be a local minimum and a solution with non-zero χ may still persist as the absolute minimization of the free energy (2.6). This is in fact the case both experimentally and theoretically for vortices in superfluid ^{3}He-B where the β_i coefficients do not satisfy (2.22), however the minimizing vortex solutions occur with either an A-phase core, or a double core vortex. Both solutions break the orbital and coordinate axial symmetry.

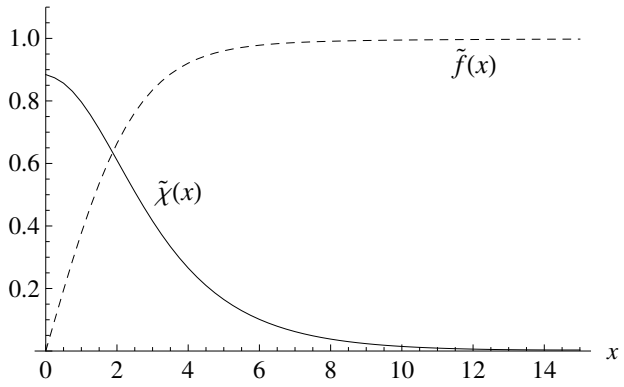

Figure 2.2: The plot shows the numerical solutions for the $\tilde{\chi}(x) \equiv \chi(x)/\Delta$ and $\tilde{f}(x)$, where $x \equiv r_\perp \sqrt{\alpha/\gamma_1}$ as previously defined. The solutions are generated by a numerical minimization of the free energy (2.6), assuming the ansatz (2.15) with the boundary conditions from (2.16). Note that so far we are working in the limit $\gamma_2, \gamma_3 \to 0$.

The existence of a non-zero $\chi(r_\perp)$ field would imply the breaking of the $SO(3)_{S+L}$ down to a $U(1)$ rotation, and thus we would expect two non-Abelian moduli from the degeneracy space

$$SO(3)_{S+L}/U(1) \simeq S^2. \tag{2.23}$$

The situation is more interesting if we consider a complex ansatz for the field $\chi^k(\vec{x}_\perp)$. In particular we consider the form

$$\vec{\chi}_A(r_\perp, \phi) = \begin{pmatrix} 1 \\ i \\ 0 \end{pmatrix} \frac{\chi_0(r_\perp)}{\sqrt{2}} + \begin{pmatrix} 1 \\ -i \\ 0 \end{pmatrix} \frac{\chi_2(r_\perp)}{\sqrt{2}} e^{2i\phi}. \tag{2.24}$$

This ansatz represents an approximate A phase vortex core that has been restricted to its trace and antisymmetric components, and is required to satisfy the condition of $U(1)_A$ axial symmetry, which we will define below. It is easy to show from the equations of motion that

$$\chi_0, \chi_2 \to \frac{c}{r_\perp} \text{ as } r_\perp \to \infty, \tag{2.25}$$

where c is a constant that must be determined by solving the equations of motion completely.

Following a similar procedure as above, we find a non-trivial χ_0 field develops if the condition (2.22) is satisfied, and thus so does the χ_2 field in order to satisfy (2.25).

Figure 2.3 shows a plot of all three non-trivial fields $f(r_\perp)$, $\chi_0(r_\perp)$, and $\chi_2(r_\perp)$, when the condition (2.22) is satisfied.

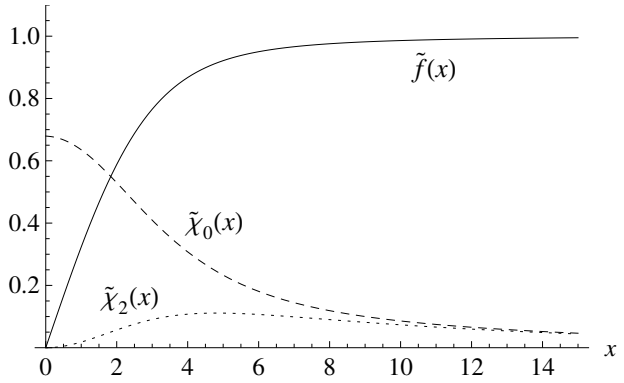

Figure 2.3: The numerical solutions for $\tilde{f}(x) = f(x)/\Delta$, $\tilde{\chi}_0(x) = \chi_0(x)/\sqrt{2}\Delta$, and $\tilde{\chi}_2(x) = \chi_2(x)/\sqrt{2}\Delta$ are plotted, where again $x \equiv r_\perp\sqrt{\alpha/\gamma_1}$. As $x \to \infty$ we have $\tilde{\chi}_0(x) = \tilde{\chi}_2(x) \to c/x$, where c is a constant that must be determined by solving completely the vortex solution.

In the case of (2.24), the non-Abelian symmetry $SO(3)_{S+L}$ is completely broken by the vortex solution and has the degeneracy space

$$SO(3)_{S+L}/1 \simeq S^3/\mathbb{Z}_2. \tag{2.26}$$

This is, of course, due to the fact that the ansatz (2.24) is not an eigenvector of a rotation about any axis. Thus the orbital $U(1)$ symmetry retained by the original ansatz (2.18) is now broken by (2.24) and we in fact have three non-Abelian moduli. However, we can see that the solution (2.24) still retains a locked $U(1)$ symmetry under simultaneous orbital, coordinate, and phase rotations,

$$\vec{\chi}(\phi) = e^{i\delta}R_z(\delta)\vec{\chi}(\phi - \delta)R_z^{-1}(\delta), \tag{2.27}$$

where $R_z(\delta)$ is the rotational matrix about the z-axis. Thus, although the orbital $SO(3)_{S+L}$ symmetry is completely broken, one of the additional modes will be equivalent to the $U(1)_A$ axial mode.

We may further increase the complexity of the ansatz by generalizing (2.24) to the

following

$$\vec{\chi}_{\rm dc}(r_\perp,\phi) = \begin{pmatrix} \chi_0(r_\perp) \\ i\zeta_0(r_\perp) \\ 0 \end{pmatrix} \frac{1}{\sqrt{2}} + \begin{pmatrix} \chi_2(r_\perp) \\ -i\zeta_2(r_\perp) \\ 0 \end{pmatrix} \frac{e^{2i\phi}}{\sqrt{2}}. \tag{2.28}$$

This ansatz would represent the case of an approximate double core vortex restricted to anti-symmetric off diagonal components. Again, to satisfy the requirement of cylindrical symmetry and the equations of motion at large distances from the vortex axis we must have

$$\chi_0,\ \chi_2,\ \zeta_0,\ \zeta_2 \to \frac{c}{r_\perp} \text{ as } r_\perp \to \infty. \tag{2.29}$$

Figures 2.4 and 2.5 show plots of the functions $\chi_0(r_\perp)$, $\chi_2(r_\perp)$, $\zeta_0(r_\perp)$, and $\zeta_2(r_\perp)$.

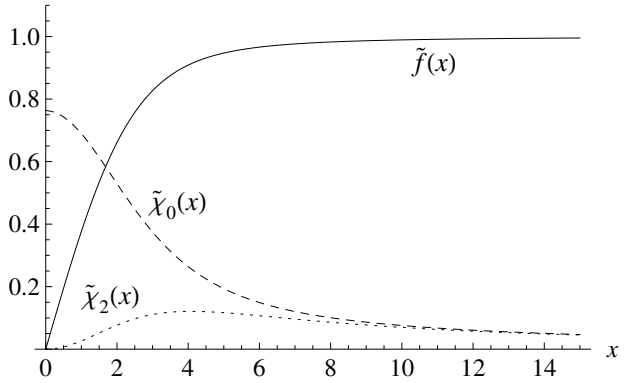

Figure 2.4: The numerical solutions for $\tilde{f}(x) = f(x)/\Delta$, $\tilde{\chi}_0(x) = \chi_0(x)/\sqrt{2}\Delta$, and $\tilde{\chi}_2(x) = \chi_2(x)/\sqrt{2}\Delta$ are plotted, where again $x \equiv r_\perp\sqrt{\alpha/\gamma_1}$.

Generally speaking a double core vortex would have four moduli from the complete breaking of $SO(3)_{S+L} \times U(1)_A$ since no hidden symmetry is necessarily preserved for arbitrary functions $\chi_0(r_\perp)$, $\chi_2(r_\perp)$, $\zeta_0(r_\perp)$, and $\zeta_2(r_\perp)$.

2.4 Low energy excitations and Counting Gapless Moduli

In this section, we will discuss the low energy excitations of vortices in the B phase from a general point of view. We will determine the moduli fields and their interactions by considering the broken symmetries of the free energy (2.6). In the following section, we will write out the effective free energy for the gapless and quasi-gapless modes for the specific cases (2.15), (2.18), (2.24), and (2.28) considered in the previous section.

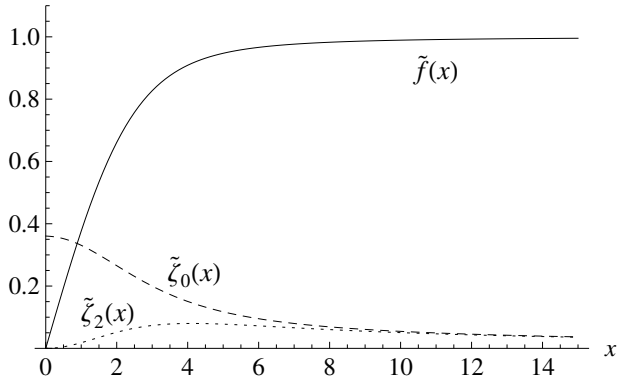

Figure 2.5: The numerical solutions for $\tilde{\zeta}_0(x) = \zeta_0(x)/\sqrt{2}\Delta$, and $\tilde{\zeta}_2(x) = \zeta_2(x)/\sqrt{2}\Delta$ are plotted.

Generally the modulus fields of the vortex are determined by the continuous symmetries of the vacuum that are broken by the vortex solution. We consider first the case that $\gamma_2, \gamma_3 = 0$, and thus we have the addition coordinate rotational $SO(3)_{\rm coord}$ symmetry. Thus the continuous symmetries of (2.6) including the coordinate rotations $SO(3)_{\rm coord}$ and translations t are given by the group

$$\mathcal{G} = U(1)_P \times SO(3)_S \times SO(3)_L \times SO(3)_{\rm coord} \times t. \tag{2.30}$$

We denote the elements of this group in the following way [48]

$$\begin{aligned}
&U_\theta = e^{i\hat{I}\theta},\ \hat{I}e_{\mu i} = e_{\mu i},\ \hat{I}e^\star_{\mu i} = -e^\star_{\mu i},\\
&\hat{S}_\beta e_{\mu i} = -i\varepsilon_{\beta\alpha\nu}e_{\nu i},\\
&\hat{L}^{\rm int}_j e_{\mu i} = -i\varepsilon_{jik}e_{\mu k},\\
&\hat{L}^{\rm ext}_j e_{\mu i} = -i\varepsilon_{jlk}x_l\frac{\partial}{\partial x_k}e_{\mu i},\\
&t_{\vec{x_0}}e_{\mu i}(\vec{x}) = e_{\mu i}(\vec{x} - \vec{x_0}),
\end{aligned} \tag{2.31}$$

where $U_\theta \in U(1)_P$. We distinguish the orbital and coordinate rotation generators by $\hat{L}^{ext}$ and $\hat{L}^{int}$ respectively.

The moduli fields are determined from the broken generators of $\mathcal{G}$ which leave the order parameter far away from the vortex core invariant. We already know that in the vacuum far from the vortex core the order parameter takes the form

$$e_{\mu i} \to e^{i\phi}\Delta\delta_{\mu i},\ \text{as } r \to \infty. \tag{2.32}$$

The asymptotic form (2.32) is invariant under the symmetry group $H_B = SO(3)_{S+L}$ as well as translations t and coordinate rotations about the x and y axes. The solution is not invariant under coordinate rotations about the z-axis, however it is invariant under a simultaneous coordinate rotation about the z-axis and a corresponding phase rotation. The element of this transformation is given by

$$U_\phi = e^{i\hat{Q}\phi},\ \hat{Q} = \hat{L}_z^{ext} - \hat{I},\ \hat{L}_z^{ext} = -i\frac{\partial}{\partial\phi}. \tag{2.33}$$

We denote the group of the transformations (2.33) as $U(1)_A$. Solutions invariant under $U(1)_A$ are known as axially symmetric, although they are strictly speaking not axially symmetric because of the phase winding $e^{i\phi} \in U(1)_P$.

Thus we have three generators $\omega_{x,y,z}$ from $SO(3)_{S+L}$, one generator δ from the axial symmetry $U(1)_A$, two generators $\hat{L}_{x,y}^{ext}$ from the remaining coordinate rotations of the degeneracy space $SO(3)_{\text{coord}}/SO(2)_z$, and two from translations in the x and y directions. We exclude translations in the z direction as we will assume the vortex solution is independent of z everywhere. In addition, it is a simple matter to show that coordinate rotations about the x and y axes can be written as z dependent translations in the xy-plane [14, 49, 50, 51]. We will denote the two generators of translations as $\xi_{x,y}$. Thus, we actually have a total of six possible gapless moduli of the vortex solution associated with spin-orbit rotations, axial rotations from $U(1)_A$, and translations:

$$\omega_x,\ \omega_y,\ \omega_z,\ \xi_x,\ \xi_y,\ \text{and}\ \delta. \tag{2.34}$$

The particular moduli that appear in the effective theory depend on which of these generators act non-trivially on the vortex solutions (2.18), (2.24), and (2.28). Table 1 includes a summary of the type of moduli, total number of moduli, and the degeneracy space of the vortex forms (2.17), (2.18), (2.24), and (2.28) we considered in the previous section.

When $\gamma_2, \gamma_3 \neq 0$ the $SO(3)_L \times SO(3)_{\text{coord}}$ symmetry is explicitly broken to $SO(3)_{L+\text{coord.}}$, which we will simply write as $SO(3)_L$. The generator of coordinate rotations is thus

$$\hat{L}_k = \hat{L}_k^{\text{int}} + \hat{L}_k^{\text{ext}}. \tag{2.35}$$

Thus the orbital rotations about the x and y axes from $SO(3)_{S+L}$ are correlated with the corresponding coordinate rotations. The $SO(3)_{S+L}$ rotations about the x and y axes

are also correlated with the translations in the xy-plane due to the local equivalence of the coordinate rotations and translations. Only axial transformations about the z-axis from $U(1)_A$ are distinct. We have only three available gapless moduli fields in this case:

$$\xi_x,\ \xi_y,\ \text{and}\ \delta. \tag{2.36}$$

When γ_2, γ_3 are small but non-zero we may include all six moduli fields from (2.34). However as we will see below some of the moduli will acquire a small mass gap proportional to γ_{23}. In addition, we will find that the moduli $\omega_{x,y}$ will acquire interactions with $\xi_{x,y}$ due to the equivalence of coordinate rotations and translations. We will call the moduli with a small mass gap, quasi-gapless.

Table 2.1: A summary of degeneracy space and associated moduli for the vortex solutions when $\gamma_2, \gamma_3 = 0$ considered in the previous section is shown. The first column indicates the core type solution. Columns 2-5 indicate the moduli fields emerging in the various solutions. The degeneracy spaces in the sixth column are denoted with subscripts indicating the group associated with the degeneracy. Additionally, we have defined $J \equiv S + L$. The last column shows the total number of emerging moduli. We have also indicated the equivalence of ω_z and δ moduli in the A-phase core vortex.

Core Type	$\vec{\xi}_\perp$	$\omega_{x,y}$	ω_z	δ	Degeneracy	# moduli
$\vec{\chi} = 0$	✓	×	×	×	S^2_t	2
$\vec{\chi} = \chi_z(r_\perp)\hat{z}$	✓	✓	×	✓	$S^2_J \times S^1_A \times S^2_t$	5
A-phase	✓	✓	1/2	1/2	$S^2_{J+A} \times S^1_{J_z+A_z}$	5
Double core	✓	✓	✓	✓	$\left(S^3/\mathbb{Z}_2\right)_J \times S^1_A \times S^2_t$	6

2.5 Classical Effective Theory of Vortex Moduli Fields

In the previous section we considered the symmetries of the free energy (2.6) to determine the possible moduli fields appearing on the effective theory of vortex excitations in the B-phase. In this section we will determine the effective field theory for the specific vortex solutions (2.15), (2.18), (2.24), and (2.28) considered above. We will begin by

outlining the general procedure for determining the low energy effective theory of vortex fluctuations (see [13] and [2]). For this purpose we will follow the construction outlined in [14].

In general, the effective field theory can be determined by considering fluctuations of the vortex solution

$$e_{\mu i}(\vec{x}_\perp) = e^{\text{vort}}_{\mu i}(\vec{x}_\perp) + \delta e_{\mu i}(x, y, z, t). \tag{2.37}$$

We insert (2.37) into the free energy (2.6) and consider terms of second order in $\delta e_{\mu i}$. Integrating by parts in the spatial gradient terms we arrive at the following equation

$$\begin{aligned} \delta^2 F_{\text{GL}} &= i\delta e_{\mu i}\partial_t \delta e^\star_{\mu i} + \delta e_{\mu i} L_{ij,\mu\nu}\delta e^\star_{\nu j}, \\ L_{ij,\mu\nu} &= -\gamma_1 \delta_{ij}\delta_{\mu\nu}\vec{\partial}^2 - \gamma_{23}\delta_{\mu\nu}\partial_i\partial_j + (\partial_{e^\star_{\mu i}}\partial_{e_{\nu j}} V). \end{aligned} \tag{2.38}$$

Here we have consolidated the spatial gradient and potential terms to the operator $L_{ij,\mu\nu}$. For our present purposes it will only be necessary to consider $\delta^2 F_{\text{GL}}$ up to second order in $\delta e_{\mu i}$. Allowing $\delta e_{\mu i}$ to depend only on $\vec{x}_\perp$ for the moment and varying (2.38) with respect to $\delta e_{\mu i}$ we arrive at an eigenvalue equation

$$L_{ij}(\vec{x}_\perp) e^{(n)}_{\mu j}(\vec{x}_\perp) = E^{(n)} e^{(n)}_{\mu i}(\vec{x}_\perp), \tag{2.39}$$

where the fluctuations $\delta e_{\mu i}$ are written in terms of the eigenmodes $e^{(n)}_{\mu i}$

$$\delta e_{\mu i}(x, y, z, t) = \sum_n c_n(t, z) e^{(n)}_{\mu i}(x, y). \tag{2.40}$$

Here we have restored the t and z dependences in $\delta e_{\mu i}$ by assuming the adiabatic approximation. The gapless modes are determined by the eigenmodes with eigenvalues $E^{(n)} = 0$. They are defined by transformations of the vortex solution $e^{\text{vort}}_{\mu i}$ that leave the Ginzburg-Landau free energy (2.6) invariant. The set of moduli defining these symmetry transformations are denoted by m^a and we may write the gapless fluctuations as

$$\delta e_{\mu i}(x, y, z, t) = \sum_a m^a(t, z) \frac{\partial}{\partial m^a} e^{\text{vort}}_{\mu i}(x, y, m). \tag{2.41}$$

Inserting (2.41) into the free energy (2.38) and ignoring all other modes with non-zero energy $E^{(n)}$ and integrating over x and y we arrive at the effective field theory of $m^a(t, z)$

describing the string like dynamics of the vortex solution. If the moduli we consider are strictly gapless we will find the free energy can be written as

$$\begin{aligned} F_{\text{eff}} &= iG_{ab}(m)m^a\partial_t m^b + G_{ab}(m)\partial_z m^a \partial_z m^b, \\ G_{ab} &= \int d^2\vec{x}_\perp \frac{\partial e^{\text{vort}}_{\mu i}(\vec{x}_\perp, m)}{\partial m^a}\frac{\partial e^{\text{vort}}_{\nu j}(\vec{x}_\perp, m)}{\partial m^b} \end{aligned} \tag{2.42}$$

where G_{ab} is a function of the moduli fields m^a, and is symmetric in a and b.

For the particular problem under consideration the moduli fields m^a are given by (2.34), however some of these moduli may not appear in the effective free energy if their generators annihilate the vortex solution.

When we switch on $\gamma_2, \gamma_3 \neq 0$, the number of gapless moduli appearing in (2.34) will be restricted to (2.36) and the remaining moduli will acquire either a mass gap proportional to γ_{23} or acquire interactions with the gapless moduli from (2.36). We will expect these interactions to occur for the case of $\xi_{x,y}$ and $\omega_{x,y}$. Only a combination of these moduli fields will be strictly gapless. This is simply a reflection of the locking of coordinate and orbital rotations, and the equivalence of coordinate rotations with z-dependent translations when γ_2, γ_3 are non-zero. If we assume γ_2, γ_3 are small compared to γ_1 we may consider the additional moduli as quasi-gapless.

We proceed by first considering the ansatz (2.15) with χ^k field given by (2.18). We assume for the moment that $\gamma_{23} = 0$ and thus the translational moduli ξ_a and rotational moduli ω_a decouple. The moduli appear as the following transformations

$$\begin{aligned} &e_{\mu i}(\vec{x}_\perp) \to e_{\mu i}(\vec{x}_\perp - \vec{\xi}_\perp), \;\; \xi \in t \\ &\chi^i(r_\perp) \to R_{ij}(\vec{\omega})\chi^j(r_\perp), \;\; R_{ij} \in SO(3)_{S+L} \\ &\chi^i(r_\perp) \to e^{i\delta}\chi^i(r_\perp), \;\; e^{i\delta} \in U(1)_A, \end{aligned} \tag{2.43}$$

where $\vec{\xi}_\perp$, $\vec{\omega}$, and δ are functions of z and t. Additionally, it will be particularly convenient to consider the rotational moduli in the form

$$\chi^i = R_{ij}(\vec{\omega})\chi^j \equiv S^i(t,z)\chi(r_\perp), \;\; |S|^2 = 1, \tag{2.44}$$

and consider the real moduli fields $\vec{S}(t,z)$ instead of $\vec{\omega}(t,z)$. We are permitted to make this switch of variables because the particular vortex solution (2.18) retains an orbital $SO(2)$ symmetry and thus the solution has only two moduli fields from the

degeneracy space $SO(3)_{S+L}/SO(2)$, which define the unit vector $S^k(t,z)$ in the direction of $\chi^k(r_\perp, z, t)$.

Performing the general procedure outlined above we may immediately write out the effective theory of the moduli fields

$$\begin{aligned} F_{\text{eff}} &= F_{\text{trans}} + F_{O(3)} + F_{U(1)}, \\ F_{\text{trans}} &= \frac{T}{2}\partial_z\vec{\xi}_\perp\partial_z\vec{\xi}_\perp, \\ F_{O(3)} &= \frac{1}{2g^2}\partial_z\vec{S}\partial_z\vec{S},\ |S|^2 \equiv 1, \\ F_{U(1)} &= \frac{1}{2g^2}\partial_z\delta\partial_z\delta, \end{aligned} \tag{2.45}$$

where we are omitting the time derivatives. We note that strictly speaking the field ρ cannot be dynamical, since it's time derivative term in the free energy could be written as a total derivative. The couplings T and g^2 are determined from the integration over $\vec{x}_\perp$:

$$\begin{aligned} \frac{T}{2} &\sim \int d^2\vec{x}_\perp 3\gamma_1 \frac{f^2}{r_\perp^2} \to \gamma_1\Delta^2 \log\left(\frac{\alpha R^2}{\gamma_1}\right), \\ \frac{1}{g^2} &\sim \int d^2\vec{x}_\perp \gamma_1\chi^2 \to \frac{\gamma_1^2}{2\beta_{12}+\beta_{345}}, \end{aligned} \tag{2.46}$$

As expected $\vec{S}$ and $\vec{\xi}_\perp$ decouple, and the effective theory takes the form of an $O(3)$ sigma model in one spatial dimension, plus a translational part that describes the Kelvin excitations, and a $U(1)_A$ part describing axial rotations. We see that the theory (2.45) has a total of five gapless moduli fields.

At this point we switch on a small but non-zero γ_{23}. We will assume that γ_{23} is small enough that we may neglect the corrections to the vortex solutions of $f(r_\perp)$ and $\chi(r_\perp)$, as well as the constants T and g^2. Aside from these uninteresting numerical corrections (2.46) remains of the same form, however there are additional terms representing the breaking of the $SO(3)_{S+L} \times SO(3)_{\text{coord}}$ symmetries. They appear as follows

$$F_{\text{eff}} \to F_{\text{eff}} - \Delta F_{\text{eff}}, \tag{2.47}$$

where ΔF_{eff} represents symmetry breaking terms, which in this case are given by

$$\Delta F_{\text{eff}} = M^2(\vec{S}_\perp - S^3\partial_z\vec{\xi}_\perp)^2 + \frac{\varepsilon}{2g^2}\left\{(S^3\partial_z\delta)^2 + (\partial_z S^3)^2\right\}. \tag{2.48}$$

Here $\varepsilon \sim \gamma_{23}/\gamma_1$, and M represents a mass gap parameter given by

$$M^2 \sim \int d^2\vec{x}_\perp \gamma_{23}(\partial_\perp \chi)^2 \to \frac{\gamma_{23}\alpha}{2(2\beta_{12}+\beta_{345})}. \tag{2.49}$$

In this form M is known as the "twisted mass" [52, 53].

If we expand the first term in (2.48) we find that the mass gap M^2 represents a negative mass term (if $\gamma_{23} > 0$) for $\vec{S}_\perp$ and implies a minimum energy for $|S_\perp|^2 = 1$, and thus $S^3 \to 0$. This characterizes the explicit $O(3)$ symmetry breaking in which the lowest energy state retains a $U(1)$ degeneracy. If $\gamma_{23} < 0$ the mass term will be positive and we will find $\vec{S}_\perp \to 0$, in which case the $O(3)$ is completely broken with no degeneracy of the ground state. We also note that the first term of (2.48) implies a correlation between the translational moduli $\vec{\xi}_\perp$ and the rotational moduli $\vec{S}_\perp$. If $S^3 \neq 0$ we find the free energy is minimized for $\partial_z \vec{\xi}_\perp$ antiparallel to $\vec{S}_\perp$. This is of course to be expected due to the locking of the coordinate and orbital rotations when $\gamma_{23} \neq 0$.

We point out the agreement of the results (2.45) and (2.48) with the low energy effective dynamics of moduli fields emerging on the ANO string (see [23] and [45]). Note that since we consider a global $U(1)_P$ phase symmetry we have the additional axial modulus $\delta(z,t)$ appearing in the effective theory (2.45).

We may extend this analysis to the anti-symmetric A-phase ansatz (2.24). Here the translational moduli $\vec{\xi}_\perp(z)$ are generated as in the previous example in (2.43). The $SO(3)_{S+L}$ and $U(1)_A$ moduli are generated by

$$\vec{\chi}_A(r_\perp, \phi) \to e^{i\delta}\chi_0(r_\perp)\vec{S} + e^{-i\delta}\chi_2(r_\perp)\vec{S}^\star e^{2i\phi}, \tag{2.50}$$

where δ and $\vec{S}$ are functions of z. Here the unit vector field $\vec{S}$ has been promoted to a complex vector

$$\vec{S} \equiv (\vec{S}_R + i\vec{S}_I)/\sqrt{2}, \tag{2.51}$$

with the following conditions:

$$|\vec{S}_R| = |\vec{S}_I| = 1, \text{ and } \vec{S}_R \cdot \vec{S}_I = 0. \tag{2.52}$$

At this point we perform the same procedure as the previous example to determine the form of the effective free energy describing the moduli dynamics. We again write

$F_{\rm eff}$ as a combination of γ_1 and symmetry breaking γ_{23} terms. For $\gamma_{23}=0$ we have

$$\begin{aligned} F_{\rm eff} &= F_{\rm trans} + F_{O(3)+U(1)}, \\ F_{\rm trans} &= \frac{T}{2}(\partial_z \vec{\xi}_\perp)^2, \\ F_{O(3)+U(1)} &= \frac{1}{2g^2}|\partial_z \vec{S} + i\vec{S}\partial_z\delta|^2, \end{aligned} \tag{2.53}$$

where T is similar to the case in (2.46). However, g^2 is now given by

$$\frac{1}{2g^2} \sim \int d^2\vec{x}_\perp \gamma_1 \chi_{0,2}^2 \to \frac{\gamma_1^2}{\alpha}\Delta^2 \log\left(\frac{\alpha R^2}{\gamma_1}\right), \tag{2.54}$$

due to the $1/r_\perp$ nature of $\chi(r_\perp)$ as $r_\perp \to \infty$.

We have written $F_{O(3)+U(1)}$ in (2.53) in a form emphasizing the symmetry (2.27). Thus, although the complex nature of $\vec{S}$ implies a complete breaking of $SO(3)_{S+L}$ and hence three complete non-Abelian moduli, the hidden symmetry (2.27) reduces the total number of moduli by one. In this case we have a total of five gapless moduli.

We continue by including the corrections when $\gamma_{23} \neq 0$. Writing

$$F_{\rm eff} \to F_{\rm eff} - \Delta F_{\rm eff}, \tag{2.55}$$

with

$$\Delta F_{\rm eff} = M^2|\vec{S}_\perp - S^3\partial_z\vec{\xi}_\perp|^2 + \frac{\varepsilon}{2g^2}|\partial_z S^3 + iS^3\partial_z\delta|^2. \tag{2.56}$$

Here $\varepsilon = \gamma_{23}/\gamma_1$ as previously and M^2 is given by

$$M^2 \sim \int d^2\vec{x}_\perp \gamma_{23}(\partial_\perp \chi_{0,2})^2 \to \gamma_{23}\Delta^2 \times C(\beta_i), \tag{2.57}$$

where $C(\beta_i)$ is a constant dependent on the β_i coefficients. We see again that (2.56) shows the correlation between the orbital $SO(3)_{S+L}$ rotations and z-dependent translations due to the breaking of $SO(3)_L \times SO(3)_{\rm coord} \to SO(3)_{L+R} \equiv SO(3)_L$ by the non-zero γ_2, γ_3 in the gradient terms of (2.6).

We complete this analysis by considering the moduli fields of the more general double core vortex ansatz (2.28). Again, the translational moduli $\vec{\xi}_\perp(z)$ are generated by the transformation in (2.43). We represent the $SO(3)_{S+L}$ and $U(1)_A$ moduli by

$$\begin{aligned} \vec{\chi}_{\rm dc}(r_\perp,\phi) \to & \frac{1}{\sqrt{2}}(e^{i\delta}\chi_0(r_\perp) + e^{-i\delta}\chi_2(r_\perp)e^{2i\phi})\vec{S} \\ & + \frac{i}{\sqrt{2}}(e^{i\delta}\zeta_0(r_\perp) - e^{-i\delta}\zeta_2(r_\perp)e^{2i\phi})\vec{n}, \end{aligned} \tag{2.58}$$

where $\vec{S}$ and $\vec{n}$ are both real unit vectors, which are orthogonal to each other

$$\vec{S} \cdot \vec{n} \equiv 0. \tag{2.59}$$

For $\gamma_{23} = 0$ we write the effective free energy following the same procedure as previously

$$\begin{aligned} F_{\text{eff}} = & \frac{T}{2}(\partial_z \vec{\xi}_\perp)^2 + \frac{1}{2g_\delta^2}(\partial_z \delta)^2 + \frac{1}{2g_\chi^2}(\partial_z \vec{S})^2 + \frac{1}{2g_\zeta^2}(\partial_z \vec{n})^2 \\ & + \frac{1}{g_{\chi\zeta}^2}(\partial_z \delta)(\vec{S} \cdot \partial_z \vec{n} - \vec{n} \cdot \partial_z \vec{S}), \end{aligned} \tag{2.60}$$

where the tension T is similar in value to the previous examples, and the couplings g_χ, g_ζ, $g_{\chi\zeta}$, and g_δ are given by

$$\begin{aligned} \frac{1}{2g_\chi^2} &= \frac{1}{2}\int d^2\vec{x}_\perp \gamma_1 \chi_{0,2}^2 \to \frac{\gamma_1^2}{\alpha}\Delta^2 \log\left(\frac{\alpha R^2}{\gamma_1}\right), \\ \frac{1}{2g_\zeta^2} &= \frac{1}{2}\int d^2\vec{x}_\perp \gamma_1 \zeta_{0,2}^2 \sim \frac{1}{2g_\chi^2}, \\ \frac{1}{2g_{\chi\zeta}^2} &= \frac{1}{2}\int d^2\vec{x}_\perp \gamma_1 (\chi\zeta)_{0,2} \sim \frac{1}{2g_\chi^2}, \\ \frac{1}{2g_\delta^2} &= \frac{1}{2g_\chi^2} + \frac{1}{2g_\zeta^2}. \end{aligned} \tag{2.61}$$

As long as $1/g_{\chi\zeta}^2 \neq 1/g_\chi g_\zeta$ there is no hidden symmetry, and we indeed find a total of six independent moduli from the complete breaking of $SO(3)_{S+L} \times U(1)_A \times t$ by the double core vortex.

Turning on γ_{23} we would again find correlations between $(\vec{S}, \vec{n})$, and $\vec{\xi}_\perp$ as well as mass terms for S^3 and n^3, all proportional to γ_{23}. The complete form for ΔF_{eff} for the double core vortex is however complex and we omit it here.

2.6 Discussion and Conclusions

In the analysis considered here we have explored the Ginzburg-Landau description of superfluid ^{3}He and similar systems with tensorial order parameter and non-Abelian group structure. The symmetry structure of such systems allows for the investigation of non-Abelian gapless and quasi-gapless moduli localized on mass vortices. We have attempted to illustrate these concepts by applying techniques standard in high energy

physics to condensed matter systems like superfluid ^{3}He-B. In particular, we have given a general procedure for determining effective theory describing the low energy excitations of vortices in superfluid ^{3}He.

Additionally we have applied this procedure to a specific case (as suggested in [14]) and derived the low energy effective theories for the gapless and quasi-gapless excitations of topological vortices appearing in the B-phase of superfluid ^{3}He. This was accomplished by considering the ansatz for the order parameter given by (2.15), with anti-symmetric components given by (2.18) and (2.24). We have chosen this specific ansatz because it illustrates the process of determining the non-Abelian moduli fields without introducing large amounts of calculation. However, it is well known both theoretically [30, 31] and experimentally [19, 20, 21] that the minimizing solutions contain additional terms in the order parameter. Considering more complex vortex solutions would not change the moduli involved in the low energy theory, however their interactions and coefficients may change depending on the symmetries respected by the vortex solution.

The low energy effective field theories we have derived given by (2.38) and (2.53) with the respective γ_{23} corrections (2.48) and (2.56), exhibit the form of one-dimensional $O(3)$ sigma models whose moduli fields interact with translational moduli generating the well known Kelvin modes [15, 16, 17, 18, 19, 20, 21]. In particular, the model (2.38) with (2.48), is very similar to the $1+1$-dimensional model describing the low energy dynamics of ANO strings in Yang-Mills theories [46, 47]. We do however point out that the present theory has the additional $U(1)$ modulus δ appearing due to the global phase symmetry $U(1)_P$ of (2.6). In the Yang-Mills theories describing the ANO strings, the $U(1)$ modulus δ can be removed by a corresponding gauge transformation. This is not possible in the present situation and thus the $U(1)$ modulus δ is unavoidable. It is however emphasized that the modulus δ does not propagate since its corresponding time derivative term in the free energy (2.6) reduces to a total derivative.

We wish to emphasize that our analysis of the effective field theory is purely classical, and we have made no attempt to discuss quantization. It is expected that after quantization the number gapless excitations appearing in the effective theory may be different from the number of moduli fields. This is of course well known for the case of the Kelvin mode, in which two moduli describing translational excitations, actually

imply only a single mode after quantization. This is a manifestation of the Goldstone theorem applied to non-relativistic systems in which the number of modes may be equal to or less than the number of broken symmetries [34, 35, 36]. We expect that such a reduction of non-Abelian modes may appear in a similar fashion to the Kelvin modes. The next chapter will be devoted to this investigation.

Chapter 3

Non-Abelian Vortices in Superfluid ^{3}He-B

In this chapter, which appeared in [54], we extend the results of the previous chapter on vortices in systems with tensorial order parameters. Specifically, we focus our attention on systems with a GinzburgLandau free energy with a global $U(1)_P \times SO(3)_S \times SO(3)_L$ symmetry in the phase, spin and orbital degrees of freedom. We consider axially symmetric vortices appearing on the spin-orbit locked $SO(3)_{S+L}$ vacuum. We determine the conditions required on the Ginzburg-Landau parameters to allow for an axially symmetric vortex with off diagonal elements in the order parameter to appear. The collective coordinates of the axial symmetric vortices are determined. These collective coordinates are then quantized using the time dependent Ginzburg-Landau free energy to determine the number of gapless modes propagating along the vortex.

3.1 Introduction

In the previous chapter [6], we considered emergent collective coordinates on vortices in systems with a Ginzburg-Landau free energy with a $U(1)_P \times SO(3)_S \times SO(3)_L$ symmetry group. Here, $U(1)_P$ represents the phase symmetry of the order parameter, and $SO(3)_{S,L}$ are the spin and orbital rotation groups. In particular, we considered vortices appearing in the bulk spin-orbit locked $SO(3)_{S+L}$ vacuum, much like the B-phase of superfluid ^{3}He. In that work, we provided a method for determining the type and

number of collective coordinates appearing on mass vortices in the $SO(3)_{S+L}$ vacuum. This was performed under the restriction that the 3×3 matrix order parameter $e_{\mu i}$ contained only its diagonal ($\delta_{\mu i}$) and antisymmetric off-diagonal ($\varepsilon_{\mu ik}\chi_k$) elements, setting its symmetric-traceless part to zero. This restriction allowed the calculations to be carried out with relative ease while still providing enough depth to illustrate the development of non-Abelian collective coordinates. We were also able to illustrate the interactions of the non-Abelian collective coordinates with the well studied translational degrees of freedom leading to the familiar Kelvin modes [15, 16, 17, 18, 19, 20, 21, 55]. The presentation of that work was purely classical and we made no attempt to discuss time dependence or quantization. Including quantization may alter the number of gapless excitations determined from the naive counting of collective coordinates. In this work, we aim to continue the analysis and discuss vortices that are more closely related to those studied both experimentally [19, 20, 21, 30, 55], and theoretically [30, 31], in superfluid ^{3}He-B. Specifically, we will discuss vortices respecting an axial $O(2)$ symmetry, which we will define below. We will also explore the effects of time dependence and quantization on the gapless excitations of axial symmetric vortices.

Condensed matter systems with tensorial order parameters such as superfluid 3He have drawn attention from the high-energy physics community [3, 7]. The non-Abelian group structure inherent to such condensed matter systems suggests interesting parallels with high energy systems with similar non-Abelian symmetries. One example of this parallel behavior is the case of low energy excitations of vortices in systems similar to superfluid ^{3}He-B, which can be compared with the low energy excitations of Abrikosov-Nielsen-Olesen-like (ANO) flux tubes [46, 47] appearing in Yang-Mills theories [8, 9, 10, 11, 12, 13]. Under a particular choice of the Ginzburg-Landau free energy parameters, the vortices in such condensed matter systems develop internal non-Abelian collective excitations whose low energy dynamics follow a non-linear O(3) sigma model [14]. The same O(3) sigma model emerges for the collective modes of the flux tubes strings in Yang-Mills theories [2, 23, 45]. This example is illustrating the universality of effective field theories in condensed matter, high energy, and cosmological systems [3].

The model we consider is described by a Ginzburg-Landau free energy with a continuous $U(1)_P \times SO(3)_S \times SO(3)_L$ symmetry. This structure appears near a critical temperature in the BCS theory of orbital P-wave pairing of identical fermions [24]. To

satisfy the anti-symmetric condition, the fermion pair must be in a spin triplet state. Thus, the order parameter describing the system is a complex 3×3 matrix $e_{\mu i}$, where μ and i describe the spin and orbital degrees of freedom, respectively. This is what happens, in particular, in superfluid ^{3}He [25, 26, 27]. We hasten to point out that the models we consider below are inspired by considerations of superfluid ^{3}He. However, aside from initial inspirations and similarities in terminology, we do not wish to invite this comparison any further in what follows.

The free energy, from which we start, contains an enhancement of the orbital rotation symmetry whereby the internal and external rotations will be considered separately (see the example in [56]). By external coordinate rotation, we are referring to a transformation resulting from a rotation of the coordinate system without a corresponding rotation of the orbital index. In this case, we can consider the orbital index as an internal degree of freedom. Thus, the continuous symmetry of the model is

$$\mathcal{G} = U(1)_P \times SO(3)_S \times SO(3)_{L_{\text{int}}} \times SO(3)_{L_{\text{ext}}} \times T \tag{3.1}$$

where the enhanced $SO(3)_L \to SO(3)_{L_{\text{int}}} \times SO(3)_{L_{\text{ext}}}$ is explicitly written. The group T represents the translational symmetry. We refer to the internal part of $\mathcal{G}$ as $G = U(1)_P \times SO(3)_S \times SO(3)_{L_{\text{int}}}$. This type of symmetry can be approximately achieved in an ultra-cold fermi gas with p-wave pairing. Additionally, this situation is reminiscent of the theory of elasticity where an unphysical vanishing of the bulk modulus leads to an enhanced symmetry of rotations $O(2) \to O(2) \times O(2)$. This leads to the equivalence of scale and conformal transformations [22]. In this work, it will be necessary to consider the entire symmetry group including both the internal and external symmetries (see Figures 3.1 and 3.2).

In the vacuum, a spontaneous breaking of the internal symmetry G to a spin-orbit locked symmetry

$$G \to H = SO(3)_{S+L_{\text{int}}} \tag{3.2}$$

occurs, similar to the mechanism of color-flavor locking in color superconductivity [28, 57]. This vacuum has a degeneracy given by

$$G/H = U(1)_P \times SO(3)_{S-L_{\text{int}}}. \tag{3.3}$$

This type of degeneracy allows for the existence of topologically stable vortices of the $\mathbb{Z}\times$

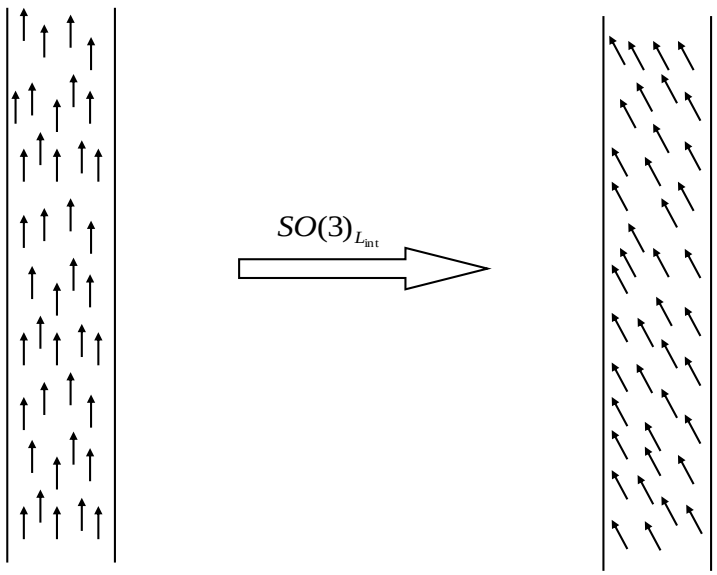

Figure 3.1: The result of an internal rotation of the vortex orbital index is shown. The vortex density function does not change, however, the directors of the vortex are rotated.

$\mathbb{Z}_2$ type [29]. The specific vortex solutions are determined by minimizing the Ginzburg-Landau free energy for the required boundary conditions.

To accomplish this task, we consider several forms of the order parameter and minimize the free energy under the assumed boundary conditions. Previously, the vortex order parameters were searched for by initially decomposing the order parameter into its trace, symmetric, and antisymmetric components [14, 6]

$$\begin{aligned} e_{\mu i} &= \frac{1}{3} e_{\sigma\sigma}\, \delta_{\mu i} + e^S_{\mu i} + e^A_{\mu i}, \\ e^S_{\mu i} &= e_{\{\mu i\}} - \frac{1}{3} e_{\sigma\sigma} \delta_{\mu i}, \\ e^A_{\mu i} &= e_{[\mu i]} \equiv \varepsilon_{\mu i k} \chi^k. \end{aligned} \tag{3.4}$$

For the illustrative purposes, in the previous chapter [6], it was sufficient to consider

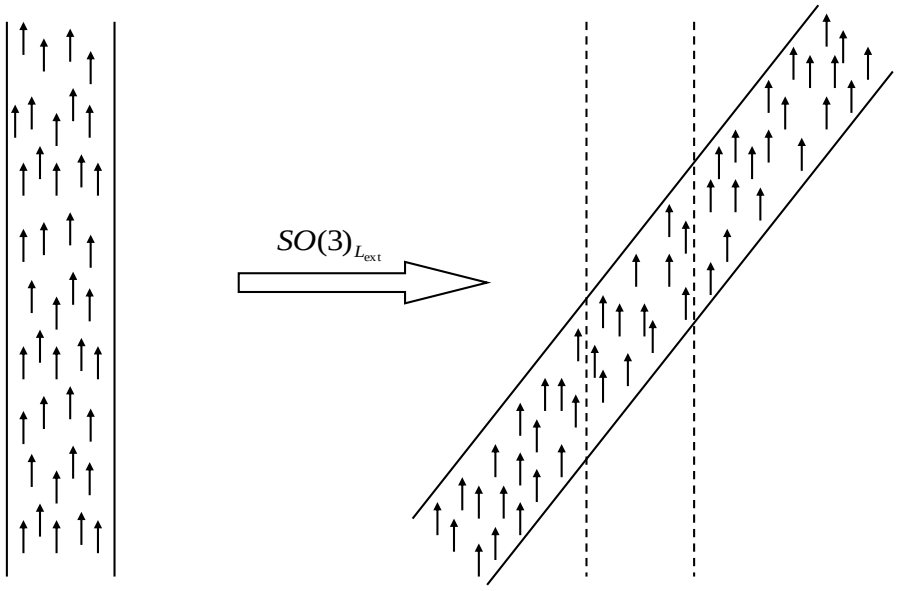

Figure 3.2: The result of an external coordinate rotation of the vortex axis is shown. The directors of the vortex solution are not rotated. A complete $SO(3)_L$ rotation would rotate both the density function and the directors.

just the trace and antisymmetric components of the order parameter

$$e_{\mu i} = \mathrm{e}^{\mathrm{i}\phi} f(\vec{x}_\perp)\delta_{\mu i} + \varepsilon_{\mu i k}\chi_k(\vec{x}_\perp), \tag{3.5}$$

where $\vec{x}_\perp \equiv (x, y)$ are the coordinates in the plane perpendicular to the vortex axis, and ϕ is the polar angle in this plane. The functions f and χ are determined by minimizing the free energy. This is indeed most simple context allowing for the maximal number of moduli fields to emerge on the vortex. In the present work we wish to continue that analysis by extending the order parameter ansatz to include all the necessary components appearing in an axially symmetric solution. These will include new symmetric-traceless components. In the absence of these terms the low energy effective theory can be described by translations (Kelvin modes) and rotations of the χ^i fields resulting in an emergent $O(3)$ sigma model for the unit vector λ^i describing the director of χ^i. We will

find that the addition of symmetric-traceless components does not change the number of collective coordinates appearing on the mass vortex. However, we will observe changes to the gradient and interaction terms in the free energy.

The other goal of this paper is to characterize the time dependence of the collective coordinates to determine the quantized modes appearing on the mass vortex. It is well known that, after quantization, the two translational collective coordinates appearing on the vortex solution result in a single Kelvin mode. This is the result of the application of Goldstones theorem [32, 33] to non-relativistic systems where the number of quantized modes is less than or equal to the number of broken group generators [34, 35, 36].[1] Additionally, it is a simple matter to show that the collective coordinates generated by the broken coordinate rotational symmetry $SO(3)_{L_{\text{ext}}}$ are equivalent to the (x, y) translations [14, 50, 51, 61]. Figure 3.3 illustrates this equivalence. Thus, the four collective coordinates generated from coordinate rotations and translations reduce to only one gapless mode. We will extend this analysis to the quantization of the non-Abelian collective coordinates appearing from the broken $SO(3)_{S+L_{\text{int}}}$.

The organization of our presentation is as follows. We will begin with a discussion of the Ginzburg-Landau free energy emerging from the symmetry structure (3.1). The following section will present a classification of vortices according to the symmetries they respect. We will determine the general form of the order parameter for an axially symmetric vortex. In particular, we will determine some specific requirements for the axially symmetric components to emerge from the trace-only solution. In the following sections, we will determine the static low-energy theory for the translational and non-Abelian collective coordinate fields localized on the mass vortex with the modifications due to the symmetric components of the axially symmetric vortex. Finally, we will find the precise number and type of quantized gapless modes appearing on the axially symmetric vortex by considering the Goldstone theorem in non-relativistic systems. We will discuss the effects of quantization on the classically gapless modes. We will not discuss quantum corrections coming from loops in the effective potential. For such an analysis, we turn the reader to the discussion presented in [62].

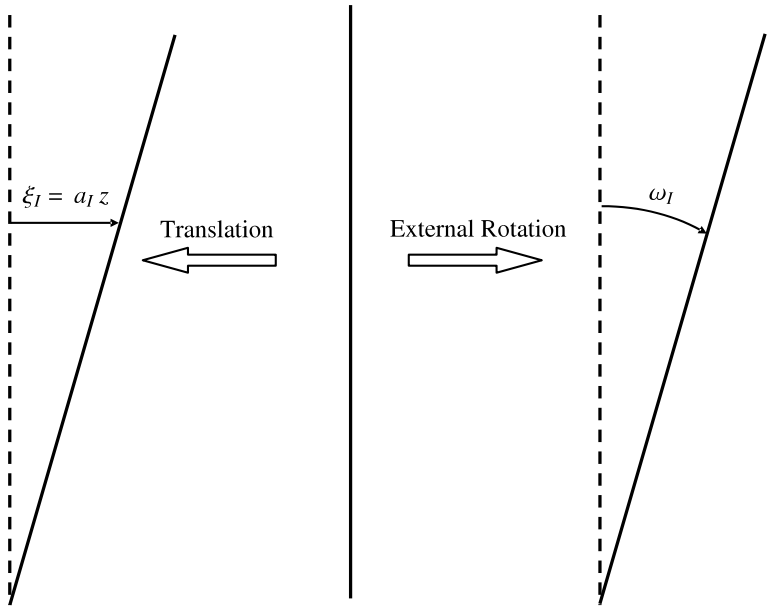

Figure 3.3: We illustrate the equivalence of a z-dependent translation $\xi_I(z)$ where $I = 1, 2$, and an (external) rotation of an infinitesimal segment of the vortex. The translational transformation is of the form $\phi(x_I) \to \phi(x_I \xi_I(z))$ where ϕ is a generic function illustrating the vortex profile, and $\xi_I(z) = a_I z$ where a_I is a constant. The rotational transformation is of the form $\phi(x_I) \to \phi(x_I \epsilon_{IJ} \omega_J z)$. If we select $a_I = \epsilon_{IJ}\omega_J$, then the transformations are equivalent [14, 50, 51, 61].

3.2 The Ginzburg-Landau description

In this section, we will review the Ginzburg-Landau description of condensed matter systems following the descriptions outlined in [3, 37, 40]. As we discussed in the introduction, the order parameter is a complex 3×3 matrix $e_{\mu i}$ that transforms as a vector under both spin and (internal) orbital rotations [25, 26, 27]

$$e_{\mu i} \to \mathrm{e}^{\mathrm{i}\psi} S_{\mu\nu} L_{ij} e_{\nu j}, \tag{3.6}$$

where $S_{\mu\nu}$ and L_{ij} are spin and orbital rotations respectively. We will consider internal and external orbital rotations as distinct and thus the continuous symmetry group is

$$\mathcal{G} = U(1)_P \times SO(3)_S \times SO(3)_{L_{\rm int}} \times SO(3)_{L_{\rm ext}} \times T, \tag{3.7}$$

where $U(1)_P$ is the group of phase rotations $\mathrm{e}^{\mathrm{i}\psi}$, and $SO(3)_{S,L}$ are the groups of spin and orbital rotations. The internal part of $\mathcal{G}$ is

$$G = U(1)_P \times SO(3)_S \times SO(3)_L, \tag{3.8}$$

.

The most general (time-dependent) Ginzburg-Landau free energy containing this symmetry is given by [26, 31, 38, 39]

$$\begin{aligned}
F_{\rm GL} &= F_{\rm time} + F_{\rm grad} + V, \\
F_{\rm time} &= \mathrm{i} e_{\mu i} \partial_t e^\star_{\mu i}, \\
F_{\rm grad} &= \gamma_1 \partial_i e_{\mu j} \partial_i e^\star_{\mu j} + \gamma_2 \partial_i e_{\mu i} \partial_j e^\star_{\mu j} + \gamma_3 \partial_i e_{\mu j} \partial_j e^\star_{\mu i}, \\
V &= -\alpha e_{\mu i} e^\star_{\mu i} + \beta_1 e^\star_{\mu i} e^\star_{\mu i} e_{\nu j} e_{\nu j} + \beta_2 e^\star_{\mu i} e_{\mu i} e^\star_{\nu j} e_{\nu j} + \beta_3 e^\star_{\mu i} e^\star_{\nu i} e_{\mu j} e_{\nu j} \\
&\quad + \beta_4 e^\star_{\mu i} e_{\nu i} e^\star_{\nu j} e_{\mu j} + \beta_5 e^\star_{\mu i} e_{\nu i} e_{\nu j} e^\star_{\mu j},
\end{aligned} \tag{3.9}$$

where γ_i, α, and β_i are phenomenological parameters whose values can be determined from the BCS theory [27]. The time-dependent part $F_{\rm time}$ of (3.9) is typically discussed for non-equilibrium dynamics where quasi-static approximations are not valid (see for example [42, 43]).

We note the similarity of the free energy (3.9) with that of superfluid 3He whose gradient part is given by:

$$(F_{\rm grad})_{^3\rm He} = \gamma_1 \partial_i e_{\mu j} \partial_i e^\star_{\mu j} + \gamma_2 \partial_i e_{\mu i} \partial_j e^\star_{\mu j} + \gamma_3 \partial_i e_{\mu j} \partial_j e^\star_{\mu i}. \tag{3.10}$$

In this case, the non-zero values of $\gamma_{2,3}$ explicitly break the $SO(3)_{L_{\rm int}} \times SO(3)_{L_{\rm ext}}$ down to the traditional $SO(3)_L$. For superfluid ^{3}He the Ginzburg-Landau parameters γ_i, β_i, and α can be calculated in the weak coupling limit at zero pressure from the BCS theory. Strong coupling corrections for the specific case of superfluid ^{3}He have been determined in [41].

In the present paper, we will not be concerned with the precise values of all of the free energy parameters. We will simply require that $\gamma_{2,3} \to 0$, and that the β_i

parameters satisfy conditions for a stable $SO(3)_{S+L}$ symmetric vacuum to exist. We do not consider the model (3.9) to be an appropriate description of superfluid ^{3}He, so we do not claim that the results below are consistent with superfluid ^{3}He. Our conclusions will only be appropriate for systems with the symmetry structure (3.7). However, whenever appropriate, we will note analogies between our model and superfluid ^{3}He for illustrative purposes.

Minimizing the free energy (3.9) results in several different vacuum structures, one of which is given by the retention of a spin-orbit locked $SO(3)_{S+L_{\rm int}}$ symmetry

$$G \to H_B = SO(3)_{S+L_{\rm int}}. \tag{3.11}$$

In this case, the bulk order parameter is given by

$$(e_B)_{\mu i} = \mathrm{e}^{\mathrm{i}\psi}\Delta(R_0)_{\mu i},\ \Delta = \frac{\alpha}{6\beta_{12}+2\beta_{345}}, \tag{3.12}$$

where $(R_0)_{\mu i}$ is a generic rotation matrix and the gap parameter Δ is determined by minimization of (3.9). In superfluid ^{3}He, this would be recognized as the B phase ground state. Here and throughout this analysis we will make use of the shorthand notation

$$\begin{aligned}\gamma_{abc...} &= \gamma_a + \gamma_b + \gamma_c + ...,\\ \beta_{abc...} &= \beta_a + \beta_b + \beta_c + ...\end{aligned} \tag{3.13}$$

We can see that the order parameter (3.12) is invariant under simultaneous orbital L_{ij} and spin $S_{\mu\nu}$ rotations satisfying $S = R_0 L R_0^T$.

The vacuum order parameter (3.12) has a ground state degeneracy given by

$$G/H_B = U(1)_P \times SO(3)_{S-L_{\rm int}}. \tag{3.14}$$

Thus, we are free to select the state with $(R_0)_{\mu i} = \delta_{\mu i}$ as our ground state. Considering the first fundamental group of the degeneracy space (3.14)

$$\pi_1(G/H_B) = \pi_1(U(1)) + \pi_1(SO(3)) = \mathbb{Z} + \mathbb{Z}_2 \tag{3.15}$$

we see that the B-phase admits topologically stable mass vortices with integer topological charge $n \in \mathbb{Z}$. Additionally, spin vortices with $\mathbb{Z}_2$ winding $\nu \in (0,1)$ also appear in the vacuum. We will only consider the mass vortices with windings $n = \pm 1$ and $\nu = 0$.

The precise form of the single vortex ($n = 1$) order parameter must be determined by minimization of the free energy (3.9). For this purpose we will consider solutions of the form

$$e_{\mu i} = e^{i\phi} f(\vec{x}_\perp)\delta_{\mu i} + \varepsilon_{\mu ik}\chi_k(\vec{x}_\perp) + S_{\mu i}(\vec{x}_\perp), \tag{3.16}$$

where f, χ_k, and $S_{\mu i}$ are functions to be determined by minimization and $S_{ii} = 0$. Here ϕ regers to the azimuthal angle about the vortex axis. To satisfy the asymptotic boundary condition, we must require

$$f \to \Delta,\ \chi_i \to 0,\ \text{and } S_{\mu i} \to 0 \text{ as } |\vec{x}_\perp| \equiv r \to \infty. \tag{3.17}$$

Additionally, f must vanish as $r_\perp \to 0$ to satisfy the winding condition at the origin.

3.3 Symmetry classification of vortices and axially symmetric solutions

3.3.1 Symmetry structure of vortices

In this section we will discuss the topic of vortex classification by considering the symmetries broken by specific vortex solutions. The results of this section will allow us to determine vortex solutions by reducing the number of components of the order parameter to those that satisfy invariance under unbroken symmetries. Additionally, by simply considering the broken generators we will be able to determine the moduli fields emerging on the mass vortex, and draw general conclusions about their kinetic terms and interactions in a low energy effective theory. The presentation of this section will follow closely the approaches given in [3, 26, 48].

We consider the complete symmetry group $\mathcal{G}$ of the free energy (3.9), along with the discrete symmetries

$$\mathcal{G} \to \mathcal{G} \times \mathcal{G}_{\text{dis}}, \tag{3.18}$$

where

$$\mathcal{G}_{\text{dis}} = \mathcal{T} \times P. \tag{3.19}$$

The discrete symmetries $\mathcal{T}$ and P represent the time reversal and parity transformations.

The effect of these transformations on the order parameter $e_{\mu i}$ are given by the following

$$\begin{aligned}
&U_\theta = \mathrm{e}^{\mathrm{i}\hat{I}\theta} \in U(1)_P, \text{ where } \hat{I}e_{\mu i} = e_{\mu i},\ \hat{I}e^\star_{\mu i} = -e^\star_{\mu i},\\
&\hat{S}_\beta e_{\mu i} = -\mathrm{i}\varepsilon_{\beta\mu\nu}e_{\nu i},\ \mathrm{e}^{\mathrm{i}\vec{\omega}\cdot\hat{S}} \in SO(3)_S\\
&\hat{L}^{\mathrm{int}}_j e_{\mu i} = -\mathrm{i}\varepsilon_{jik}e_{\mu k},\ \mathrm{e}^{\mathrm{i}\vec{\omega}\cdot\hat{L}^{\mathrm{int}}} \in SO(3)_L\\
&\hat{L}^{\mathrm{ext}}_j e_{\mu i} = -\mathrm{i}\varepsilon_{jlk}x_l\frac{\partial}{\partial x_k}e_{\mu i},\ \mathrm{e}^{\mathrm{i}\vec{\omega}\cdot\hat{L}^{\mathrm{ext}}} \in SO(3)_{\mathrm{coord}},\\
&t_{\vec{\xi}_0}e_{\mu i}(\vec{x}) = e_{\mu i}(\vec{x}-\vec{\xi}_0),\ t_{\vec{\xi}_0} \in t\\
&\hat{T}e_{\mu i} = e^\star_{\mu i},\ \hat{T} \in T\\
&\hat{P}e_{\mu i}(\vec{x}) = -e_{\mu i}(-\vec{x}),\ \hat{P} \in P.
\end{aligned} \tag{3.20}$$

In the first line of (3.20), θ represents the phase angle. We will employ the shorthand notations

$$\hat{L} \equiv \hat{L}_{\mathrm{int}} + \hat{L}_{\mathrm{ext}},\ \ \hat{J}_{\mathrm{int}} \equiv \hat{L}_{\mathrm{int}} + \hat{S},\ \ \hat{J} \equiv \hat{L} + \hat{S}. \tag{3.21}$$

In the $SO(3)_{S+L_{\mathrm{int}}}$ vacuum state, where we may select for our ground state

$$e_{\mu i} = \mathrm{e}^{\mathrm{i}\psi}\Delta\delta_{\mu i}, \tag{3.22}$$

we can see that the preserved continuous symmetries from $\mathcal{G}$ are

$$\mathcal{H} = SO(3)_{J_{\mathrm{int}}} \times SO(3)_{L_{\mathrm{ext}}} \times T. \tag{3.23}$$

The discrete symmetries are given by the transformations

$$U_\psi\hat{\mathcal{T}}U_{-\psi},\ \text{and}\ \hat{P}U_\pi. \tag{3.24}$$

In the presence of a vortex in the spin-orbit locked phase, the determination of the continuous symmetries preserved in the asymptotic limit is somewhat more subtle. Far away from the vortex core the order parameter approaches the form

$$e_{\mu i} \to \mathrm{e}^{\mathrm{i}\phi}\Delta\delta_{\mu i},\ \text{as } r \to \infty. \tag{3.25}$$

Clearly the asymptotic form retains the spin-orbit locking $SO(3)_{J_{\mathrm{int}}}$ symmetry, as well as invariance under translations $T_{\vec{\xi}_0}$. It is also not difficult to show that coordinate rotations about the x and y axis also leave the order parameter invariant in the asymptotic

limit. However, it is clear that the order parameter is not invariant under independent phase and external coordinate rotations about the z-axis. Instead the order parameter is invariant under axial $O(2)_A$ transformations, which are generated by a linear combination of the generators of phase and z-axis external coordinate rotations:

$$\hat{Q} = \hat{L}_z^{\rm ext} - \hat{I},\ U_\delta = {\rm e}^{{\rm i}\delta\hat{Q}} \in O(2)_A. \tag{3.26}$$

A specific example of an axial transformation generated by $\hat{Q}$ is shown in Figure 3.4.

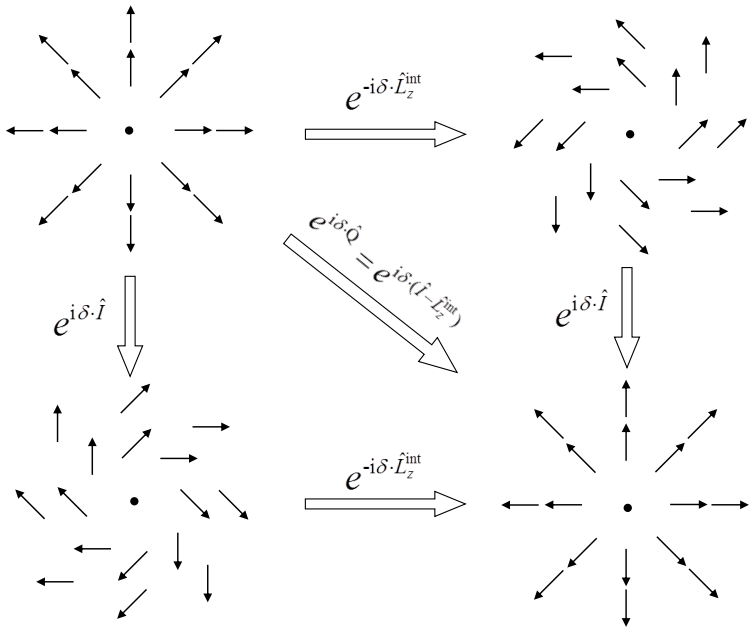

Figure 3.4: The phase vectors of an axial $O(2)_A$ symmetric vortex solution are mapped onto the perpendicular plane to the vortex axis. The two transformations generated by $\hat{L}_z^{\rm int}$ and $\hat{I}$ are shown in the upper right and lower left corner respectively. When these transformations are performed in succession by equal and opposite angle δ, they are known as axial $O(2)_A$ transformations generated by $\hat{Q}$. Axially symmetric solutions are invariant under $O(2)_A$ transformations, as illustrated in the lower right corner.

Thus, summarizing the continuous symmetries of the $SO(3)_{S+L_{\rm int}}$ phase with an

$n = 1$ vortex in the asymptotic limit

$$(\mathcal{H}_B)_{n=1} = SO(3)_{J_{\rm int}} \times O(2)_A \times T. \tag{3.27}$$

Additionally, in the asymptotic limit, the order parameter is invariant under the discrete transformations

$$\hat{P}_1 \equiv \hat{P}\mathrm{e}^{\mathrm{i}\pi\hat{I}},\ \hat{P}_3 \equiv \hat{\mathcal{T}}\mathrm{e}^{\mathrm{i}\pi\hat{J}_x} \tag{3.28}$$

Note that $\hat{J}_x$ generates rotations of both the internal and external degrees of freedom.

The degeneracy space associated with a particular mass vortex solutions is characterized by the possible symmetry breaking pattern of the continuous group (3.27). Clearly the existence of a vortex core breaks translations in the x and y directions as well as rotations about any axis in the $x-y$ plane. Additionally, vortices are invariant under translations in the z direction. Thus, vortices are classified according to their transformation properties under the group

$$O(2)_A \times SO(3)_{J_{\rm int}} \times (\mathbb{Z}_2 \times \mathbb{Z}_2)_{P_1 \times P_3} \tag{3.29}$$

whose continuous group elements are generated by $\hat{Q}$, $\hat{J}_{\rm int}$, with discrete group elements given in (3.28).

3.3.2 Vortices in the spherical tensor basis

In searching for vortex solutions that minimize the free energy, we may consider forms of the order parameter the break some or all of the symmetries in (3.29). In this light, it is most convenient to expand the vortex solution in terms of eigenfunctions of $\hat{Q}$, $\hat{S}_z$, and $\hat{L}_z^{\rm int}$.

$$\begin{aligned} e_{\mu i} &= \sum_{\rho,\nu=\pm1,0} \sum_n C_{\rho\nu,n}(r)\lambda_\mu^\rho \lambda_i^\nu \mathrm{e}^{\mathrm{i}n\phi}, \\ \hat{S}_z\lambda_\mu^\rho &= \rho\lambda_\mu^\rho, \\ \hat{L}_z^{\rm int}\lambda_i^\nu &= \nu\lambda_\mu^\nu, \end{aligned} \tag{3.30}$$

where the $\hat{J}_z$ eigenfunctions written in the cartesian (x, y, z) basis as

$$\lambda_\alpha^\pm = 1/\sqrt{2}(\hat{x}_\alpha \pm i\hat{y}_\alpha),\ \lambda_\alpha^0 = \hat{z}_\alpha. \tag{3.31}$$

The most trivial example of a solution is a vortex that is axially $O(2)_A$ symmetric and invariant under $SO(3)_{J_{\rm int}}$

$$\hat{Q}e_{\mu i} = \hat{J}_{\rm int}e_{\mu i} = 0. \tag{3.32}$$

In this case the solution is constrained to $n = 1$, as well as $\rho + \nu = 0$. Here $C_{+-} = C_{00} = C_{-+} = f(r)$, and all other $C_{\rho\nu}$ vanish. Additionally, the invariance under the $(\mathbb{Z}_2 \times \mathbb{Z}_2)_{P_1\times P_3}$ requires $f(r)$ to be real. This would represent the trace-only vortex solution

$$e^t_{\mu i}(x, y) = \mathrm{e}^{\mathrm{i}\phi} f(r)\delta_{\mu i}. \tag{3.33}$$

A more interesting ansatz occurs when we consider solutions that are invariant under a locked $O(2)_{A+J_z}$ symmetry, which is a subgroup of the classification group (3.29). The $O(2)_{A+J_z}$ group is generated by

$$\hat{Q}'e_{\mu i} = 0, \text{ where } \hat{Q}' \equiv \hat{Q} + \hat{J}^{\rm int}_z = \hat{J} - \hat{I}. \tag{3.34}$$

This results in the constraint $n + \rho + \nu = 1$, and thus we may express the amplitudes $C_{\rho\nu,n}$ as

$$\sum_n C_{\rho\nu,n} = \begin{pmatrix} C_{++}\mathrm{e}^{-\mathrm{i}\phi} & C_{+0} & C_{+-}\mathrm{e}^{\mathrm{i}\phi} \\ C_{0+} & C_{00}\mathrm{e}^{\mathrm{i}\phi} & C_{0-}\mathrm{e}^{2\mathrm{i}\phi} \\ C_{-+}\mathrm{e}^{\mathrm{i}\phi} & C_{-0}\mathrm{e}^{2\mathrm{i}\phi} & C_{--}\mathrm{e}^{3\mathrm{i}\phi} \end{pmatrix} \tag{3.35}$$

The $O(2)_{A+J_z}$ vortices are further categorized by their transformations under the $(\mathbb{Z}_2 \times \mathbb{Z}_2)_{P_1\times P_3}$. This results in five subclasses of axisymmetric vortices. We will consider the subclass given by

$$\hat{P}_1\hat{P}_3 e_{\mu i} = e_{\mu i}, \tag{3.36}$$

which reduces to the constraint that the $C_{\rho\nu}$ amplitudes are real.

To identify the trace, symmetric, and anti-symmetric components of $e_{\mu i}$ for the axially symmetric solutions, we rearrange the solution in terms of the irreducible multiplets in the (J, J_z) basis. Following this procedure, we may write the antisymmetric and symmetric-traceless parts of the order parameter $e_{\mu i}$ as follows

$$e_{\mu i} = \mathrm{e}^{\mathrm{i}\phi} f(r)\delta_{\mu i} + \varepsilon_{\mu ij}\chi_j(r, \phi) + S_{\mu i}(r, \phi), \tag{3.37}$$

where we write the χ_i and $S_{\mu i}$ tensors in terms of the spherical tensor components χ_{m_J} and S_{m_J}:

$$\vec{\chi}(r,\phi) = \mathrm{i}\left(\chi_1\vec{\lambda}^{+} + \chi_0 \mathrm{e}^{\mathrm{i}\phi}\vec{\lambda}^{0} + \chi_{-1}\mathrm{e}^{2\mathrm{i}\phi}\vec{\lambda}^{-}\right) \tag{3.38}$$

and

$$\begin{aligned} S_{\mu i} =& s_2 \mathrm{e}^{-\mathrm{i}\phi}\lambda^{+}_{\{\mu}\lambda^{+}_{i\}} + s_1\lambda^{+}_{\{\mu}\lambda^{0}_{i\}} + s_0\mathrm{e}^{\mathrm{i}\phi}\left(\lambda^{+}_{\{\mu}\lambda^{-}_{i\}} - 2\lambda^{0}_{\{\mu}\lambda^{0}_{i\}}\right) \\ &+ s_{-1}\mathrm{e}^{2\mathrm{i}\phi}\lambda^{-}_{\{\mu}\lambda^{0}_{i\}} + s_{-2}\mathrm{e}^{3\mathrm{i}\phi}\lambda^{-}_{\{\mu}\lambda^{-}_{i\}}. \end{aligned} \tag{3.39}$$

The following relations between the (J, J_z) and the $(L_z^{\mathrm{int}}, S_z)$ bases are useful and easy to derive from the Clebsch-Gordon coefficients:

$$\begin{aligned} & f = \frac{1}{3}(C_{+-} + C_{-+} + C_{00}), \\ & \chi_0 = \frac{1}{2}(C_{+0} - C_{0+}),\ \chi_1 = \frac{1}{2}(C_{-+} - C_{+-}),\ \chi_2 = \frac{1}{2}(C_{-0} - C_{0-}), \\ & s_{-1} = C_{++},\ s_0 = \frac{1}{2}(C_{+0} + C_{0+}),\ s_1 = \frac{1}{6}(C_{+-} + C_{-+} - 2C_{00}) \\ & s_2 = \frac{1}{2}(C_{-0} + C_{0-}),\ s_3 = C_{--}. \end{aligned} \tag{3.40}$$

In the context of superfluid ^{3}He-B the solutions (3.36) are known as the v-vortices [48]. Physically, they are characterized by a core with mixed A-phase (C_{+0}) and ferromagnetic β-phase (C_{0+}) components. In the following section we will argue that these components will typically arise spontaneously from the trace only solution (3.22). Thus, the vortex will contain symmetric and anti-symmetric components, resulting in additional gapless excitations of the vortex core.

3.4 Emergence of off-diagonal components in the vortex core

In the previous chapter we considered the conditions under which a single antisymmetric component $\varepsilon_{\mu ik}\chi_k(r_\perp)$ of the vortex order parameter would spontaneously develop in the core of solution (3.22). To accomplish that task we employed the methods of [44] considered for superconducting strings. Initially, the χ_k field is set to zero and the free energy (3.9) is minimized numerically by $f(r)$ (see Figure 3.5).

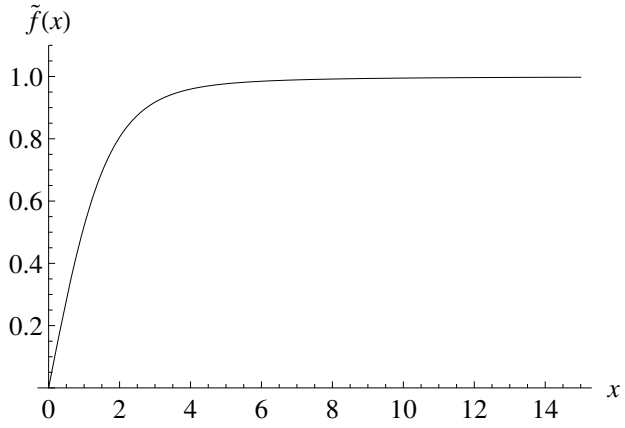

Figure 3.5: The numerical solution $\tilde{f}(x) = f(x)/\Delta$ is plotted. Here we have defined $x \equiv r_\perp \sqrt{\alpha/\gamma_1}$. For $x \ll 1$ the solution follows the form $\tilde{f}(x) \sim 0.583x$. In the opposite limit $x \gg 1$ the function $\tilde{f}(x) \to 1 - 1/2x^2 + \mathcal{O}(x^{-4})$.

At this point a small $\chi_k(r)$ field is considered in the free energy (3.9) such that the quartic terms of χ_k may be neglected. Since we consider $\gamma_{2,3} = 0$ we are free to set

$$\vec{\chi}(r) \equiv (0, 0, \chi(r)). \tag{3.41}$$

Thus, the $\chi(r)$ dependent part of the free energy is

$$F_\chi = \int r_\perp dr_\perp \left\{ i\chi \frac{\partial \chi}{\partial t} + \chi L_2 \chi + \mathcal{O}(\chi^4) \right\}, \tag{3.42}$$

where L_2 is given given by:

$$\begin{aligned} L_2 &= -2\gamma_1 \frac{1}{r_\perp} \frac{\partial}{\partial r_\perp} \left(r_\perp \frac{\partial}{\partial r_\perp} \right) + V(r_\perp), \\ V(r_\perp) &= 4(3\beta_2 + 2\beta_4) f^2(r_\perp) - 2\alpha. \end{aligned} \tag{3.43}$$

In this context, L_2 acts as a Schrodinger operator whose eigenvalues and eigenvectors are given by solving

$$L_2 \chi_n = \omega_n \chi_n, \text{ where } \chi(r) = \sum_n a_n \chi_n(r). \tag{3.44}$$

It can be shown that a negative eigenvalue ω_0 will exist under the condition

$$\frac{1}{2} \leq \frac{3\beta_2 + 2\beta_4}{6\beta_{12} + 2\beta_{345}} \lesssim 0.76. \tag{3.45}$$

If this condition is satisfied a non-zero $\chi(r)$ field will emerge spontaneously from the trace-only solution (3.22).

We may take this analysis one step further by considering a more general ansatz for χ_k, which satisfies the $O(2)_{A+J_z^{\rm int}}$ axial symmetry condition:

$$\vec{\chi}_A(r,\phi) = \mathrm{i}\left(\chi_1(r)\vec{\lambda}^+ + \chi_{-1}(r)\mathrm{e}^{2\mathrm{i}\phi}\vec{\lambda}^-\right). \tag{3.46}$$

The stability is determined by considering the equations of motion linearized in $\chi_\pm$

$$\begin{aligned}
\frac{\gamma_1}{r}\frac{\partial}{\partial r}\left(r\frac{\partial\chi_1}{\partial r}\right) &= ((6\beta_2+4\beta_4)f(r)^2-\alpha)\chi_1 + (6\beta_1-2\beta_4+2\beta_{35})f(r)^2\chi_{-1},\\
\frac{\gamma_1}{r}\frac{\partial}{\partial r}\left(r\frac{\partial\chi_{-1}}{\partial r}\right) &= \frac{4\chi_{-1}}{r^2} + ((6\beta_2+4\beta_4)f(r)^2-\alpha)\chi_1 + (6\beta_1-2\beta_4+2\beta_{35})f(r)^2\chi_1.
\end{aligned} \tag{3.47}$$

Considering the case far from the vortex core, a non-trivial solution to the coupled equations (3.47) exists for any β_i with the asymptotic condition

$$\chi_1(r) \simeq \chi_{-1}(r) \sim \frac{1}{r} + \mathcal{O}(r^{-3}) \tag{3.48}$$

Near the vortex core it is clear that $\chi_{-1}(r\to 0)\to 0$ due to the winding. However, the field χ_1 is not constrained at the origin by any winding and thus may develop a non-trivial value in the core. This value must be determined by solving the full equations of motion. Numerical solutions for $\chi_{\pm 1}$(r) are shown in Figure 3.6 for a typical set of β_i values.

Having demonstrated the spontaneous emergence of antisymmetric components χ_1 and χ_{-1}, we continue the analysis by considering symmetric-traceless components as perturbations on the antisymmetric solution. For this we consider the symmetric ansatz

$$S_{\mu i}(r,\phi) = s_1\lambda^+_{\{\mu}\lambda^0_{i\}} + s_0\mathrm{e}^{2\mathrm{i}\phi}\lambda^+_{\{\mu}\lambda^0_{i\}}. \tag{3.49}$$

Considering the equations of motion linearized in s_1 and s_{-1} we arrive at

$$\begin{aligned}
\frac{\gamma_1}{r}\frac{\partial}{\partial r}\left(r\frac{\partial s_1}{\partial r}\right) &= 2(\beta_5-\beta_3)\chi_1^3 + (\text{terms}\propto s_{\pm1}),\\
\frac{\gamma_1}{r}\frac{\partial}{\partial r}\left(r\frac{\partial s_{-1}}{\partial r}\right) &= 2(\beta_5-\beta_3)\chi_{-1}^3 + (\text{terms}\propto s_{\pm1}).
\end{aligned} \tag{3.50}$$

where, for our purposes, it will only be necessary to consider the first terms on the right hand side of (3.50). It is readily apparent that non-zero $\chi_{\pm}(r)$ fields act as sources for the symmetric-traceless fields $s_{\pm 1}(r)$. Numerical solutions for $s_{\pm 1}(r)$ are shown in Figure 3.7. Thus, all four off diagonal fields $\chi_{\pm 1}$ and $s_{\pm 1}$ spontaneously develop from the trace-only solution (3.22). The remaining four elements of the axial solution (numerically plotted in Figure 3.8) also arise spontaneously from (3.22) due to their couplings with the symmetric $s_{\pm 1}$ and antisymmetric $\chi_{\pm 1}$ solutions. However, these are typically small, and will have little impact on the low energy effective theory we discuss in the following sections.

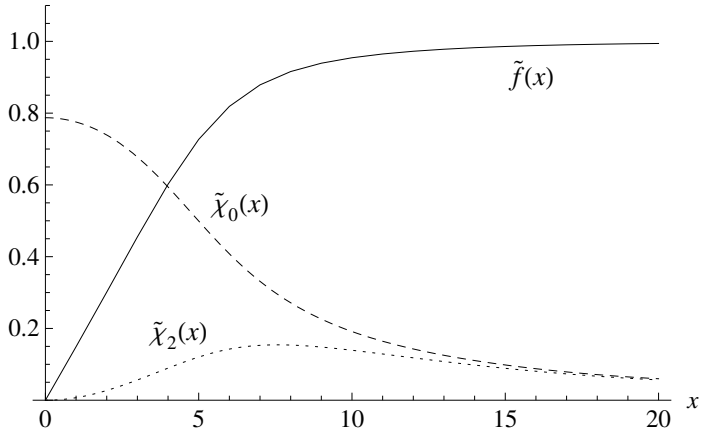

Figure 3.6: The numerical solutions for $\tilde{f}(x) = f(x)/\Delta$, $\tilde{\chi}_0(x) = \chi_0(x)/\Delta$, and $\tilde{\chi}_2(x) = \chi_2(x)/\Delta$ are plotted, where again $x \equiv r_\perp \sqrt{\alpha/\gamma_1}$. As $x \to \infty$ we have $\tilde{\chi}_0(x) \simeq \tilde{\chi}_2(x) \to c/x$, where c is a constant that must be determined by solving completely the vortex solution.

3.5 Broken symmetries and non-Abelian moduli localized on vortex

Having established the spontaneous emergence of non-trace elements of the $n = 1$ vortex order parameter we may proceed to address the effective field theory describing the gapless excitations of the vortex string. At the classical level this can be accomplished by determining the broken symmetries of a particular vortex solution. The number of broken symmetries determines the number of gapless moduli appearing in the low energy

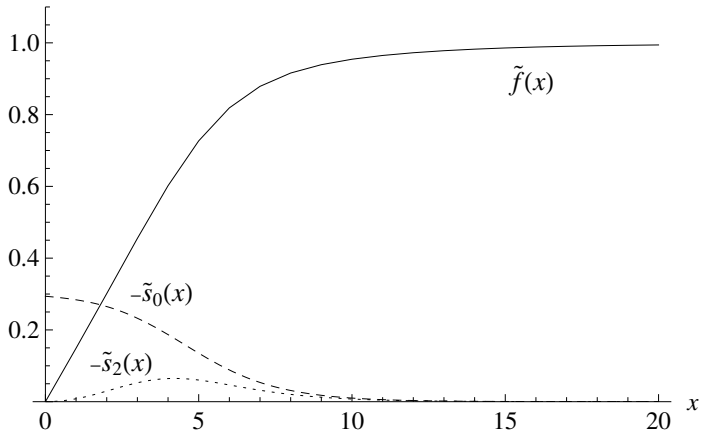

Figure 3.7: The numerical solutions for $\tilde{f}(x) = f(x)/\Delta$, $\tilde{s}_0(x) = s_0(x)/\Delta$, and $\tilde{s}_2(x) = s_2(x)/\sqrt{2}\Delta$ are plotted, where again $x \equiv r_\perp\sqrt{\alpha/\gamma_1}$.

theory. For relativistic systems this is precisely the number of quantized Goldstone modes appearing in the effective theory. However, for non-relativistic systems, the Goldstone theorem is more subtle and care must be taken to determine how many gapless modes survive the quantization procedure. In this section we will simply discuss the collective coordinates determined from symmetry considerations and determine the classical effective theory. In the following section we will consider quantization.

In section 4 we discussed that at large distances from the vortex core, the order parameter was required to be invariant under the continuous symmetry group (3.27)

$$(\mathcal{H}_B)_{n=1} = SO(3)_{J_{\rm int}} \times SO(3)_{A+L_\perp^{\rm ext}} \times T \tag{3.51}$$

The collective coordinates generating gapless modes for a particular vortex solution are determined from the broken generators of the group (3.27). In particular, all vortex lines break the translational symmetries in the xy plane resulting in two Abelian moduli generating the Kelvin excitations. Additionally, vortex solutions that break the axial $U(1)_A$ symmetry generate an additional Abelian mode. We may also consider the coordinate rotations about the x and y axes, which would naively be expected to generate two additional rotational collective coordinates. However, it is a simple matter to show that the coordinate rotations about the x and y directions are equivalent to a z-dependent translation in the $x-y$ plane. Thus, there are a total of three potential Abelian moduli arising on the vortex string. These are well studied in both condensed

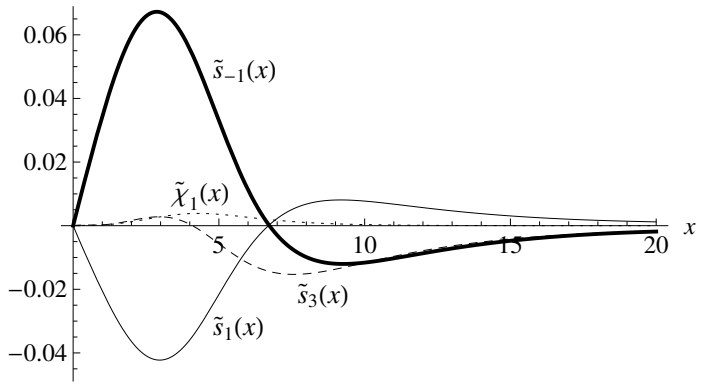

Figure 3.8: The numerical solutions for $\tilde{s}_{-1}(x) = s_{-1}(x)/\Delta$, $\tilde{s}_1(x) = s_1(x)/\Delta$, and similar definitions for the remaining functions are plotted, where again $x \equiv r_\perp \sqrt{\alpha/\gamma_1}$. These functions necessarily develop in response to the development of non-zero $\chi_{0,2}$ and $s_{0,2}$. They are however typically small for most values of β_i.

matter and high energy systems with topological vortex strings.

We are however interested in the additional non-abelian collective coordinates occurring from the breaking of the $SO(3)_{J_{\rm int}}$ symmetry in the vortex core. There will be an additional two or three collective coordinates appearing on the vortex depending on the symmetry breaking pattern of $SO(3)_{J_{\rm int}}$. If the vortex solution retains a $O(2)$ symmetry from the breaking of $SO(3)_{J_{\rm int}}$ then there will appear two modes ω_x and ω_y living on the degeneracy space

$$SO(3)_{J_{\rm int}}/U(1)_{J_z^{\rm int}} \simeq S^2. \tag{3.52}$$

An example of such a vortex solution is given by the case of an order parameter with a single real valued antisymmetric component $\vec{\chi}(r) = \chi(r)\hat{z}$ as discussed in at the beginning of the previous section.

If the vortex completely breaks $SO(3)_{J_{\rm int}}$, all three potential moduli ω_x, ω_y, and ω_z will appear in the effective theory living on the space

$$SO(3)_{J_{\rm int}}/1 \simeq S^3/Z_2. \tag{3.53}$$

The axial vortices preserving the $O(2)_{A+J_z^{\rm int}}$ symmetry are characterized by a complete breaking of $SO(3)_{J_{\rm int}}$. However, due to the preserved $O(2)_{A+J_z^{\rm int}}$ symmetry only two of the moduli from the broken $SO(3)_{J_{\rm int}}$ will be independent of the axial modulus δ

from $O(2)_A$. Table 1 summarizes the degeneracy space and associated moduli fields developing on particular vortex solutions.

Table 3.1: A summary of degeneracy space and associated moduli for the vortex solutions when $\gamma_2, \gamma_3 = 0$ considered in the previous section is shown. The first column indicates the core type solution. Columns 2-5 indicate the moduli fields emerging in the various solutions. The degeneracy spaces in the sixth column are denoted with subscripts indicating the group associated with the degeneracy. Additionally, we have defined $J_{\rm int} \equiv S + L_{\rm int}$. The last column shows the total number of emerging moduli. We have also indicated the equivalence of ω_z and δ moduli in the A-phase core vortex.

Core Type	$\vec{\xi}_\perp$	$\omega_{x,y}$	ω_z	δ	Degeneracy	# moduli
$\vec{\chi} = 0,\ f = f(r)$	✓	×	×	×	S^2_t	2
$\vec{\chi} = 0,\ f = f(x,y)$	✓	×	×	×	$S_A \times S^2_t$	3
$\vec{\chi} = \chi_z(r_\perp)\hat{z} \in \mathbb{R}^3$	✓	✓	×	✓	$S^2_{J_{\rm int}} \times S^1_A \times S^2_t$	5
Preserved $O(2)_{A+J^{\rm int}_z}$	✓	✓	1/2	1/2	$S^2_{J_{\rm int}+A} \times S^1_{J^{\rm int}_z+A_z}$	5
Broken $O(2)_{A+J^{\rm int}_z}$	✓	✓	✓	✓	$\left(S^3/\mathbb{Z}_2\right)_{J^{\rm int}} \times S^1_A \times S^2_t$	6

For the case of axially asymmetric vortices the group $O(2)_A \times SO(3)_{J_{\rm int}}$ is completely broken, and thus all four moduli from the internal space will appear independently in the classical effective theory. Physical examples include the double core vortex in superfluid ^{3}He-B. We will avoid further discussion of the axially asymmetric solutions of this form here.

We may this analysis to the case of small but non-zero $\gamma_{2,3}$. It is readily seen from (3.9) that the associated gradient terms no longer have the separate $SO(3)_{L_{\rm int}} \times SO(3)_{L_{\rm ext}}$ from the internal and external rotations. Instead the gradient terms preserve only the complete orbital rotations $SO(3)_{L^{\rm ext}+L^{\rm int}}$, which we will simply refer to as $SO(3)_L$ for the moment. Thus due to the equivalence of coordinate rotations about the x and y axes to translations in the xy-plane we will find that only the translational moduli $\xi_{x,y}$ and the axial $O(2)_A$ modulus δ will be independent. The collective coordinates from the remaining generators will develop a mass gap proportional to γ_{23}. In addition interactions between $\omega_{x,y}$, and $\xi_{x,y}$ will appear illustrating the equivalence of coordinate

rotations and translations.

3.6 Low energy effective field theory of gapless excitations

After demonstrating the existence of vortex solutions that spontaneously break the non-Abelian symmetry $SO(3)_{S+L}$ in the vortex core, we may write down the effective low energy theory of the gapless excitations arising from the broken symmetries. In this section we will summarize the general procedure for determining this low energy theory by considering perturbations of the vortex line. We will find that at least classically, the combinations of perturbations corresponding to the broken generators will contain no mass gap. Upon quantization we will observe the number of gapless modes emerging from the classical collective coordinates. In the following section we will consider the specific solutions from the previous section and use the procedure discussed here to determine the quantized low energy theory of the gapless excitations.

We begin by considering fluctuations of the vortex line given by

$$e_{\mu i}(\vec{x}_\perp) = e_{\mu i}^{\text{vort}}(\vec{x}_\perp) + \delta e_{\mu i}(x, y, z, t). \tag{3.54}$$

Inserting (3.54) into the free energy (3.9) and expanding to second order in $\delta e_{\mu i}$, we obtain upon integrating by parts in the spatial gradients

$$\begin{aligned} \delta^2 F_{\text{GL}} &= i\delta e_{\mu i}\partial_t \delta e^\star_{\mu i} + \delta e_{\mu i} L_{ij,\mu\nu}\delta e^\star_{\nu j}, \\ L_{ij,\mu\nu} &= -\gamma_1 \delta_{ij}\delta_{\mu\nu}\vec{\partial}^2 - \gamma_{23}\delta_{\mu\nu}\partial_i\partial_j + (\partial_{e^\star_{\mu i}}\partial_{e_{\nu j}} V), \end{aligned} \tag{3.55}$$

where we have consolidated the spatial gradient and potential terms into the operator $L_{ij,\mu\nu}$. For non-zero $\gamma_{2,3}$, we will have an additional term $\gamma_{23}\delta_{\mu\nu}\partial_i\partial_j$ appearing in $L_{ij,\mu\nu}$. Unless we specify otherwise, we will remain in the $\gamma_{2,3} = 0$ regime. At this point, we consider an adiabatic mode expansion for $\delta e_{\mu i}(\vec{x}_\perp, z, t)$

$$\delta e_{\mu i}(\vec{x}_\perp, z, t) = \sum_n c_n(t, z) e_{\mu i}^{(n)}(\vec{x}_\perp), \tag{3.56}$$

where the functions $e_{\mu i}^{(n)}(\vec{x}_\perp)$ are eigenfunctions of $L_{ij,\mu\nu}$:

$$L_{ij}(\vec{x}_\perp) e_{\mu j}^{(n)}(\vec{x}_\perp) = E^{(n)} e_{\mu i}^{(n)}(\vec{x}_\perp). \tag{3.57}$$

In the low energy approximation, we may restrict the expansion (3.56) to eigenfunctions $e^{(n)}_{\mu i}(\vec{x}_\perp)$, for which $E^{(n)}$ is small compared to the free energy density of the unperturbed vortex solution.

For the current problem, we are specifically interested in the zero-modes where $E^{(n)} = 0$. These modes are generated by the non-trivial symmetry transformations of $e^{\rm vort}_{\mu i}(\vec{x}_\perp)$ that leave free energy invariant. For each broken generator, we parameterize the associated transformation of the vortex solution by a collective coordinate m^a, and consider the family of equivalent vortex solutions $e^{\rm vort}_{\mu i}(\vec{x}_\perp, m^a)$. We define the ground state solution as $e^{\rm vort}_{\mu i}(\vec{x}_\perp, 0) \equiv e^{\rm vort}_{\mu i}(\vec{x}_\perp)$. The gapless fluctuations are thus generated by the collective coordinate fields m^a varying in space and time. Specifically, for the adiabatic approximation where $m^a = m^a(z,t)$, the gapless fluctuations are given by

$$\delta e_{\mu i}(x,y,z,t) = \sum_a m^a(t,z) \frac{\partial}{\partial m^a} e^{\rm vort}_{\mu i}(x,y,m). \tag{3.58}$$

Inserting (3.58) into (3.55), and integrating over $\vec{x}_\perp$, we arrive at a low energy effective field theory of gapless excitations localized on the mass vortex. If the fluctuations we consider are strictly gapless, we will find the free energy can be written as

$$\begin{aligned} F_{\rm eff} &= iG^t_{ab}(m) m^a \partial_t m^b + G^z_{ab}(m) \partial_z m^a \partial_z m^b, \\ G^{t,z}_{ab}(m) &= \int d^2\vec{x}_\perp \frac{\partial e^{\rm vort}_{\mu i}(\vec{x}_\perp, m)}{\partial m^a} \frac{\partial e^{{\rm vort}\star}_{\nu j}(\vec{x}_\perp, m)}{\partial m^b}, \end{aligned} \tag{3.59}$$

where G_{ab} is a function of the fields m^a. We hasten to point out that the functions $G^{t,z}_{ab}(m)$ in (3.59) are symbolic in the sense that their particular form depends on how the indices i, j, μ, and ν are paired.

The second term of $F_{\rm eff}$ in (3.59) describes the energy expense from fluctuations of the collective coordinates from the broken generators. To study the classical theory, this is all that is required. The first term is the dynamical term, which must be considered to determine the number of independent gapless modes emerging from the Goldstone fields. For Lorentz invariant systems, the corresponding dynamical term (which would include two time derivatives) would show that the number of quantized gapless modes is precisely given by the number of broken generators. However, for a non-relativistic system, the Goldstone theorem is more subtle. The simplest example of a non-relativistic system includes two collective coordinate fields (such as the translational collective

coordinates) m_1 and m_2 where $G_{ab} \propto \varepsilon_{ab}$. In this case, the time dependent part of the free energy assumes the form

$$F_t = \text{constant} \times (m_1 \dot{m}_2 - m_2 \dot{m}_1). \tag{3.60}$$

In this case, the collective coordinates are the conjugate momenta of each other. Thus, they form a single Goldstone mode with quadratic dispersion. Goldstone modes with quadratic dispersion are referred to as type II modes, as opposed to type I Goldstone modes that have linear dispersion. Typically, type I modes derive from a single collective coordinate, whereas type II modes result from conjugate pairing of two collective coordinates. There are some subtle exceptions to this rule (see [35]), however, we will not need to consider them here.

On the other hand, if $G^t_{ab} \propto \delta_{ab}$, the diagonal terms proportional to $m_a \dot{m}_a$ in the effective free energy are total derivatives at quadratic order, and are non-dynamical. In such cases where $F^t \propto m_a \dot{m}_a$, amore careful consideration of the interactions of m_a with non-zero modes is required. Typically, this results in an effective theory of relativistic type I Goldstone modes with linear dispersion. These modes are known as Bogoliubov modes. Both type I and II Goldstone modes appear in the effective theories of the gapless excitations on mass vortices.

We hasten to point out that the Bogoliubov modes we discuss cannot always be considered as low energy excitations, since their dispersion relations depend on their interaction with non-zero (gapped) modes. If the gap parameter associated with the non-zero mode is high, the propagation velocity of the Bogoliubov mode will be large, and the excitation will disappear from the spectrum. In what follows below, we will assume that the non-zero modes have a small enough gap for the associated Bogoliubov mode to be considered in the low energy spectrum.

In the axially $O(2)_{A+J_z^{\text{int}}}$ symmetric cases considered in the next section, we will find that the classical low energy theory predicts the existence of two separate translational collective coordinates, as well as three collective coordinates from the internal symmetry breaking $SO(3)_{J_{\text{int}}} \times O(2)_A \to O(2)_{A+J_z^{\text{int}}}$. However, the quantized theory will show only one type II translational mode, one $O(2)$ Abelian type I mode, and one non-Abelian type II mode. The reduction of two translational collective coordinates to one quantized mode is of course well understood from the study of Kelvin excitations of vortices, and

follows from the general result (3.60). The $O(2)$ mode will follow from the breaking of the axial $O(2)_A$ symmetry. The remaining two independent collective coordinates $\omega_{x,y}$ will form a single quantized type II non-Abelian zero mode. For an axially asymmetric vortex that completely breaks the $SO(3)_{J_{\rm int}} \times O(2)_A$, an additional zero mode from $O(2)_{J_z^{\rm int}}$ would appear.

Before proceeding to a detailed discussion of axially symmetric vortex excitations, we wish to illustrate this method in detail by applying it to the case of a vortex with real vector $\vec{\chi} = \chi(r)\hat{z}$ and $S_{\mu i} \equiv 0$, considered in the previous section. This ansatz is not axially $O(2)_{A+J_z^{\rm int}}$ symmetric, so we do not make any initial claims about the number and type of quantized zero modes in this case. Applying general translations, rotations, and $O(2)_A$ transformations the collective coordinates appear in

$$\begin{aligned} &e_{\mu i}(\vec{x}_\perp) \to e_{\mu i}(\vec{x}_\perp - \vec{\xi}_\perp), \;\; \xi \in t \\ &\chi^i(r_\perp) \to R_{ij}(\vec{\omega})\chi^j(r_\perp), \;\; R_{ij} \in SO(3)_{S+L} \\ &\chi^i(r_\perp) \to e^{i\delta}\chi^i(r_\perp), \;\; e^{i\delta} \in U(1)_A, \end{aligned} \tag{3.61}$$

where $\vec{\xi}_\perp$, $\vec{\omega}$, and δ are functions of z and t. Additionally, it will be particularly convenient to consider the rotational moduli in the form

$$\chi^i = R_{ij}(\vec{\omega})\chi^j \equiv S^i(t,z)\chi(r_\perp), \;\; |S|^2 = 1, \tag{3.62}$$

and consider the real collective coordinates $\vec{S}(t,z)$ instead of $\vec{\omega}(t,z)$.

Inserting this solution into (3.9) and integrating over x and y we arrive at the following low energy theory

$$\begin{aligned} F_{\rm eff} &= F_{\rm trans} + F_{O(3)} + F_{U(1)}, \\ F_{\rm trans} &= \frac{T_1}{2}\epsilon_{ab}\xi_a\partial_t\xi_b + \frac{T_2}{2}\partial_z\vec{\xi}_\perp \cdot \partial_z\vec{\xi}_\perp, \\ F_{O(3)} &= \frac{1}{2g^2}\partial_z\vec{S}\cdot\partial_z\vec{S}, \; |S|^2 \equiv 1, \\ F_{U(1)} &= \frac{1}{2g^2}\partial_z\delta\partial_z\delta, \end{aligned} \tag{3.63}$$

where ϵ_{ab} is the 2×2 antisymmetric matrix. The couplings $T_{1,2}$ and g^2 are determined

from the integration over $\vec{x}_\perp$:

$$\frac{T_{1,2}}{2} \sim \int d^2\vec{x}_\perp 3\gamma_1 \frac{f^2}{r_\perp^2} \to \gamma_1 \Delta^2 \log\left(\frac{\alpha R^2}{\gamma_1}\right),$$
$$\frac{1}{g^2} \sim \int d^2\vec{x}_\perp \gamma_1 \chi^2 \to \frac{\gamma_1^2}{2\beta_{12}+\beta_{345}}, \tag{3.64}$$

The low energy theory derived here shows the emergence of an $O(3)$ sigma model analogous to the low energy theory of gapless excitations of ANO strings in Yang-Mills theories. For comparison see [45]. Classically, the low energy theory contains five collective coordinates from $\xi_{x,y}$, $S_{1,2}$, and δ.

The $O(2)_A$ collective coordinate δ appears in (3.63) with a time derivative term at quadratic order. This term follows from the fluctuations of the magnitude of the χ field in the vortex core. Considering these fluctuations $\chi(x,y) \to \chi(x,y) + h(x,y,z,t)$ to quadratic order in h in the free energy, we arrive at a term linear in h of the form

$$F \supset 2\chi(r) h \dot{\delta}. \tag{3.65}$$

Integrating out the massive field h, and performing the integrations over the perpendicular coordinates (x,y), we arrive at the quadratic time derivative term for δ in (3.63). We note that the $F_{O(3)}$ part of (3.63) contains no time derivative terms, since these terms only appear as total derivatives (to quadratic order in $\vec{S}$). Thus, they do not contribute to the low energy effective theory. Naively, it might be expected that the coupling of $\vec{S}$ to non-zero modes would produce quadratic time derivative terms of the form $\dot{S}_i \dot{S}_j$ in the effective free energy similar to the case of δ. However, a careful analysis shows that this is not the case. Instead, when we consider fluctuations of the form $\chi_i \chi(r) S_i(z,t) + h_i(z,t)$, the fluctuating non-zero modes h_i coupling to S_i appear in the effective theory as

$$F_{h_i} \supset 2\mathrm{i}\chi(r)\left(S_i \partial_t h_i + h_i \partial_t S_i\right) + \mathcal{O}(h_i^2), \tag{3.66}$$

which is a total derivative at linear order in h_i. Thus, it cannot contribute to the dynamical degrees of freedom. This result follows from the requirement of time reversal symmetry. If we relax the constraint that $\vec{}$ be a real vector, then we may consider complex fluctuations $h_i \in \mathbb{C}^3$. In this case, the time derivative terms of S_i will no longer be total derivatives. Thus, two propagating non-Abelian modes may appear as

Bogoliubov modes in form

$$F_{\dot{S}_i} = \frac{1}{2g_s^2\gamma_1}\partial_t\vec{S}\cdot\partial_t\vec{S},$$
$$\frac{1}{g_s^2} \sim \frac{\gamma_1^2}{2\beta_2 - 2\beta_1 + \beta_4}. \tag{3.67}$$

Summarizing the analysis, the quantized effective theory (3.63) describes the propagation of a translational Kelvin mode with quadratic dispersion and an axial $O(2)_A$ mode δ with linear dispersion. These appear along with potentially two additional non-Abelian Bogoliubov modes from (3.67). The non-Abelian modes follow from the tensorial nature of the order parameter.

The results of the previous analysis were determined for a Ginzburg-Landau free energy with a separate internal and external orbital rotation symmetry $SO(3)_{L_{\text{int}}} \times SO(3)_{L_{\text{ext}}}$. It is interesting to observe the effects of a non-zero $\gamma_{2,3}$ on the low energy effective field theory, where only the traditional orbital $SO(3)_L$ symmetry exists in the Ginzburg-Landau free energy. We will assume that γ_{23} is small enough that we may neglect the corrections to the vortex solutions of $f(r)$ and $\chi(r)$, and the constants $T_{1,2}$ and $g_{1,2}^2$. Aside from these uninteresting numerical corrections, the individual terms in (3.64) remain of the same form. However, there are additional terms representing the explicit breaking of the $SO(3)_{J_{\text{int}}} \times SO(3)_{L_{\text{ext}}} \to SO(3)_L$ symmetries. They appear as follows:

$$F_{\text{eff}} \to F_{\text{eff}} - \Delta F_{\text{eff}}, \tag{3.68}$$

where ΔF_{eff} represents symmetry breaking terms. In this case, they are given by

$$\Delta F_{\text{eff}} = M^2\left(\vec{S}_\perp - S^3\partial_z\vec{\xi}_\perp\right)^2 + \frac{\varepsilon}{2g^2}\left\{(S^3\partial_z\delta)^2 + (\delta_z S^3)^2\right\}. \tag{3.69}$$

Here $\varepsilon \sim \gamma_{23}/\gamma_1$, M represents a mass gap parameter given by

$$M^2 \sim \int d^2\vec{x}_\perp \gamma_{23}\left(\partial_\perp\chi\right)^2 \to \frac{\gamma_{23}\alpha}{2(2\beta_{12} + \beta_{345})}. \tag{3.70}$$

In this form, M is known as the twisted mass [52, 53].

For the case that $M^2 > 0$, the free energy will be minimized at $\vec{S}_\perp = 0$. Thus, both fields $S_{1,2}$ will no longer be gapless. If $M^2 < 0$, $|\vec{S}_\perp| = 1$, so the effective theory will retain one non-Abelian collective coordinate. In both cases, the Kelvin and axial $O(2)_A$ modes will remain gapless.

3.7 Gapless modes of axially symmetric vortices

At this point, we may consider the low energy excitations of the $O(2)_{A+J_z^{\rm int}}$ axially symmetric vortices. As mentioned in the previous sections, in the case that $\gamma_{23} = 0$ we expect to observe five collective coordinates for the classical theory. Following the quantization, these collective coordinates will be reduced to one translational and one axial $O(2)_A$ zero mode, along with additional non-Abelian zero modes.

We proceed by writing the axial vortex solution in the $\hat{Q}, \hat{S}_z, \hat{L}_z^{\rm int}$ eigenbasis, and performing translational, rotational, and $O(2)_A$ transformations

$$e_{\mu i} = \sum_{\rho,\nu} C_{\rho\nu}(r_\perp)\lambda_\mu^\rho \lambda_i^\nu e^{i(1-\rho-\nu)\phi} \to \sum_{\rho,\nu} C_{\rho\nu}(r'_\perp)\lambda_\mu^\rho(\vec{\omega})\lambda_i^\nu(\vec{\omega}) e^{i(1-\rho-\nu)\phi'} e^{i(\rho+\nu)\delta},$$
$$\lambda_a^\rho(\vec{\omega}) = R_{ab}(\vec{\omega})\lambda_b^\rho, \tag{3.71}$$

where $(r'_\perp, \phi')$ are the new coordinates generated by the translations $\vec{\xi}_\perp(z,t)$, and $R_{ab}(\vec{\omega})$ is a $SO(3)_{J_{\rm int}}$ rotation given as a function of the moduli $\vec{\omega}(z,t)$. Henceforth, λ_a^ρ will refer to the $\vec{\omega}$-dependent $\lambda_a^\rho(\vec{\omega})$. Additionally, the $O(2)_A$ modulus δ is a function of z and t. Decomposing (3.71) into the trace, antisymmetric, and symmetric parts and converting to the $(J^{\rm int}, J_z^{\rm int})$-basis, we find

$$\begin{aligned} e_{\mu i}(r_\perp,\phi,z,t) = {} & f e^{i\phi}\delta_{\mu i} + \chi_0 \lambda^+_{[\mu}\lambda^0_{i]} e^{i\delta} + \chi_1 e^{i\phi}\lambda^+_{[\mu}\lambda^-_{i]} + \chi_2 e^{2i\phi}\lambda^-_{[\mu}\lambda^0_{i]} e^{-i\delta} \\ & + s_{-1} e^{-i\phi}\lambda^+_{\{\mu}\lambda^+_{i\}} e^{2i\delta} + s_0 \lambda^+_{\{\mu}\lambda^0_{i\}} e^{i\delta} + s_1 e^{i\phi}\left(\lambda^+_{\{\mu}\lambda^-_{i\}} - 2\lambda^0_\mu\lambda^0_i\right) \\ & + s_2 e^{2i\phi}\lambda^-_{\{\mu}\lambda^0_{i\}} e^{-i\delta} + s_3 e^{3i\phi}\lambda^-_{\{\mu}\lambda^-_{i\}} e^{-2i\delta}. \end{aligned} \tag{3.72}$$

We neglect $s_{\pm 2,0}$ and χ_0 in (3.72). These components are typically much smaller than f, $\chi_{\pm 1}$ and $s_{\pm 1}$, and contribute only small corrections to the low energy effective theory. Additionally, these contributions will not affect the number of quantized modes appearing in the theory.

Proceeding with these assumptions, and the requirement that $\gamma_{23} = 0$ we may apply the methods of the previous section to arrive at the following low energy effective theory:

$$\begin{aligned} F_{\rm eff} = {} & \frac{T_1}{2}\varepsilon_{ab}\xi_a\partial_t\xi_b + \frac{T_2}{2}\partial_z\vec{\xi}\cdot\partial_z\vec{\xi} + \frac{\mathrm{i}}{2g_1^2}\vec{\lambda}^+\cdot\partial_t\vec{\lambda}^- + \frac{1}{2g_2^2}|\vec{\lambda}^-\cdot(\partial_t\vec{\lambda}^+ + \mathrm{i}\vec{\lambda}^+\partial_t\delta)|^2 \\ & + \frac{1}{2g_3^2}|\partial_z\vec{\lambda}^+ + i\vec{\lambda}^+\partial_z\delta|^2 - \frac{1}{2g_4^2}|\vec{\lambda}^-\cdot(\partial_z\vec{\lambda}^+ + i\vec{\lambda}^+\partial_z\delta)|^2, \end{aligned} \tag{3.73}$$

where again ϵ_{ab} is the 2×2 antisymmetric symbol and $T_{1,2}$ and $1/2g^2_{1,2,3}$ are given by

$$\begin{aligned}
\frac{T_{1,2}}{2} &\sim \int d^2\vec{x}_\perp 3\gamma_1 \frac{f^2}{r_\perp^2} \to \gamma_1 \Delta^2 \log\left(\frac{\alpha R^2}{\gamma_1}\right), \\
\frac{1}{g^2_{1,3}} &\sim \int d^2\vec{x}_\perp \gamma_1 \left(\chi_1^2 + \chi_{-1}^2 + s_1^2 + s_{-1}^2\right) \to \frac{\gamma_1^2}{\alpha}\Delta^2 \log\left(\frac{\alpha R^2}{\gamma_1}\right), \\
\frac{1}{g_2^2} &\sim \int d^2\vec{x}_\perp \gamma_1 \left(\chi_1^2 - \chi_{-1}^2 + s_1^2 - s_{-1}^2\right) \to \frac{\gamma_1^2}{4\beta_2 + 2\beta_4 + \beta_{35}}, \\
\frac{1}{g_4^2} &\sim \int d^2\vec{x}_\perp \gamma_1 \left(s_1^2 + s_{-1}^2\right) \to \frac{\gamma_1^2}{4\beta_2 + 2\beta_4 + \beta_{35}}.
\end{aligned} \tag{3.74}$$

The interesting features to point out from (3.73) include the last two lines showing the $O(2)_{A+J_z}$ symmetry respected by the vortices. Thus, as expected there are only five independent collective coordinates from the broken translational and internal non-Abelian generators. Additionally, the expected single Kelvin mode emerging from the dynamical term has appeared just as in the previous examples.

The first term in the second line, which describes the time dependence of the non-Abelian zero modes, is new. In the limit of small oscillations, we may consider rotations to the first order in $\vec{\omega}(z,t)$, and consider

$$\lambda_i^\rho(\vec{\omega}) = R_{ij}(\vec{\omega})(\lambda_0)_j^\rho \simeq (\lambda_0)_i^\rho - \omega_j \epsilon_{ijk}(\lambda_0)_k^\rho. \tag{3.75}$$

This gives the following result for the time dependent term

$$\mathrm{i}\vec{\lambda}^+ \cdot \partial\vec{\lambda}^- \simeq \omega_x\dot{\omega}_y - \omega_y\dot{\omega}_x. \tag{3.76}$$

Thus, we see that only one independent mode emerges from the collective coordinates after quantization, since the fields $\omega_{x,y}$ are the conjugate momenta of each other. This mode is a type II Goldstone mode with quadratic dispersion relation. Additionally, the second term in the second line of (3.73) also includes a term quadratic in the time derivative of δ. This implies that the $O(2)_A$ Bogoliubov mode appears due to the coupling of δ with the massive oscillations of $\chi_{\pm 1}$ and $s_{\pm 1}$, as in the previous section. After integrating out these oscillations, we arrive at the corresponding term in (3.73). It is clear that this term also preserves the $O(2)_{A+J_z^{\mathrm{int}}}$ symmetry.

For completeness we consider the additional gradient terms in the free energy (3.9) when $\gamma_{23} \neq 0$. For the purposes of illustration we will omit the contributing terms

from $s_{\pm 1}(r)$, since they are notationally complex but do not introduce any additional interesting effects. As before, we assume that the γ_{23} corrections have negligible effect on the functions $f(r)$ and $\chi_{\pm 1}(r)$. Thus we find the following additional terms to $F_{\text{eff}} \to F_{\text{eff}} - \Delta F_{\text{eff}}$:

$$\begin{aligned}\Delta F_{\text{eff}} \supset & M^2 |\vec{\lambda}_\perp^+ - \lambda_3^+ \partial_z \vec{\xi}_\perp|^2 + \left\{ M_{ab}^2 \left(\lambda_a^+ - \partial_z \xi_a \lambda_3^+\right)\left(\lambda_b^+ - \partial_z \xi_b \lambda_3^+\right) e^{2i\delta} + \text{h.c.} \right\} \\ & + \frac{\varepsilon}{2g^2} |\partial_z \lambda_3^+ + i\lambda_3^+ \partial_z \delta|^2, \end{aligned} \tag{3.77}$$

where $\varepsilon = \gamma_{23}/\gamma_1$. We also have

$$M^2 \sim \int d^2\vec{x}_\perp \gamma_{23} (\partial_\perp \chi_{\pm 1})^2 \to \gamma_{23} \Delta^2 \times C(\beta_i), \tag{3.78}$$

where $C(\beta_i)$ is a constant determined by the β_i parameters. M_{ab}^2 represents a symmetric mass matrix illustrating the crossing factors between χ_1 and χ_{-1}:

$$M_{ab} = \int d^2\vec{x}_\perp \gamma_{23} \partial_a \chi_1 \partial_b (\chi_{-1} e^{-2i\phi}). \tag{3.79}$$

The emerging mass terms in (3.77) are again the result of the breaking of $SO(3)_{L_{\text{int}}} \times SO(3)_{L_{\text{ext}}} \to SO(3)_L$ for non-zero $\gamma_{2,3}$. Thus, only a certain combination of the internal rotational collective coordinates $\vec{\lambda}_\perp^+$ and the translational $\vec{\xi}_\perp$ coordinates remain massless. Additionally, only the quantized mode associated with this combination will be strictly gapless. Thus, we have a total of two gapless excitations, since the gapless mode associated with the axial $O(2)_A$ symmetry is not broken by these additional terms. The non-Abelian mode becomes quasi-gapless.

Although, we will not consider the axial $O(2)_{A+J_z^{\text{int}}}$ asymmetric case in detail here (see [63] for a detailed discussion), we will make a few brief remarks on the number and type of zero modes of the vortex. The most important change that is observed is that the collective coordinates ω_z and δ are no longer equivalent. Thus, the single mode for the axial symmetric case will divide into two type I Goldstone modes with linear dispersion for the axial asymmetric case. The other collective coordinates remain the same. Thus, a total of four zero modes exist for the axially asymmetric vortex. Again, when a small but non-zero $\gamma_{2,3}$ exists, the non-Abelian mode from $\omega_{x,y}$ coordinate will become quasigapless. Table 2 summarizes the number and type of modes emerging for the various core types.

Table 3.2: A summary of the type and number of quantized modes appearing on the vortex when $\gamma_{2,3} = 0$ is shown. For each core type, the particular collective coordinates appearing on the vortex string are listed. Additionally, whether the specific collective coordinate results in a type I or II mode after quantization is indicated. A star (*) indicates that the mode only exists if $\gamma_{2,3} = 0$ and receives a mass gap if $\gamma_{2,3} \neq 0$. We have also indicated the equivalence of ω_z and δ modes for the preserved $O(2)_{A+J_z^{\rm int}}$ core.

Core Type	$\vec{\xi}_\perp$	$\omega_{x,y}$	ω_z	δ	# modes ($\gamma_{2,3} = 0$)	# modes ($\gamma_{2,3} \neq 0$)
$\vec{\chi} = 0$, $f = f(r)$	II	$\times$	$\times$	$\times$	1	1
$\vec{\chi} = 0$, $f = f(x, y)$	II	$\times$	$\times$	I	2	2
$\vec{\chi} = \chi_z(r_\perp)\hat{z} \in \mathbb{R}^3$	II	$\times$	$\times$	I	2	2
$\vec{\chi} = \chi_z(r_\perp)\hat{z} \in \mathbb{C}^3$	II	I*	$\times$	I	4	2
Preserved $O(2)_{A+J_z^{\rm int}}$	II	II*	1/2	1/2	3	2
Broken $O(2)_{A+J_z^{\rm int}}$	II	II*	I	I	4	3

3.8 Conclusions

In this work, we have extended the analysis of the previous chapter to include a description of gapless excitations of axially symmetric vortices. This was demonstrated for systems with a Ginzburg-Landau free energy with symmetry $G = U(1)_P \times SO(3)_S \times SO(3)_{L_{\rm int}} \times SO(3)_{L_{\rm ext}}$ that is spontaneously broken to the spin-orbit locked $SO(3)_{S+L_{\rm int}}$ vacuum. We have shown that the classical low energy theory includes the translational collective coordinates presenting the well studied Kelvin excitations (see [15, 16, 17, 18, 19, 20, 21, 55]). In addition, the theory contains three additional collective coordinates from the breaking of the non-Abelian $O(2)_A \times SO(3)_{J_{\rm int}}$ to the locked orbital-phase $O(2)_{A+J_z^{\rm int}}$ group. These results have been developed using standard techniques of high energy physics to determine the classical low energy theory.

Additionally, we have introduced the time dependent part of the Ginzburg-Landau free energy to facilitate the discussion of quantization of the gapless excitations. In particular, we have discussed the number of gapless excitations emerging from the classical

collective coordinates, determined from the broken symmetry generators. In the present context, the procedure of determining the gapless Goldstone modes is somewhat subtle due to the non-Lorentz invariance of the action [34, 36, 21]. Specifically, we have shown that out of the five collective coordinates emerging from the broken symmetry, only three appear as independent Goldstone modes after quantization. Two of these are the type II Kelvin mode and the type I axial $O(2)_A$ mode, which have been well studied both experimentally and theoretically [15, 16, 17, 18, 19, 20, 21]. The additional mode is the type II internal non-Abelian mode resulting from the breaking of $SO(3)_{J_{\rm int}}$ by the vortex line.

Additionally, upon introduction of small but non-zero γ_{23} terms in the free energy (3.9) the translational and rotational $SO(3)_{J_{\rm int}}$ collective coordinates develop additional interactions. This is due to the explicit breaking of the separate internal and external rotations $SO(3)_{L_{\rm int}} \times SO(3)_{L_{\rm ext}}$ to the rotational $SO(3)_L$. Since the external rotations of the vortex line about the x and y axes are equivalent to local translations, we see that the translational collective coordinates couple to the $SO(3)_{J_{\rm int}}$ coordinates with coefficients proportional to γ_{23} in the free energy. In addition, the new terms imply that only a particular combination of the translational and non-Abelian collective coordinates remain strictly gapless. The other two non-Abelian collective coordinates are considered quasi-gapless. This results in the usual Kelvin and $O(2)_A$ gapless modes, along with a single type II quasi-gapless non-Abelian mode after quantization.

We point out that although we have extended our analysis from the previous chapter [6] to include the effects of quantization on our classically gapless modes, we have neglected to include the effects of higher order loop corrections to the effective potential. In the context of condensed matter systems, such as superfluid ^{3}He, these corrections will have little effect on the conclusions of the present work. However, for an application of these corrections to the case of non-abelian strings, see the analysis presented in [62].

We wish to conclude by pointing out the similarities between the present discussion of the excitations of mass vortices in condensed matter systems to the excitations of ANO-like strings [46, 47] in four-dimensional Yang-Mills theories. The low energy theory describing the gapless excitations of axially symmetric vortices is analogous to the emergent $1+1$-dimensional $O(3)$ sigma model of non- Abelian modes of ANO strings in Yang-Mills theories [45]. However, in the present case, the $U(1)_P$ phase symmetry

is considered as a global symmetry, in contrast to the case of Yang-Mills ANO strings where the phase symmetry is a $U(1)$ gauge symmetry. Thus, in our case, the phase symmetry presents a collective coordinate on the low energy theory, which would not be the case for ANO-like strings in Yang-Mills theories. This collective coordinate δ leads to the $O(2)_A$ Bogoliubov mode with linear dispersion.

Chapter 4

$U(1)$ Vortices in Cholesterics

In this chapter, which was presented originally in [64], we discuss flux tubes in systems with $U(1)$ gauge, and spin-orbit locked $SO(3)_{S+L}$ symmetry. The spin-orbit locking is achieved explicitly in the Lagrangian by introducing a parity violating twist term which causes the spontaneous breaking of $SO(3)_{S+L} \to SO(2)$. Additionally, this term causes a spontaneous breaking of the translational symmetry along a particular direction. Thus, the system appears with a cholesteric vacuum under certain conditions of the parameter space. With this term, the system admits $U(1)$ topologically stable vortices with additional structure in the vortex cores. This added structure leads to additional moduli appearing in the low energy dynamics. We determine these solutions and their low energy theory.

4.1 Introduction

Both, superconductivity of the second kind, with the Abrikosov flux tubes inherent to it, and cholesteric crystals (also known as chiral nematic crystals) are among the most venerable physical discoveries which acquired multiple practical applications. Recent studies of the so-called non-Abelian flux tubes (which originally emerged in supersymmetric field theories, see e.g. [65] for a review) led us to consider models which can have both phenomena simultaneously. The ground state in such models presents a superconductor with a cholesteric structure. Topological defects of the flux tube type that are supported in these models carry (non-Abelian) moduli, i.e. gapless (or quasigapless)

excitations of rotational type. A related dynamical pattern that arises in condensed matter physics was discussed in [66].

The specific model we consider is characterized with the symmetry group

$$G = U(1)_{\text{gauge}} \times SO(3)_{S+L} \times T, \tag{4.1}$$

where $SO(3)_{S+L}$ is the spin-orbit locked symmetry group of rotations, and T is the translational group in three spatial dimensions. The spin-orbit locking is achieved with an explicit parity violating term added to the Lagrangian, that preserves only the locked subgroup $SO(3)_{S+L} \subset SO(3)_S \times SO(3)_L$. An additional feature of this term is the spontaneous breaking of the spatial translational symmetry along a particular direction when certain conditions of the parameters are met. We choose this direction as our z axis:

$$T \to T_x \times T_y. \tag{4.2}$$

Additionally, this term causes the spontaneous breaking of $SO(3)_{S+L}$. However, a particular combination of the z translations and the $SO(2)$ rotations about the z axis will be preserved by the vacuum.

The spontaneous breaking of the $U(1)$ gauge or global symmetry leading to the Abrikosov-Nielsen-Olsen flux-tubes in the vacuum is well reviewed [46, 47]. Our goal in this chapter is to discuss the response of the additional fields appearing in the model when the added parity violating term is included. As this additional term does not involve either the Higgs or the gauge vector field, the $U(1)$ charged vortices will remain topologically stable in this model. They will however acquire additional structure due to the breaking of translational symmetry in the vacuum.

When the parity violating term is small we may discuss the perturbative effect on the low energy dynamics of the vortex. It is well known that the dynamics of vortices in the $U(1)$ model without the parity violating term reduce to a $1+1$ dimensional model of excitations propagating along the vortex axis. These propagating modes follow from the translational symmetry breaking (Kelvin excitations), and other broken non-Abelian rotational symmetries which typically follow the dynamics of a sigma model (see [23, 45, 67]). In the case of a broken $SO(3)$ rotational symmetry, the additional excitation form an $CP(1)$ model on the vortex. We will see that the additional parity violating term will lift some of the $CP(1)$ degrees of freedom.

We will begin by discussing the model in general and introducing the parity violating twist term. The following section will be devoted to exploring the vacuum structure of the model and determining the conditions on the parameter space required for each vacuum to be the minimum. Section 5 will discuss the vortices and discuss the details of the numerical procedure used to obtain solutions. Section 6 will develop the low energy dynamics of the vortices. We will discuss the results and conclude in section 7.

4.2 The system

The simplest model supporting flux tubes of the Abrikosov type, with non-Abelian excitantions localized on the tube was suggested in [68] based on an extension of [44] and further studied in [23, 45, 67]. Its Lagrangian has the form

$$\begin{aligned}
\mathcal{L} &= \mathcal{L}_0 + \mathcal{L}_\chi \\
\mathcal{L}_0 &= -\frac{1}{4e^2} F_{\mu\nu}F^{\mu\nu} + |D_\mu \phi|^2 - \lambda(|\phi|^2 - v^2)^2 \\
\mathcal{L}_\chi &= \partial_t \chi_i \partial_t \chi_i - \partial_i \chi_j \partial_i \chi_j - \gamma \left[(-\mu^2 + |\phi|^2)\chi_i \chi_i + \beta(\chi_i \chi_i)^4 \right],
\end{aligned} \tag{4.3}$$

where the subscript i runs over $i = 1, 2, 3$. The field χ_i can be viewed as spin field. The covariant derivative is defined in a standard way

$$D_\mu = \partial_\mu - iA_\mu \,. \tag{4.4}$$

Under an appropriate choice of parameters the charged field ϕ is condensed in the ground state,

$$|\phi|_{\rm vac} = v \,. \tag{4.5}$$

Moreover, if $\mu < v$, the field χ is not excited in the vacuum

$$(\chi_i)_{\rm vac} = 0 \,. \tag{4.6}$$

The model obviously supports the Abrikosov flux tube. Inside the tube, the "spin" field χ_i is excited giving rise to gapless (or quasigapless) excitations of non-Abelian type, localized on the flux tube.

Now we would like to make the next step and introduce a twist term $\mathcal{L}_\varepsilon$ which violates parity through mixing of the "spin term" with angular momentum,

$$\mathcal{L} = \mathcal{L}_0 + \mathcal{L}_\chi + \mathcal{L}_\varepsilon\,, \qquad \mathcal{L}_\varepsilon = -\eta\varepsilon_{ijk}\chi_i\partial_j\chi_k\,, \tag{4.7}$$

where η is a deformation parameter. The spatial kinetic terms of χ_i including the twist $\mathcal{L}_\varepsilon$, is recognized as the FrankOseen free energy density of an isotropic chiral nematic liquid crystal [69]. Note that the twist term is linear in derivatives. If η is large enough, a vacuum expectation value of χ_i develops with a cholesteric structure. It should also be pointed out that this type of behavior has been studied in the context of superfluid ^{3}He B phase where the so called w vortices exhibit a cholesteric spiral in the core. When a collection of such vortices are coherently orientated in a rotating cryostat the spiral structure appears in the bulk superfluid [70]. The vortices we consider below will be closely related to the w vortices in superfluid ^{3}He-B.

$\mathcal{L}_\varepsilon$ also breaks the orbital rotational part of the Lorentz symmetry implying a spin-orbit locked symmetry of the full Lagrangian,

$$SO(3)_L \times SO(3)_S \to SO(3)_{S+L}. \tag{4.8}$$

The energy density derived from the Lagrangian (4.7) is

$$\begin{aligned} E &= \frac{1}{4e^2}F_{ij}F^{ij} + |D_i\phi|^2 + \lambda(|\phi|^2 - v^2)^2 + \partial_i\chi_j\partial_i\chi_j \\ &+ \eta\varepsilon_{ijk}\chi_i\partial_j\chi_k + \gamma\left[(-\mu^2 + |\phi|^2)\chi_i\chi_i + \beta(\chi_i\chi_i)^2\right]. \end{aligned} \tag{4.9}$$

Our first task is to study the vacuum (ground state) of the dynamical system described by (4.7) or (4.9).

4.3 Generalities

Assuming that all couplings of the model at hand are small in what follows we will solve static classical equations of motion (i.e. we will limit ourselves to the quasiclassical approximation). The Lagrangian (4.7) contains a number of constants: e, λ, β and γ (dimensioneless couplings) and dimensionful parameters v, μ and η. The mass of the elementary excitations of the charged field ϕ is

$$m_\phi^2 = 4\lambda v^2\,. \tag{4.10}$$

In the next sections we will rescale all quantities to appear below to make them dimensionless, for instance, distance in the direction of the flux tube axis

$$\tilde{z} = m_\phi z \,, \tag{4.11}$$

distance in the perpendicular direction

$$\rho = m_\phi \sqrt{x^2 + y^2} \,, \tag{4.12}$$

and so on. Other dimensionless parameters are

$$b = \frac{\gamma(c-1)}{4\lambda c} \,, \quad c = \frac{v^2}{\mu^2} \,, \quad a = \frac{e^2}{2\lambda} \,, \quad \tilde{\eta} = \eta/m_\phi \,. \tag{4.13}$$

The field χ_i being represented in Cartesian coordinates takes the form

$$\chi_i = \frac{\mu}{\sqrt{2\beta}} \left\{ \tilde{\chi}_x(x,y,z),\ \tilde{\chi}_y(x,y,z),\ \tilde{\chi}_z(x,y,z) \right\} . \tag{4.14}$$

The static classical equations of motion are derived by extremization of energy (4.9), in a general coordinate system they read

$$\nabla_i \left(\sqrt{-g} g^{ij} \nabla_j \chi_k \right) - \eta \epsilon_{kji} \nabla_j \chi_i - \frac{\partial V}{\partial \chi_k} = 0 \,, \tag{4.15}$$

$$D_i \left(g^{ij} \sqrt{-g} D_j \phi \right) + \sqrt{-g} \left(2\lambda \left(|\phi|^2 - v^2 \right) + \gamma g^{ij} \chi_i \chi_j \right) \phi = 0 \,, \tag{4.16}$$

$$\partial_i \left(\sqrt{-g} g^{ji} g^{kl} F_{jk} \right) - ie^2 \sqrt{-g} \left(\phi^* D^l \phi - \phi D^l \phi^* \right) = 0 \,, \tag{4.17}$$

where

$$\frac{\partial V}{\partial \chi_k} = \sqrt{-g} \gamma \left(\left(-\mu^2 + |\phi|^2 \right) + 2\beta g^{ij} \chi_i \chi_j \right) \chi_k \,, \tag{4.18}$$

and

$$\nabla_i \chi_j = \partial_i \chi_j - \Gamma^k_{ij} \chi_k \tag{4.19}$$

is the standard curved space covariant derivative.

4.4 Ground state

Inspection of $\mathcal{L}_\eta$ in the Lagrangian (4.7) – in particular, the fact that it is of the first order in derivative – prompts us that, generally speaking, in the ground state translational invariance will be spontaneously broken. One can always assume that this breaking is aligned in the z direction. Then minimization of energy argument suggests that the spin field χ_i is oriented in the x, y plane and rotates as we move in the z direction. In other words, a cholesteric structure appears in the ground state

$$\begin{aligned} \chi_i &= \chi_0\, \epsilon_i(z)\,, \qquad \chi_i = \frac{\mu}{\sqrt{2\beta}} \tilde{\chi}_0\, \epsilon_i(z)\,, \\ \vec{\epsilon}(z) &= \Big\{ \cos kz,\ \sin kz,\ 0 \Big\}\,, \end{aligned} \tag{4.20}$$

where k is a wave vector (more exactly, the wave vector is $\vec{k}$, but with our choice of the reference frame it has only the z component, $\vec{k} \to \{0,\ 0,\ k\}$). Since the coupling between the fields ϕ and χ occurs only through $\chi_i \chi_i = \chi_0^2$ we can also put

$$\phi = \phi_0\,, \qquad A_i = 0\,, \tag{4.21}$$

where ϕ_0 is a constant. Then equations of motion (4.15) - (4.17) imply

$$\begin{aligned} &\chi_0 \left(-k^2 + \eta k - \gamma((-\mu^2 + \phi_0^2) + 2\beta\chi_0^2) \right) = 0\,, \\ &\phi_0 \left(2\lambda(\phi_0^2 - v^2) + \gamma\chi_0^2 \right) = 0\,. \end{aligned} \tag{4.22}$$

First we minimize over the wavevector k and obtain

$$k = \eta/2 \tag{4.23}$$

demonstrating that the translational symmetry is unbroken only if $\eta = 0$.

For consistency with later sections of the chapter we use here the dimensionless field definitions

$$\begin{aligned} \tilde{E}_{\rm vac} &= \frac{1}{m_\phi^2 v^2} E_{\rm vac} \\ \tilde{\chi}_0 &= \frac{\sqrt{2\beta}}{\mu} \chi_0 \\ \varphi &= \frac{\phi}{v}. \end{aligned} \tag{4.24}$$

Generally speaking the system of equations (4.22) has three independent solutions,

(I)

$$(\varphi_0^2)^I = \frac{1 - \frac{b}{\beta(c-1)} - \frac{\tilde{\eta}^2}{4\beta}}{1 - \frac{bc}{\beta(c-1)}}, \quad (\tilde{\chi}_0^2)^I = (c-1)\frac{\frac{\tilde{\eta}^2}{4b} - 1}{1 - \frac{bc}{\beta(c-1)}},$$

$$\tilde{E}^I_{vac} = -\frac{(c-1)^2(\eta^2 - 4b)^2}{\beta(c-1) - bc} \tag{4.25}$$

(II)

$$(\varphi_0^2)^{II} = 1, \quad (\tilde{\chi}_0)^{II} = 0, \quad \tilde{E}^{II}_{vac} = 0, \tag{4.26}$$

(III)

$$(\varphi_0)^{III} = 0, \quad (\tilde{\chi}_0^2)^{III} = 1 + (c-1)\frac{\tilde{\eta}^2}{4b},$$

$$\tilde{E}^{III}_{vac} = \frac{16bc(c-1)\beta - ((c-1)\eta^2 + 8b)^2}{64bc(c-1)\beta}. \tag{4.27}$$

In this chapter we always assume

$$c > 1, \quad b > 0, \quad \beta > 0 \quad \text{and} \quad a > 0. \tag{4.28}$$

It will be necessary to determine which vacuum is the minimum for the given parameters in (4.28). For the moment we will make the additional assumption that

$$\beta(c-1) > bc. \tag{4.29}$$

Vacuum I represents the case where both the translational and $U(1)$ gauge symmetries are broken by the non-zero vacuum expectation values of χ_0 and ϕ_0. It is easy to show from (4.25) that this vacuum exists and is a minimum if in addition to (4.29),

$$4b < \eta^2 < 4\beta\left(1 - \frac{b}{\beta(c-1)}\right), \tag{4.30}$$

Vacuum II as given in (4.26) implies the breaking of the $U(1)$ gauge symmetry, while preserving the translational symmetry in the vacuum. When $\eta^2 < \eta^2_{\text{crit}_1} \equiv 4b$ vacuum II (4.26) is the energy minimizing solution. As η^2 crosses over $\eta^2_{\text{crit}_1}$ there is a second order phase transition from vacuum II to vacuum I.

We can also see that there is a second critical point

$$\eta^2_{\text{crit}_2} \equiv 4\beta\left(1 - \frac{b}{\beta(c-1)}\right), \tag{4.31}$$

where there is another phase transition from vacuum I to vacuum III as η^2 crosses over $\eta^2_{\text{crit}_2}$. As $\phi_0 = 0$ in vacuum III the $U(1)$ gauge symmetry is preserved. Thus, vortices with $U(1)$ topological charge do not exist in vacuum III. We will briefly discuss this case further in the sections below, however our main focus for the chapter will be on vortices in vacua I or II. Figure 4.1 illustrates the vacuum energy as a function of η.

We may also consider the condition

$$bc > \beta(c-1). \tag{4.32}$$

We can see from (4.25) that the vacuum energy of I is greater than the vacuum energy of II in all cases, and is thus never a minimizing solution. In this case we can see from (4.26) that the minimizing vacuum is II when

$$\eta^2 < \eta^2_{\text{crit}_3} = \frac{\sqrt{(c-1)bc\beta} - b}{(c-1)}. \tag{4.33}$$

Additionally, when the critical point $\eta^2_{\text{crit}_3}$ exists, there is a first order transition from vacuum II to vacuum III at that critical point. If however,

$$(c-1)c\beta < b, \tag{4.34}$$

then $\eta^2_{\text{crit}_3}$ is non-existent, and vacuum III is the only true vacuum for all η^2. The vacuum energy for the case $bc > \beta(c-1)$ is shown in Figure 4.2.

Corresponding to the breaking of translational invariance in the vacuum I there exists a Goldstone mode related to spatially dependent phase shifts of the cholesteric structure. In general, the cholesteric phase breaks all four of the generators of the global translational and rotational generators p_z and $\vec{J}$ while still preserving the linear combination kJ_zp_z . Thus, we expect a Goldstone mode associated to the broken translational symmetry in the z direction. Namely if

$$\vec{\epsilon}(z) \to \vec{\epsilon}(x,y,z) = \big\{ \cos\left(kz + u(x,y,z)\right),\ \sin\left(kz + u(x,y,z)\right),\ 0 \big\}, \tag{4.35}$$

is inserted into (3) in which $k = \eta/2$ one finds that

$$E = E_{vac} + \frac{\chi_0^2\eta^2}{4}(\nabla_i\xi)^2, \tag{4.36}$$

where $i = (x,y,z)$. Of course the translation (33) is equivalent to a rotation of ϵ_i about the z axis by an angle $\vartheta = k\xi$, showing the preserved kJ_zp_z symmetry of the cholesteric vacuum.

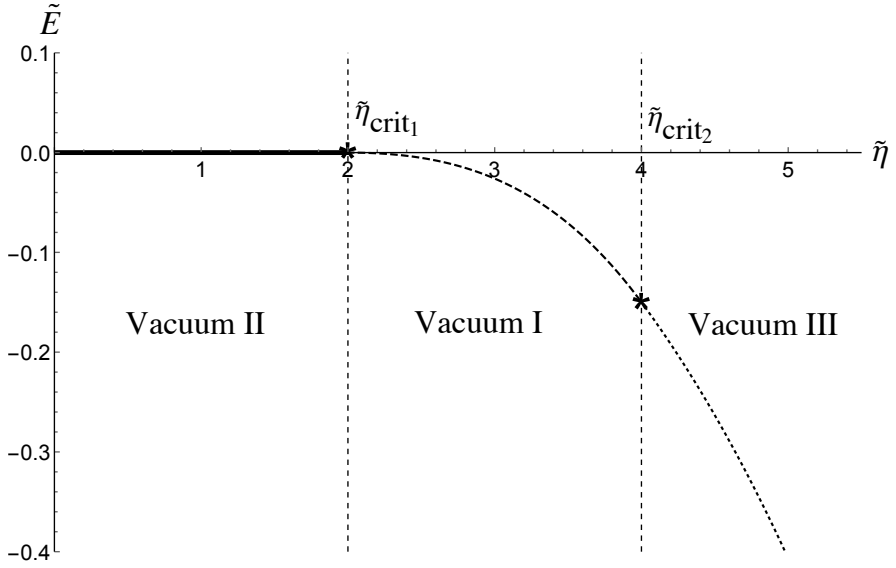

Figure 4.1: $b = 1,\ c = 1.25,\ \beta = 8$. Vacuum energy dependence on $\tilde{\eta}$ for $\beta(c-1) > bc$, the solid line corresponds to vacuum II, the dashed line to vacuum I and the dotted line to vacuum III.

Since there are three broken generators by the cholesteric vacuumJ_x, J_y, and $p_z + kJ_z$it would be naively expected that three Goldstone modes would appear in the low energy theory instead of one. However, it can be shown that the orientational moduli from J_x and J_y are lifted from the spectrum for energies much lower than the pitch $\eta/2$ of the vacuum [71]. Essentially, the additional orientational moduli from $J_{x,y}$ acquire mass gaps due to their mutual interaction and interactions with $p_z + kJ_z$ [72]. This effect will also appear on the low energy theory of vortices, which we will describe in Section 6 below.

4.5 Vortex Solutions

In this section we will discuss vortices in the three vacua discussed in the previous section. The model (4.3) admits two types of vortices of which we will discuss only one type in detail. In vacua I and II, the accumulation of the field χ in the vortex core can be considered as a response to the effective potential emerging from the topological vortex in ϕ. In these cases, the field χ does not carry a topological charge of its own.

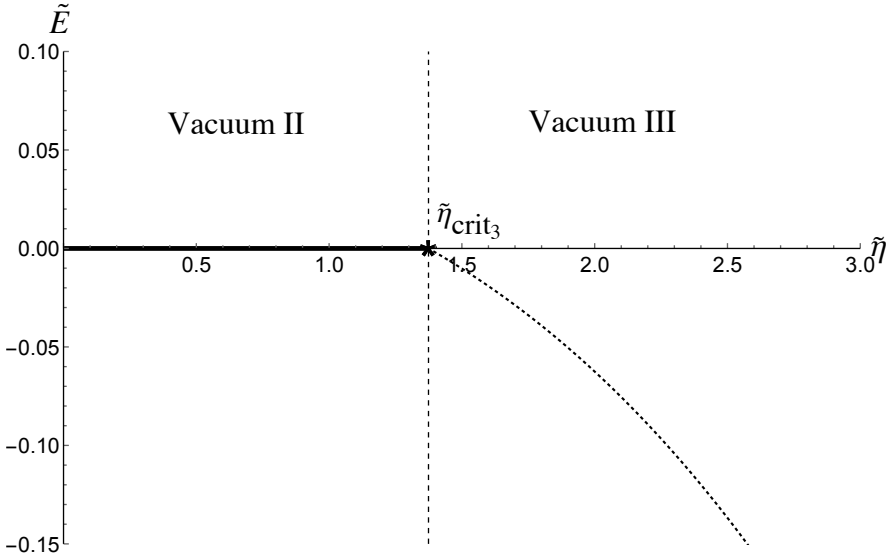

Figure 4.2: $b = 1,\ c = 1.25,\ \beta = 4$. Vacuum energy dependence on $\tilde{\eta}$ for $\beta(c-1) < bc$, the solid line corresponds to vacuum II and the dotted line to vacuum III.

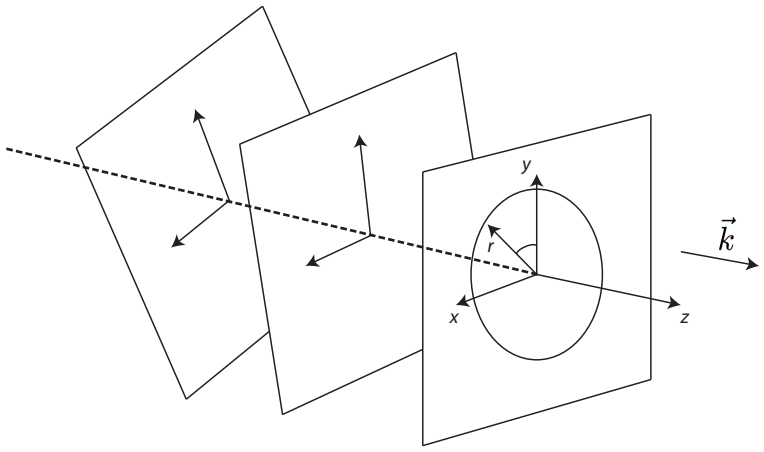

Figure 4.3: Geometric set-up of the problem. The vortex axis, in the z direction, is parallel to the wave-vector $\vec{k}$ which is normal to the cholesteric planes.

These vortices mimic the structure of w vortices appearing in superfluid ^{3}He-B [70]. These vortices will be the focus of our attention.

In contrast, we may also consider a winding of the $SO(3)_{S+L}$ global symmetry by giving χ_i a θ dependence at large distances from the vortex axis. This type of vortex is typically called a spin vortex and arises in models of superfluid ^{3}He [73]. Although, the $SO(3)$ charged vortices in this model present an interesting avenue, we will not discuss them further here.

4.5.1 $U(1)$ topological vortices

In the search of the vortex solution we will switch to polar coordinates. Note that finding a vortex in the cholesteric vacuum is a nontrivial numerical problem. We will limit ourselves to the simplest case: the vortex axis parallel to the z axis (or, which is the same, coinciding with $\vec{k}$). The geometry of our problem is illustrated in Figure 4.3. We will solve the full three dimensional numerical problem for the functions

$$\chi_i = \frac{\mu}{\sqrt{2\beta}}\tilde{\chi}_i, \quad \phi = v\varphi(\rho,\theta,\tilde{z}), \quad A_i = m_\varphi \tilde{A}_i. \tag{4.37}$$

In the equations to follow, we will omit the tilde above A, χ, z, and η to avoid cluttering the notation. We will also work in polar coordinates,

$$\vec{\chi}(r,\theta,z) = \chi^r\partial_r + \chi^\theta\partial_\theta + \chi^z\partial_z, \vec{A}(r,\theta,z) = A^r\partial_r + A^\theta\partial_\theta + A^z\partial_z. \tag{4.38}$$

Note that ϕ (and correspondingly φ) is a complex function. Additionally, we work

in the Coulomb gauge $\nabla \cdot \vec{A} = 0$. Then the equations of motion for χ_i reduce to

$$\begin{aligned}
&\frac{1}{\rho}\partial_\rho\left(\rho\partial_\rho\left(\rho\chi^\theta\right)\right) + \rho\partial_z^2\left(\chi^\theta\right) + \frac{1}{\rho}\left(\partial_\theta^2\chi^\theta - \chi^\theta + \frac{2}{\rho}\partial_\theta\chi^r\right) \\
&\qquad + \eta\left(\partial_\rho\chi^z - \partial_z\chi^r\right) - (V_\chi)\rho\chi^\theta = 0, \\
&\frac{1}{\rho}\partial_\rho\left(\rho\partial_\rho\chi^r\right) + \partial_z^2\chi^r + \frac{1}{\rho^2}\left(\partial_\theta^2\chi^r - \chi^r - 2\rho\partial_\theta\chi^\theta\right) \\
&\qquad + \eta\left(\rho\partial_z\chi^\theta - \frac{\partial_\theta\chi^z}{\rho}\right) - (V_\chi)\chi^r = 0, \\
&\frac{1}{\rho}\partial_\rho\left(\rho\partial_\rho\chi^z\right) + \partial_z^2\chi^z + \frac{1}{\rho^2}\partial_\theta^2\chi^z - \eta\left(\rho\partial_\rho\chi^\theta + 2\chi^\theta - \frac{\partial_\theta\chi^r}{\rho}\right) \\
&\qquad - (V_\chi)\chi^z = 0.
\end{aligned} \tag{4.39}$$

The equations for the gauge field A reduce to

$$\begin{aligned}
&\frac{1}{\rho}\partial_\rho\left(\rho\partial_\rho\left(\rho A^\theta\right)\right) + \rho\partial_z^2 A^\theta + \frac{1}{\rho}\left(\partial_\theta^2 A^\theta - A^\theta + \frac{2}{\rho}\partial_\theta A^r\right) \\
&\qquad - \frac{a\rho}{2}\left(J^\theta + 2A^\theta|\varphi|^2\right) = 0, \\
&\frac{1}{\rho}\partial_\rho\left(\rho\partial_\rho A^r\right) + \partial_z^2 A^r + \frac{1}{\rho^2}\left(\partial_\theta^2 A^r - A^r - 2\rho\partial_\theta A^\theta\right) \\
&\qquad - \frac{a}{2}\left(J^\rho + 2A^r|\varphi|^2\right) = 0, \\
&\frac{1}{\rho}\partial_\rho\left(\rho\partial_\rho A^z\right) + \partial_z^2 A^z + \frac{1}{\rho^2}\partial_\theta^2 A^z - \frac{a}{2}\left(J^z + 2A^z|\varphi|^2\right) = 0.
\end{aligned} \tag{4.40}$$

The equation for the scalar field φ reduces to

$$\begin{aligned}
&\frac{1}{\rho}\partial_\rho\left(\rho\partial_\rho\varphi\right) + \frac{1}{\rho^2}\partial_\theta^2\varphi + \partial_z^2\varphi - 2\mathrm{i}\left(A^r\partial_\rho + A^\theta\partial_\theta + A^z\partial_z\right)\varphi \\
&\qquad - A^2\varphi - (V_\varphi)\varphi = 0,
\end{aligned} \tag{4.41}$$

where

$$V_\chi = \frac{b}{c-1}\left[-1 + c|\varphi|^2 + \chi_r^2 + \frac{\chi_\theta^2}{\rho^2} + \chi_z^2\right],$$

$$V_\phi = \frac{1}{2}\left(|\varphi|^2 - 1 + \frac{b}{\beta(c-1)}\chi^2\right),$$

$$J^i = \mathrm{i}(\varphi^*\partial_i\varphi - \varphi\partial_i\varphi^*). \tag{4.42}$$

In the polar coordinates, when $\beta(c-1) > 4bc$ and $\eta_{\mathrm{crit}_1} < \eta < \eta_{\mathrm{crit}_2}$, the vacuum solution describes a cholesteric vacuum and takes the form

$$\chi^r = \chi_0 \cos(kz - \theta), \quad \chi^\theta = \frac{\chi_0}{\rho}\sin(kz-\theta), \quad \chi_z = 0, \tag{4.43}$$

where we are assuming k and z are in dimensionless units. Note that this corresponds to a vacuum which, in terms of Cartesian vectors χ_x, χ_y and χ_z, has no $kz-\theta$ dependence. In order to find finite energy solutions in this parameter range we therefore seek solutions to these equations with the following boundary conditions in ρ:

$$\begin{aligned}
&\chi^z(\rho,\theta,z) \xrightarrow{\rho\to\infty} 0,\\
&\chi^r(\rho,\theta,z) \xrightarrow{\rho\to\infty} \chi_0\cos(kz-\theta),\\
&\chi_\theta(\rho,\theta,z)/\rho \xrightarrow{\rho\to\infty} \chi_0\sin(kz-\theta)/\rho,\\
&\varphi(0,\theta,z) = 0, \quad \varphi(\rho,\theta,z) \xrightarrow{\rho\to\infty} \varphi_0 \mathrm{e}^{\mathrm{i}\theta},\\
&A^\theta(\rho,\theta,z)/\rho \xrightarrow{\rho\to\infty} 0,\\
&A^r(0,\theta,z) = 0, \quad A^r(\rho,\theta,z) \xrightarrow{\rho\to\infty} 0,\\
&A^z(\infty,\theta,z) = 0.
\end{aligned} \tag{4.44}$$

Additionally, there are boundary conditions on χ^r, χ^θ, A^r and A^θ, at $\rho \to 0$ that are required for the solution to be analytic at the origin. The boundary condition on $\varphi(\rho \to \infty)$ ensures the $U(1)$ winding of the solution. We also demand periodicity in the angular θ direction and continuity in the z direction. Solutions for the field χ with $a = 1$, $b = 1$, $c = 1.25$, $\beta = 8$, and $\eta = 2.2$ are shown for $z = 0$ in Figures 4.4 and 4.5 where the cholesteric structure is clearly visible. A plot of the density $|\vec{\chi}|$ is shown in

Figure 4.6. Figure 4.7 shows a plot of $|\phi|$ and A as functions of ρ at $z = \theta = 0$ indicating the vortex structure at the origin of the xy plane. For these values of the parameters $\eta_{\text{crit}_1} = 2$ and $\eta_{\text{crit}_2} = 4$. In Figures 4.8-4.11 we show similar plots for the same choice of parameters a, b, c, and β but with $\eta = 0.5$. Thus, these vortices sit in vacuum II.

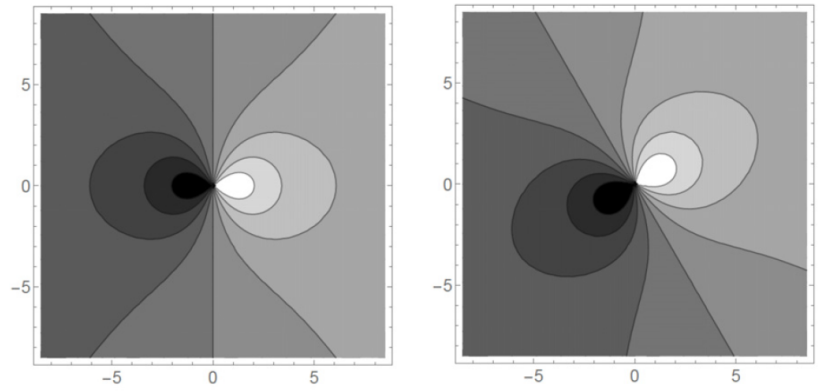

(a) χ^r, at $kz = 0$.

(b) χ^r at $kz = \pi/6$.

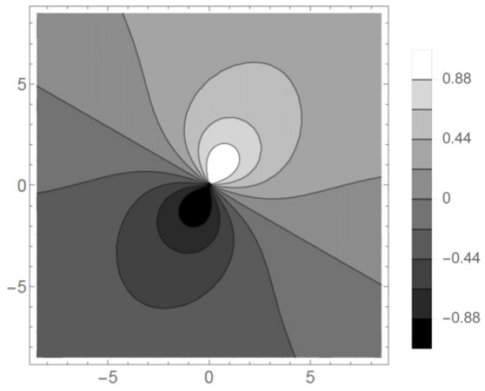

(c) χ^r at $kz = \pi/3$.

Figure 4.4: The graphs in (a), (b) and (c) show the χ^r profiles as contour plots at $kz = 0$, $\pi/6$, and $\pi/3$ respectively for $\eta = 2.2$. The three plots indicate that the χ^r profile twists with pitch $\eta/2$. This is also true of the other components χ^θ and χ^z.

4.5.2 Numerical Technique

The differential system (4.39)- (4.41) for the dynamical vortex is a coupled set of eight differential equations that must be solved in three dimensions with the boundary conditions (4.44). In order to achieve an accurate numerical solution in a reasonable amount

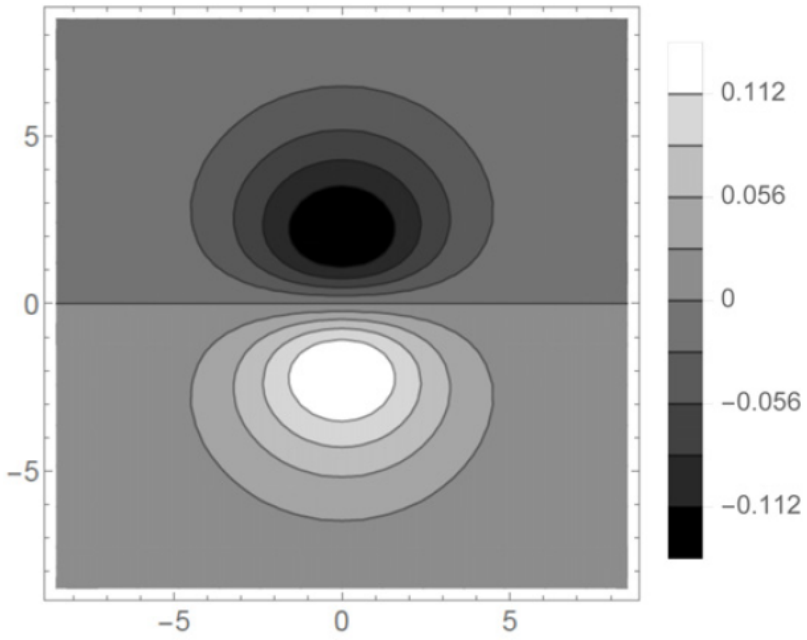

Figure 4.5: Shown in this figure is a contour plot of χ^z at $kz = 0$, for $\eta = 2.2$. The plot indicates a dipole in the χ^z profile.

of computing time and memory, we make use of the pseudo-spectral method on a collocated grid [74]. We expand the solution in θ and z coordinates in Fourier modes to exploit the periodicity expected in both coordinates. For the radial coordinate we first compactify the coordinate so that the boundary condition at infinite radius can be implemented. For this we transform the radial coordinate r to the coordinate x by

$$r = \frac{Lx}{\sqrt{1-x^2}}, \tag{4.45}$$

where L is a constant we select by choice. Typically we select $L = 2$ or 3 to achieve the best distribution of grid points. The radial solution is then expanded in Chebyshev polynomials $T_n(x)$ over a Radau collocation grid in x. We implement our boundary condition at $x \to 1$, which corresponds to the large radius $r \to \infty$. It is worth mentioning that the functions $T_n(x(r))$ are known as the rational Chebyshev functions.

Having written the solutions in terms of the expansion modes, we transform the differential equations into a coupled system of algebraic equations, which must be solved

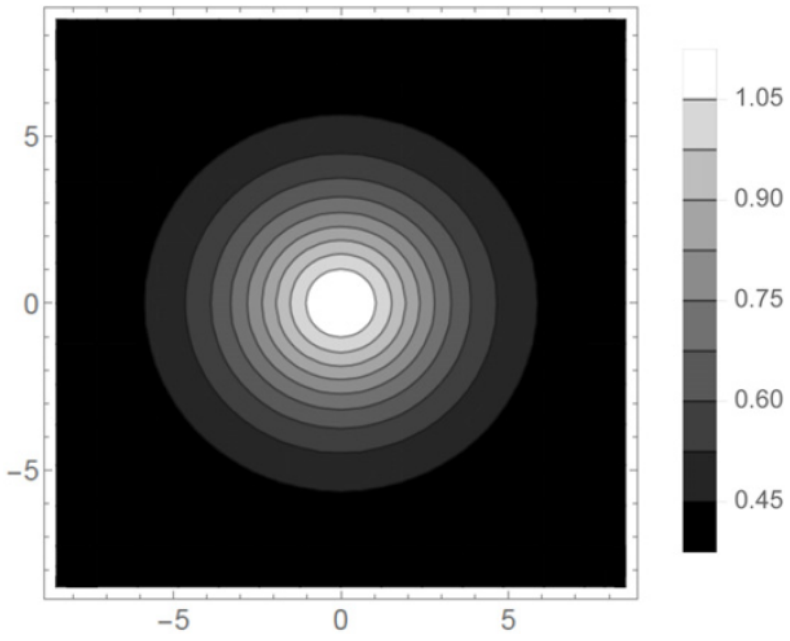

Figure 4.6: Shown in this figure is a contour plot of $\chi = \sqrt{\chi^{r2} + \rho^2 \chi^{\theta 2} + \chi^{z2}}$ at $kz = 0$, for $\eta = 2.2$. The plot indicates the near cylindrical symmetry of the field χ. This implies a minimal back reaction on ϕ and $\vec{A}$ due to the twisting of χ^i.

to determine the coefficients of the expansion modes. To solve the large system, we use a Newton's method to achieve a solution iteratively until convergence is observed. An added bonus of this method is that the stability properties of the approximate solution are shared with the linear stability of the exact solution for a large enough set of expansion modes [75]. Thus, if our method shows convergence to a stable approximation, we can be sure of the linear stability of our solution to small perturbations.

4.6 Low energy theory of vortex moduli

It is well known that in the absence of a cholesteric structure, when $\eta = 0$, the system with energy density (4.9) describes non-abelian strings. The low energy theory on their world-sheet is a $CP(1)$ model for two orientational moduli (plus the standard translational moduli of the vortex centre). When $\eta \neq 0$, once one aligns the vortex axis with the cholesteric wave-vector, the $O(3)$ rotational freedom of χ_i is broken to

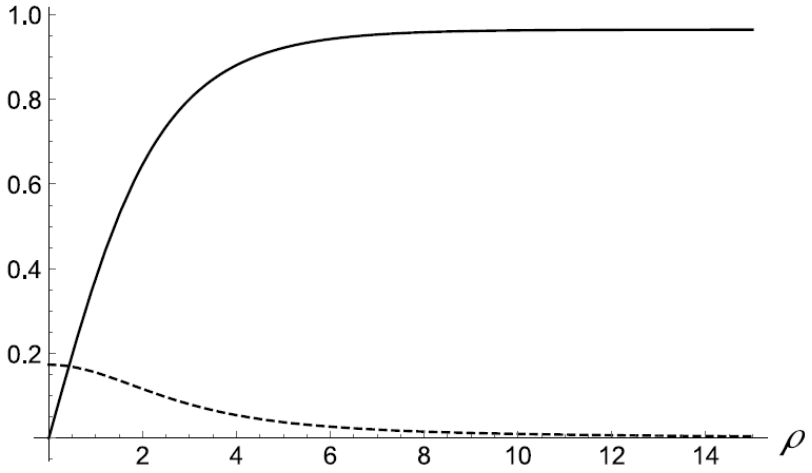

Figure 4.7: $|\phi(\rho)|$ (solid) and $A_\theta(\rho)$ (dashed) are shown at $z = \theta = 0$ for $\eta = 2.2$. The non-analytic behavior of $|\phi|$ at $\rho \to 0$ indicates the $U(1)$ topological charge of the vortex solution. The functions $A^r(\rho)$ and $A^z(\rho)$ are negligible in comparison to $A^\theta(\rho)$, and are thus not shown.

the subgroup of rotations in the plane orthogonal to $\vec{k}$. Correspondingly some of the orientational moduli have to be lifted.

To determine the low energy theory at the classical level, we rely on the symmetries of the system following the procedure in [14]. In particular, the moduli appearing on the vortex are determined by the continuous global symmetries of the vacuum, which are broken by the vortex core. The continuous global symmetry group of the Lagrangian (4.3) with the parity breaking term (4.7) is given by

$$G_{\text{global}} = SO(3)_J \times T, \tag{4.46}$$

where T is the three dimensional translation group, and J refers to the sum of generators $S + L$.

The vacua appearing in the model preserve part or all of the symmetry group G. For vacuum I in (4.25) the appearance of a non-zero χ_0 implies the symmetry breaking of translations in the direction of the wave vector $\vec{k} \equiv k\hat{z}$. Thus only the subgroup $T_x \times T_y$ of the translational group T remains invariant in this vacuum. Additionally, since $\vec{\chi}_0$ rotates in the xy-plane as one translates in the z direction, rotations about the z direction are broken. The wave vector $\vec{k}$ breaks the remainder of the $SO(3)_J$ group.

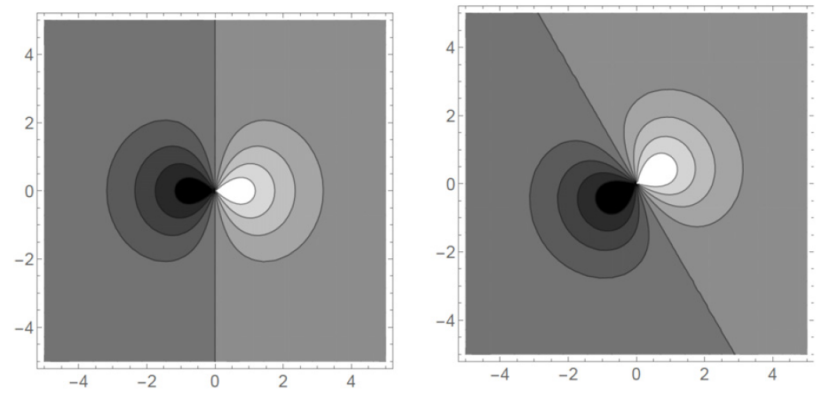

(a) χ^r, at $kz = 0$.

(b) χ^r at $kz = \pi/6$.

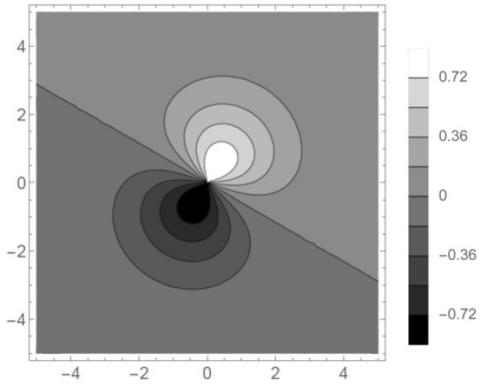

(c) χ^r at $kz = \pi/3$.

Figure 4.8: The graphs in (a), (b) and (c) show the χ^r profiles as contour plots at $kz = 0$, $\pi/6$, and $\pi/3$ respectively for $\eta = 2.2$. The three plots indicate that the χ^r profile twists with pitch $\eta/2$. This is also true of the other components χ^θ and χ^z.

However, a glance at (4.20) shows that translations in the z direction are equivalent to rotations about z in vacuum I. Thus, although vacuum I separately breaks T_z and $SO(2)_{J_z}$, a subgroup, which we will denote $SO(2)_{J'_z} \subset SO(2)_{J_z} \times T_z$ is preserved. Thus the complete symmetry of vacuum I is given by

$$H_I = T_{x,y} \times SO(2)_{J'_z}. \tag{4.47}$$

Vacuum II on the other hand does not break the translational or rotational symmetries since $\chi_0 = 0$ in this case. Thus,

$$H_{II} = G_{\text{global}}. \tag{4.48}$$

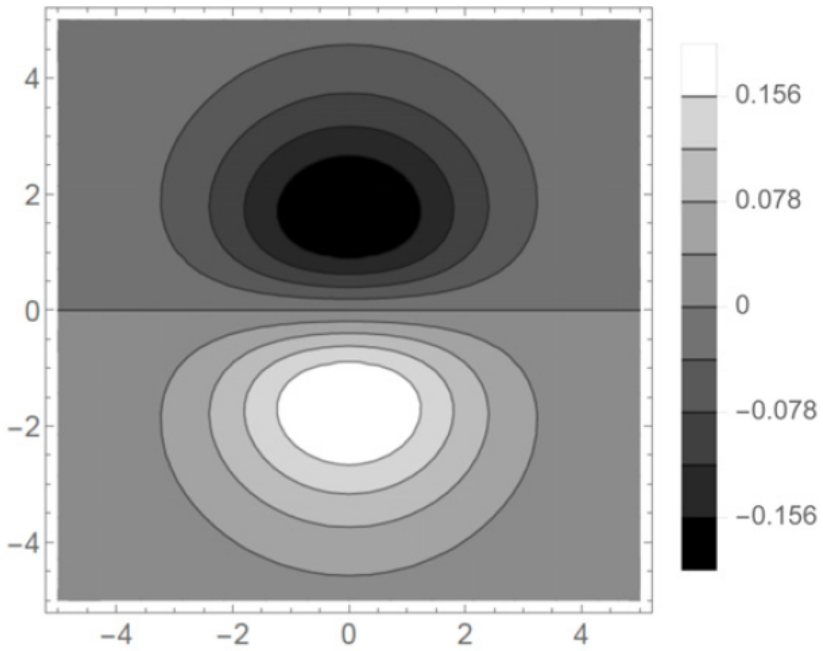

Figure 4.9: Shown in this figure is a contour plot of χ^z at $kz = 0$, for $\eta = 2.2$. The plot indicates a dipole in the χ^z profile.

The continuos global symmetries preserved by vacuum III are exactly the same as those of I. Vacuum III is only distinguished from I because III does not break the $U(1)$ gauge symmetry.

$$H_{III} = H_I. \tag{4.49}$$

The presence of vortices in these vacua further break the symmetry of the system. The generators of the vacuum subgroups H_i which are broken by the vortex solution produce the moduli fields in the low energy theory. With this in mind we may write down a low energy theory by varying the vortex solutions through their degeneracy space. For the translations in the x and y directions this can be achieved by replacing

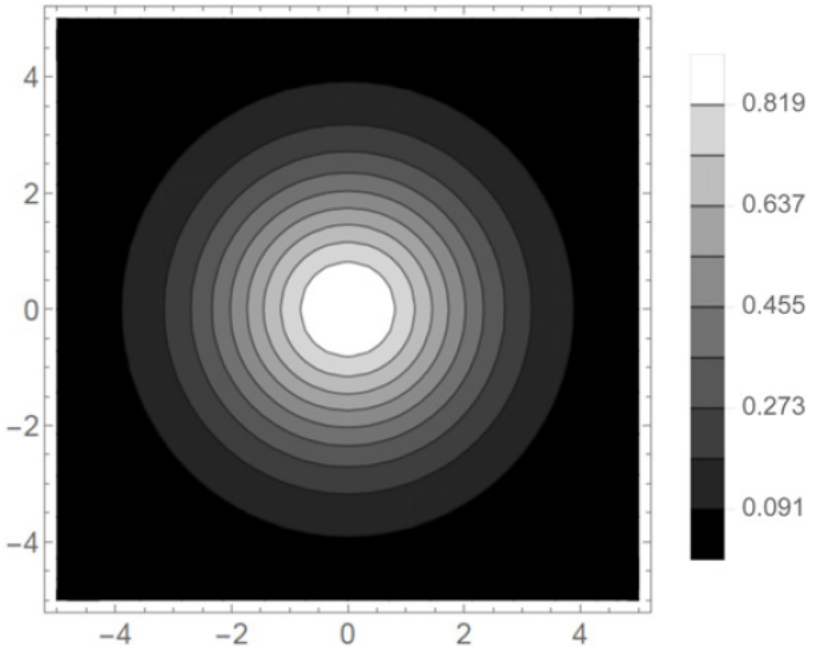

Figure 4.10: Shown in this figure is a contour plot of $\chi = \sqrt{\chi^{r2} + \rho^2 \chi^{\theta 2} + \chi^{z2}}$ at $kz = 0$, for $\eta = 2.2$. The plot indicates the near cylindrical symmetry of the field χ. This implies a minimal back reaction on ϕ and $\vec{A}$ due to the twisting of χ^i.

in the Lagrangian

$$\begin{aligned} &\chi_i(\vec{x}) \to \chi_i(\vec{x} - \vec{\xi}(t,z)), \\ &\varphi(\vec{x}) \to \varphi(\vec{x} - \vec{\xi}(t,z)), \\ &A_i(\vec{x}) \to A_i(\vec{x} - \vec{\xi}(t,z)), \end{aligned} \tag{4.50}$$

and expanding to second order in $\vec{\xi}(t,z)$. After integrating over x and y one achieves an effective Lagrangian in the modulus fields $\vec{\xi}(t,z)$. If $\eta = 0$ one may also expand the vortex solution in the orientational modulus $\vec{S}(t,z)$ where the field χ_i is replaced in the Lagrangian

$$\chi_i \to R_{ij}(t,z)\chi_j \equiv S_i(t,z)\chi(\vec{x}_\perp), \tag{4.51}$$

where $\vec{x}_\perp \equiv (x,y)$ are the coordinates perpendicular to the vortex axis. R_{ij} is the spin rotation matrix in $SO(3)_S$. We also define $\chi^2 \equiv |\vec{\chi}|^2$. Thus, $\vec{S}(t,z)$ satisfies the

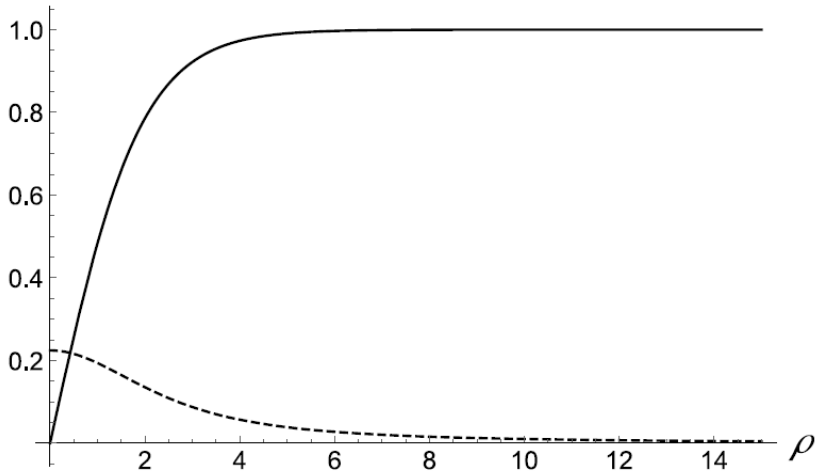

Figure 4.11: $|\phi(\rho)|$ (solid) and $A_\theta(\rho)$ (dashed) are shown at $z = \theta = 0$ for $\eta = 0.5$. Again, the functions $A^r(\rho)$ and $A^z(\rho)$ are negligible in comparison to $A^\theta(\rho)$.

constraint $|\vec{S}|^2 = 1$. Thus, when $\eta = 0$ the effective theory is given by

$$S_{\eta=0} = \int dtdz \left\{ \frac{1}{2g^2}\partial_\alpha S_i \partial_\alpha S_i + \frac{T}{2}\partial_\alpha \xi_b \partial_\alpha \xi_b \right\} \tag{4.52}$$

where g and T are calculated from the integration over x and y [**?**]. Here $\alpha = (t, z)$, and $b = (x, y)$. The component ξ_z does not appear in the low energy theory since the vortex solution in this case is independent of z.

We now switch on $\eta \neq 0$ and observe the effects on the vortex moduli in the various vacua. For this we focus our attention on the χ_i kinetic terms in the Lagrangian. For convenience in determining the moduli fields we write

$$\chi_i \equiv \chi(t, \vec{x}) S_i(t, \vec{x}), \quad \text{where } |\vec{S}|^2 \equiv 1. \tag{4.53}$$

This definition allows for a convenient form of the kinetic terms in the Lagrangian,

$$\mathcal{L}_{\text{kin}} = \partial^\mu \chi \partial_\mu \chi + \chi^2 \left(\partial^\mu S_i \partial_\mu S_i - \varepsilon_{ijk} S_i \partial_j S_k \right). \tag{4.54}$$

Let us first consider the vortices in vacuum I. Obviously, the translational moduli $\xi_{x,y}(t, z)$ are still existent. However, since the solutions no longer preserve z translational symmetry, the additional translations $\xi_z(t, z)$ along the z-direction along the vortex axis

may appear. However, the vacuum far from the vortex axis is characterized by a non-zero $\chi_i \to \chi_0 \epsilon_i(z)$. Thus, the kinetic term for $\xi_z(t,z)$ in the action is given by:

$$S_{\xi_z} = \frac{T_z}{2} \int dt dz (\partial_\alpha \xi_z)^2 \tag{4.55}$$

where the tension T is given by

$$T_z \to \int d^2\vec{x}_\perp \chi_0^2, \tag{4.56}$$

which is obviously divergent. This is expected since the vacuum I only preserves a translational symmetry in the z direction if it is accompanied by a corresponding rotation in $SO(2)_{J_z}$. However, for the parameters considered in the previous sections the vortex solutions also satisfy the $SO(2)_{J'_z}$ symmetry to a very good approximation and thus cannot produce a dynamical modulus from this group. For larger back reactions (due to large $\eta \gg \eta_{\text{crit}_2}$ for example) on the ϕ and A_i fields this approximation will no longer hold, and an $SO(2)_{J'_z}$ modulus will appear in the low energy dynamics. This $SO(2)_{J_z}$ modulus can be shown to emerge on the ϕ field due to the back reaction from the last term proportional to χ^2 in V_ϕ in (40). For large η, χ_i will have a dipole term with a $\theta - kz$ dependence, and thus χ^2 will have higher multipoles (at least quadrupole) appearing in a Fourier expansion in $\theta \equiv \theta - kz$. This will break the $SO(2)_{J_z}$ symmetry, and lead to an additional modulus appearing on the ϕ vortex solution. We will not consider this case in further detail here.

The more interesting case occurs in vacuum II where the entire global symmetry group G_{global} is preserved in the vacuum, and only the $U(1)$ gauge symmetry is broken. We will assume for this case that $0 < \eta << \eta_{\text{crit}_1}$. With this constraint we may assume a vortex solution of the form

$$\chi_i \approx \chi(\rho)\epsilon_i(z), \tag{4.57}$$

where the modulus $\chi(\rho)$ has near axial symmetry. We now apply the translational transformations (4.50) and the $SO(3)_J$ transformations,

$$\epsilon_i \to R_{ij}(\vec{\omega}(t,z))\epsilon_j \equiv S_i(t,z). \tag{4.58}$$

Expanding (4.54) to second order in $\xi(t,z)$ and integrating over x and y we find

$$\mathcal{L}_{\text{kin}} = \frac{T}{2}(\partial_\alpha \vec{\xi}_\perp)^2 + \frac{1}{2g^2}\Big[(\partial_\alpha \vec{S})^2 + (\partial_\alpha \vec{S})^2(\partial_z \xi_z)^2 + \eta \varepsilon_{ab} S_a \partial_z S_b + 2\partial_z \xi_z \left((\partial_z \vec{S})^2 - \frac{\eta}{2}\varepsilon_{ab} S_a \partial_z S_b\right)\Big], \tag{4.59}$$

where $\alpha = (t, z)$, and (a, b) are indices in (x, y). The constant g is calculated from the integration over x and y,

$$\frac{1}{2g^2} = \int d^2\vec{x}_\perp \chi(\rho)^2. \tag{4.60}$$

We emphasize for clarity that $\vec{S}$ in (57) has both the non-perturbative dynamical structure $\epsilon_i(z)$ from (18) in addition to the small perturbations on the ground state.

We first note that the second line of (4.59) can be expanded to first order in $\vec{\omega}$ with the result

$$2\partial_z\xi_z \left((\partial_z\vec{S})^2 - \frac{\eta}{2}\varepsilon_{ab}S_a\partial_z S_b\right) = -\eta\partial_z\xi_z\partial_z\omega_z + \mathcal{O}(\vec{\omega}^2). \tag{4.61}$$

Combining this with the $\mathcal{O}(\xi_z^2)$ and $\mathcal{O}(\omega_z^2)$ in the first line of (4.59) we find

$$\mathcal{L}_{\text{kin}} \supset \frac{1}{2g^2}\left[\partial_z\left(\frac{\eta}{2}\xi_z + \omega_z\right)\right]^2 \equiv \frac{1}{2g^2}\left(\partial_z\omega_z'\right)^2, \tag{4.62}$$

which simply enforces the $SO(2)_{J_z'}$ symmetry of the vortex. Thus, only one of the two moduli coming from the broken z translations and the $SO(2)_{J_z}$ rotations survives as a low energy dynamical field.

The last observation we wish to discuss is the remaining two rotational moduli $\omega_{x,y}$ from the degeneracy space $SO(3)_J/SO(2)_{J_z}$. Expanding the second line of (4.59) to second order in $\omega_{x,y}$ we arrive at

$$\partial_z S_a\partial_z S_a = \left((\partial_z\omega_x + k\omega_y)\sin kz - (\partial_z\omega_y - k\omega_x)\cos kz\right)^2 + \mathcal{O}(\omega^3). \tag{4.63}$$

To obtain this formula we expand S_i to first order in ω using

$$\vec{S} = \mathrm{e}^{\mathrm{i}\vec{\omega}\cdot\vec{L}} \approx \left(1 + \mathrm{i}\vec{\omega}\cdot\vec{L}\right)\vec{\epsilon} = \begin{pmatrix} \cos kz - \omega_z \sin kz \\ \sin kz + \omega_z \cos kz \\ \omega_x \sin kz - \omega_y \cos kz \end{pmatrix}. \tag{4.64}$$

Taking the derivative of this expression and squaring gives us the formula (61).

We observe for $\partial_z\omega_a \gg \eta\omega_a$ that

$$(\partial_z S_a)^2 \approx (\partial_z\omega_y)^2. \tag{4.65}$$

Thus, for high energy excitations in ω_a, the modulus ω_y survives as a massless degree of freedom.

On the other hand if $\partial_z \omega_a \ll \eta \omega_a$ we have

$$(\partial_z S_a)^2 \approx \frac{\eta^2}{4}\left(\omega_x^2 + \omega_y^2\right) + (\text{kinetic terms in } \omega_a). \tag{4.66}$$

As expected, at low energies the two moduli from $SO(3)_J/SO(2)_{J_z}$ are lifted due to the emerging mass terms in $\omega_{x,y}$.

The interpretation of the high energy result (4.65) is that at high momenta, the twisting structure of the vortex is decoupled from the excitations, and the original sigma model for $\eta \to 0$ reappears approximately. However, low energy excitations see an average over many cycles of the vortex twisting leading to a lifting of the moduli $\omega_{x,y}$ (see [71]). We point out that the high energy result (63) cannot be disregarded on the grounds of classical low energy dynamics. Indeed, it is quite possible for the energy of the excitation to be larger than η while still being low energy relative to the width of the vortex.

4.7 Discussion and Conclusions

We have observed some of the effects of a parity violating twist term in the Lagrangian (4.3), which is linear in the derivative. The most important of these observation is the introduction of new cholesteric vacuum field configurations which break translational and rotational symmetry. In addition, we have discussed vortex solutions with the gauge $U(1)$ topological charge in the two vacua (I and II) where such vortices are allowed classically.

We have deduced the essentials of the classical low energy excitations of such vortices. This was achieved by appealing to symmetry arguments when the twist term can be treated as a perturbation of the original Lagrangian (4.3). In particular, we have observed the emergence of a new translational modulus ω_z' appearing in (4.62). In addition, we have observed the lifting of the non-Abelian moduli $\omega_{x,y}$ of the original $(1+1)$ dimensional $O(3)$ sigma model. For the case of vortices in vacuum II this occurs for low energy excitations of $\omega_{x,y}$ which develop a mass proportional to η. On the other hand, excitations with momenta much larger than η probe the vortex line at small enough distances where the twist effect decouples.

This chapter has focused on the dynamical effects on vortices with a $U(1)$ topological

charge after introducing a parity violating twist term in the lagrangian (4.3). Such vortices mimic the structure of w-vortices in superfluid ^{3}He-B [70]. However, several topics of this system remain unanswered and could provide avenues of future research. Specifically, although we have mentioned the existence of vortices with a non-Abelian global $SO(3)_{S+L}$ charge, we have not discussed their solutions in detail. These solutions are the so called disclinations. They are similar to the vortices in a biaxial nemetic liquid crystal where the non-zero value of η and χ_0 leads to a degeneracy space $SO(3)$ with non-trivial fundamental group. The details of these vortices in cholesteric liquid crystals have been worked out (see [69, 70] or [37] for example), however their properties in the present context, with the additional $U(1)$ gauge symmetry, are yet to be discussed (although see [76, 77]).

Our discussion of the low energy excitations has been confined to a classical discussion. We have not considered the quantization of the zero modes, which is a non-trivial topic when the system is not Lorentz invariant [35, 78] and spacetime symmetries are broken [50, 51, 61, 79].

Chapter 5

Spin Vortices in Cholesterics

The chapter was originally discussed in [80]. We continue the study of $U(1)$ vortices with cholesteric vacuum structure. A new class of solutions is found which represent global vortices of the internal spin field. These spin vortices are characterized by a non-vanishing angular dependence at spatial infinity, or winding. We show that despite the topological $\mathbb{Z}_2$ behavior of $SO(3)$ windings, the topological charge of the spin vortices is of the $\mathbb{Z}$ type in the cholesteric. We find these solutions numerically and discuss the properties derived from their low energy effective field theory in $1+1$ dimensions

5.1 Introduction

This chapter presents a continuation of the previous chapter [64] which investigates the low energy theory of $U(1)$ vortices in systems with cholesteric vacuum structures. This work was inspired by considerations from supersymmetric solitons (see [66] for a review) as well as supconductivity [66] and superfluidity [70]. The kind of vortex solutions found in [64] are similar to the w vortices appearing in superfluid ^{3}He-B [70]. Indeed these w vortices, and those found in [64], develop a cholesteric spiral structure in the core. If a collection of such vortices are coherently orientated in a rotating cryostat the spiral structure appears in the bulk superfluid [70]. The main task of this chapter is to report on a different class of solutions also present in this model. These solutions are characterized by the internal spin field carrying a topological charge of its own. Typically vortices with topological windings originating from an internal $SO(3)_J$

spin group are referred to as spin vortices. However, for reasons discussed below, the solutions we obtain are distinct from the typical spin vortex observed in say superfluid ^{3}He [73] [76, 77]. Our plan is to find these solutions numerically and investigate their low energy excitations.

The model, as originally introduced in [64], has a symmetry structure given by

$$G = U(1)_{\text{gauge}} \times SO(3)_J \times T \tag{5.1}$$

where the $U(1)_{\text{gauge}}$ group represents gauge rotations of a complex Higgs field, and $SO(3)_{S+L} \equiv SO(3)_J$ represents the spin orbit locked rotational symmetry. The group T represents the three translational symmetries of the model. The spin orbit locked $SO(3)_J$ appears from the larger group $SO(3)_S \times SO(3)_L$ due to an additional term in the Largrangian coupling the spin index to the spatial gradiant. This term is parity violating and leads to spontaneous breaking of translational symmetry. The additional term thus gives rise to a cholesteric spiral structure in the vacuum under certain conditions of the parameters in the model [64].

The spontaneous breaking of the $U(1)_{\text{gauge}}$ group allows for the appearence the Abrikosov-Nielsen-Olsen [46, 47] flux tube familiar to models of type II superconductors [66] and Yang-Mills theories [66]. With no other winding of the subgroups of G these vortices represent the mass vortices that were studied in [64]. A typical spin vortex on the other hand arises from the non-trival topology of the $SO(3)_J$ group:

$$\pi_1(SO(3)_J) = \mathbb{Z}_2. \tag{5.2}$$

The spin vortices can appear regardless of the cholesteric behavior of the vacuum and only require the existence of a broken $SO(3)$ symmetry. However, the vortices we consider in this chapter are distinct from the typical spin vortex in that they are only allowed due to the broken translational symmetry of the vacuum. In particular, the vacuum of our model preserves a $U(1)_{J'_z}$ global subgroup of G which is generated by a linear combination of the translational and rotational generators about an axis oriented along the cholesteric wave vector $\vec{k}$:

$$G \to U(1)_{J'_z} \times T_{x,y}, \text{ where } U(1)_{J'_z} \subset U(1)_{J_z} \times T_z. \tag{5.3}$$

$T_{x,y}$ are the translational groups along the direction perpendicular to $\vec{k}$. Here the subgroup $U(1)_{J'_z}$ is denoted with its generator J'_z which is a linear combination of the

rotational J_z and translational p_z generators:

$$J'_z \equiv J_z - \frac{p_z}{k}, \quad k \equiv |\vec{k}|. \tag{5.4}$$

As we will discuss below this equivalence of rotations and translations in the vacuum leads to a global $U(1)$ degeneracy space of vacua in addition to the $U(1)_{\text{gauge}}$ "degeneracy" appearing from the Higgs phase. Vortices may appear with either gauge or global $U(1)$ topological windings or both:

$$\pi_1(U(1)_{\text{gauge}} \times U(1)) = \mathbb{Z} + \mathbb{Z}. \tag{5.5}$$

We must mention that the classification of topological defects in cholesteric media has additional subtleties due to the broken translational symmetry in the vacua [81]. For systems with broken translational symmetry the local behavior of the order parameter cannot be completely specified by its value at a single point. Typically, additional information on the derivatives of the order parameter are necessary for a complete specification of the local structure. As a result, the defects corresponding to physical field configurations must satisfy certain conditions requiring the compatibility of the nonlocal behavior of order parameter with the restrictions on the derivatives of the order parameter following from broken translational symmetry [81]. We will discuss these restrictions for our particular model in Section 3. Additionally, for crystalline structures the defects built from the spatial variations of the order parameter will include additional energy contributions from the distortions of the crystal lattice [81]. For the vortices considered in this chapter these subtleties are avoided because the wave vector $\vec{k}$ corresponding to the crystal layer spacing is constant along the z-direction far from the vortex core. Thus, no additional stresses appear due to crystal lattice distortions.

In this chapter we will focus our attention on the vortices with both types of charges. We hasten to point out that the vortices in this model are global. Thus, for cholesteric vacua (vacuum I as it is defined below) these vortices will have a logarithmically divergent energy functional and thus require an infrared cutoff. This is not a problem for systems in a finite volume such as superfluid ^{3}He. However, as a consequence of this finite volume, the Kelvin modes appearing on the vortex will acquire a mass gap proportional to the inverse cutoff length R. These effects were considered recently in [55], and we will apply similar arguements when we discuss the gapless excitations in section 5 below.

We will begin in sections 2 and 3 with a detailed review of the model and the vacuum structure following the procedure discussed in [64]. We will explore briefly the Goldstones appearing in the bulk cholesteric vacuum. We will discuss their relation to the spin vortices appearing in the cholesteric bulk. In section 4 we will present the equations of motion for the spin vortices and present their numerical solutions for a representative set of parameters. In section 5 we will discuss the low energy theory of the moduli appearing on the vortices. We will present an analysis of the Kelvin modes for vortices in a particular vacuum, and provide additional topological discussions of the orientational moduli. For the case of a cholesteric vacuum we will discuss the finite volume effects on the mass terms for Kelvin modes. We will provide concluding remarks in section 6.

5.2 The system

The starting point is the system used in [64]. This model is an extension of the model originally suggested in [68], inspired by Witten's superconducting string model [44], and further studied in [23, 45, 67]. Its Lagrangian has the form

$$\begin{aligned}
\mathcal{L} &= \mathcal{L}_0 + \mathcal{L}_\chi + \mathcal{L}_\varepsilon, \\
\mathcal{L}_0 &= -\frac{1}{4e^2} F_{\mu\nu}F^{\mu\nu} + |D_\mu \phi|^2 - \lambda(|\phi|^2 - v^2)^2, \\
\mathcal{L}_\chi &= \partial_t \chi_i \partial_t \chi_i - \partial_i \chi_j \partial_i \chi_j - \gamma \left[(-\mu^2 + |\phi|^2)\chi_i \chi_i + \beta(\chi_i \chi_i)^2 \right], \\
\mathcal{L}_\varepsilon &= -\eta \varepsilon_{ijk} \chi_i \partial_j \chi_k \,,
\end{aligned} \tag{5.6}$$

where the subscript i runs over $i = 1, 2, 3$. The field χ_i can be viewed as a spin field. The covariant derivative is defined in a standard way

$$D_\mu = \partial_\mu - iA_\mu \,. \tag{5.7}$$

The last term in (5.6) is the parity violating twist term with a single derivative. This term is responsible for the cholesteric behavior of the vacuum as we will show below.

Let us consider the system with $\eta = 0$ first. Then, under an appropriate choice of parameters the charged field ϕ condenses in the ground state,

$$|\phi|_{\rm vac} = v \,, \tag{5.8}$$

and, if $\mu < v$, the field χ is not excited in the vacuum

$$(\chi_i)_{\rm vac} = 0\,. \tag{5.9}$$

The system has full translational invariance T and orbital rotational symmetry $SO(3)_L$ as well as an internal rotational $SO(3)_S$ symmetry of the χ_i spin field. As is well known, the model supports the Abrikosov flux tube [46, 47]. Inside the tube, where the Higgs field vanishes, the spin field χ_i is excited giving rise to gapless (or quasigapless) excitations of non-Abelian type, localized on the vortex. The full solution is known as a non-Abelian string.

Including $\mathcal{L}_\varepsilon$, explicitly breaks the orbital rotational part of the Lorentz symmetry implying a spin-orbit locked symmetry of the full Lagrangian,

$$SO(3)_L \times SO(3)_S \to SO(3)_{S+L} \equiv SO(3)_J. \tag{5.10}$$

The energy density derived from the Lagrangian (5.6) is

$$\begin{aligned} E =& \frac{1}{4e^2}F_{ij}F^{ij} + |D_i\phi|^2 + \lambda(|\phi|^2 - v^2)^2 + \partial_i\chi_j\partial_i\chi_j \\ &+ \eta\varepsilon_{ijk}\chi_i\partial_j\chi_k + \gamma\left[(-\mu^2 + |\phi|^2)\chi_i\chi_i + \beta(\chi_i\chi_i)^2\right]. \end{aligned} \tag{5.11}$$

Note that the kinetic terms of χ_i including the linear in derivatives η term can be recognized as the Frank-Oseen free energy density of an isotropic chiral nematic liquid crystal [69].

For later convenience we rescale all couplings in the model to make them dimensionless. Hence, we take

$$\tilde{z} = m_\phi z\,, \tag{5.12}$$

to denote the distance in the longitudinal direction aligned with the string axis. We will also set the dimensionless radial distance

$$\rho = m_\phi\sqrt{x^2 + y^2}\,, \tag{5.13}$$

where the mass of the elementary excitations of the charged field ϕ is

$$m_\phi^2 = 4\lambda v^2. \tag{5.14}$$

Additional dimensionless parameters are given as

$$b = \frac{\gamma(c-1)}{4\lambda c}\,, \quad c = \frac{v^2}{\mu^2}\,, \quad a = \frac{e^2}{2\lambda}\,, \quad \tilde{\eta} = \eta/m_\phi\,. \tag{5.15}$$

We limit ourselves to the semi-classical approximation and assume all couplings in the model are small.

The field χ_i being represented in Cartesian coordinates takes the form

$$\chi_i = \frac{\mu}{\sqrt{2\beta}}\,\left\{\tilde{\chi}_x(x,y,z),\ \tilde{\chi}_y(x,y,z),\ \tilde{\chi}_z(x,y,z)\right\}. \tag{5.16}$$

The static classical equations of motion are derived by extremization of energy (5.11), in a general coordinate system they read

$$\begin{aligned}
&\nabla_i\left(\sqrt{-g}g^{ij}\nabla_j\chi_k\right) - \eta\varepsilon_{kji}\nabla_j\chi_i - \frac{\partial V}{\partial\chi_k} = 0\,,\\
&D_i\left(g^{ij}\sqrt{-g}D_j\phi\right) + \sqrt{-g}\left(2\lambda\left(|\phi|^2 - v^2\right) + \gamma g^{ij}\chi_i\chi_j\right)\phi = 0\,,\\
&\partial_i\left(\sqrt{-g}g^{ji}g^{kl}F_{jk}\right) - ie^2\sqrt{-g}\left(\phi^* D^l\phi - \phi D^l\phi^*\right) = 0\,,
\end{aligned} \tag{5.17}$$

where

$$\frac{\partial V}{\partial\chi_k} = \sqrt{-g}\gamma\left(\left(-\mu^2 + |\phi|^2\right) + 2\beta g^{ij}\chi_i\chi_j\right)\chi_k\,, \tag{5.18}$$

and

$$\nabla_i\chi_j = \partial_i\chi_j - \Gamma^k_{ij}\chi_k \tag{5.19}$$

is the standard curved space covariant derivative with Γ the Christoffel symbol.

5.3 Ground state

In this section we give a summary of the results obtained in [64] concerning the ground state structure of the model. As shown there this model has a rich ground state structure depending on the value of η and the relation between the parameters. Given the presence of the first derivative term one expects that in the ground state translational invariance will be spontaneously broken. If one assumes that this breaking is aligned in the z

direction, then a cholesteric structure appears in the ground state with the χ field rotating in the (x, y) plane

$$\begin{aligned} \chi_i &= \chi_0\, \epsilon_i(z)\,, \qquad \frac{\sqrt{2\beta}}{\mu}\,\chi_i = \tilde{\chi}_0\, \epsilon_i(z)\,, \\ \vec{\epsilon}(z) &= \Big\{ \cos kz,\ \sin kz,\ 0 \Big\}\,, \end{aligned} \tag{5.20}$$

where k is the z component of the wave vector $\vec{k}$. χ_0 is the constant amplitude of the $\vec{\chi}$ field in the vacuum to be determined below in (5.22). Then, in the ground state we may take

$$\phi = \phi_0\,, \qquad A_i = 0\,, \tag{5.21}$$

where ϕ_0 is a constant. The equations of motion (5.17) imply

$$\begin{aligned} &\chi_0 \left(-k^2 + \eta k - \gamma((-\mu^2 + \phi_0^2) + 2\beta\chi_0^2)\right) = 0\,, \\ &\phi_0 \left(2\lambda(\phi_0^2 - v^2) + \gamma\chi_0^2\right) = 0\,. \end{aligned} \tag{5.22}$$

Minimizing over the wavevector k one obtains

$$k = \eta/2. \tag{5.23}$$

Therefore, only when $\eta = 0$ we recover translational invariance (however see (5.30)). As per [64] we always assume

$$c > 1, \quad b > 0, \quad \beta > 0 \quad \text{and} \quad a > 0, \tag{5.24}$$

and we use here the same dimensionless field definitions

$$\begin{aligned} \tilde{E}_{vac} &= \frac{m_\phi}{v^2} E_{vac} \\ \tilde{\chi}_0 &= \frac{\mu}{\sqrt{2\beta}}\chi_0 \\ \varphi &= v\phi. \end{aligned} \tag{5.25}$$

There are two parameter ranges which characterize the vacuum structure. We will report here the main results and refer the reader to [64] for calculational details. For both cases the lowest energy vacuum solution is dictated by the value of $\tilde{\eta}$. This is

important in order to understand the role of the spin-vortex solutions and their winding at spatial infinity. Consider first the case where

$$\beta(c-1) > bc. \tag{5.26}$$

Then when

$$4b < \tilde{\eta}^2 < 4\beta\left(1 - \frac{b}{\beta(c-1)}\right), \tag{5.27}$$

the vacuum solution of (5.22) is

$$(\varphi_0^2)^I = \frac{1 - \frac{b}{\beta(c-1)} - \frac{\tilde{\eta}^2}{4\beta}}{1 - \frac{bc}{\beta(c-1)}}, \quad (\tilde{\chi}_0^2)^I = (c-1)\frac{\frac{\tilde{\eta}^2}{4b} - 1}{1 - \frac{bc}{\beta(c-1)}},$$

$$\tilde{E}^I_{vac} = -\frac{(c-1)^2(\tilde{\eta}^2 - 4b)^2}{\beta(c-1) - bc}. \tag{5.28}$$

In this vacuum both $\varphi_0 \neq 0$ and $\chi_0 \neq 0$ and therefore both local $U(1)$ gauge and $z-$translational symmetries are broken. This vacuum allows for the existence of local ANO vortices. If instead

$$\tilde{\eta}^2 < \tilde{\eta}^2_{\text{crit}_1} \equiv 4b \tag{5.29}$$

then the vacuum solution is

$$(\varphi_0^2)^{II} = 1, \quad (\tilde{\chi}_0)^{II} = 0, \quad \tilde{E}^{II}_{vac} = 0, \tag{5.30}$$

Note that, since $(\tilde{\chi}_0)^{II} = 0$, this vacuum preserves translational invariance. Finally, when

$$\tilde{\eta}^2_{\text{crit}_2} \equiv 4\beta\left(1 - \frac{b}{\beta(c-1)}\right), \tag{5.31}$$

the vacuum solution is given by

$$(\varphi_0)^{III} = 0, \quad (\tilde{\chi}_0^2)^{III} = 1 + (c-1)\frac{\tilde{\eta}^2}{4b},$$

$$\tilde{E}^{III}_{vac} = \frac{16bc(c-1)\beta - ((c-1)\tilde{\eta}^2 + 8b)^2}{64bc(c-1)\beta}. \tag{5.32}$$

In this vacuum translational invariance is broken but local $U(1)$ gauge invariance is preserved, hence this vacuum does not support ANO vortices. The energy of the ground states as functions of η are shown in Figure 5.1.

In the opposite case where

$$\beta(c-1) < bc, \tag{5.33}$$

the minimizing vacuum is given by (5.30) when

$$\tilde{\eta}^2 < \tilde{\eta}^2_{\text{crit}_3} = \frac{\sqrt{(c-1)bc\beta} - b}{(c-1)}. \tag{5.34}$$

When $\tilde{\eta}$ crosses the critical value $\tilde{\eta}^2_{\text{crit}_3}$, there is a first order transition from vacuum (5.30) to vacuum (5.32). This pattern of ground states is depicted in Figure 5.2.

For this chapter we will focus our attention primarily on the vacuum I and vacuum II cases where the gauge $U(1)_{\text{gauge}}$ group is broken by a non-zero ϕ field. For vacuum II none of the global symmetries $SO(3)_J$ or T are broken in the ground state. For ANO vortices in this case, cholesteric behavior of the χ_i field will only appear in the vortex core. On the other hand vacuum I has an interesting symmetry structure appearing from a linear combination of the rotational J_z and translational p_z generators:

$$J'_z = J_z - \frac{p_z}{k}. \tag{5.35}$$

From (5.20) for non-zero χ_0 it is clear that J'_z annihilates the vacuum, and thus the vacuum I ground state retains a $U(1)_{J'_z}$ symmetry in addition to the subgroup T_{xy} of translations perpendicular to $\vec{k} = k\hat{z}$. We may thus write the symmetry group of the vacuum I

$$H_I = U(1)_{J'_z} \times T_{xy}. \tag{5.36}$$

The equivalence of translations and rotations about the z axis on the vacuum state implies an additional structure on the degeneracy space of vacua in vacuum I. Consider the coset space

$$G/H_I = U(1)_{\text{gauge}} \times S^2_{J_\perp} \times U(1)_{J''_z}/\mathbb{Z}_2, \tag{5.37}$$

where

$$J''_z \equiv J_z + \frac{p_z}{k} \tag{5.38}$$

is a generator of the $U(1)_{J''_z}$ group orthogonal to J'_z. Here $S^2_{J_\perp}$ is the two sphere of directions for the wave vector $\hat{k}$. The group $U(1)_{J''_z}$ generates non-trivial rotations of the vacuum about the wave vector $\vec{k}$. Physically the group $U(1)_{J''_z}$ represents degeneracy associated with rotations of $\vec{\chi}$ about $\vec{k}$. Alternatively, due to the equivalence of

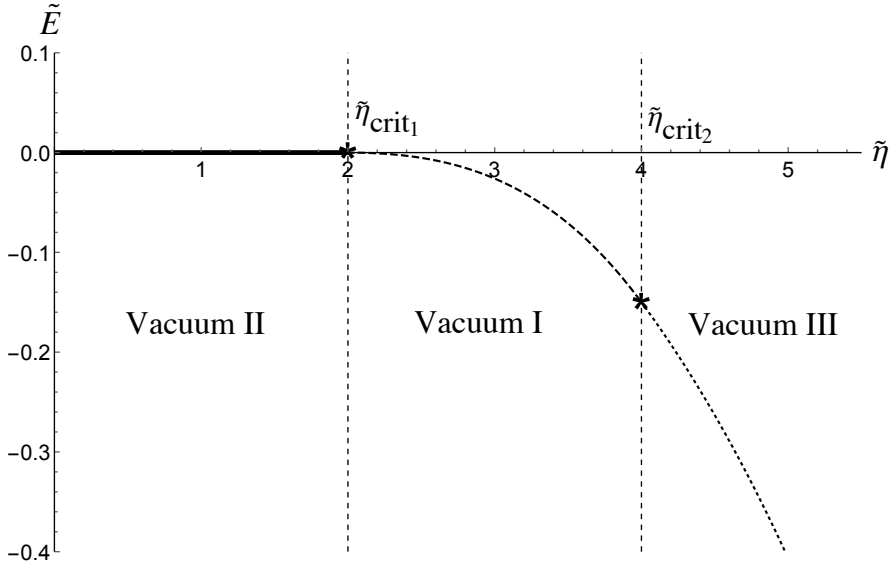

Figure 5.1: $b = 1,\ c = 1.25,\ \beta = 8$. Vacuum energy dependence on $\tilde{\eta}$ for $\beta(c-1) > bc$, the solid line corresponds to vacuum II, the dashed line to vacuum I and the dotted line to vacuum III.

translations and rotations, and the periodicity of the z translations of the vacuum, the $U(1)_{J_z''}$ may be viewed as a compactification of T_z.

Naively the topology of $S^2 \times U(1)/\mathbb{Z}_2$ supports only a $\mathbb{Z}_2$ winding. However, it was shown by [71] that for low energy excitations the generators J_x and J_y acquire a mass gap through an effective Higgs mechanism. For the vacuum state this implies that only a single Goldstone mode associated with phase rotations of the vacuum appear, instead of the naively expected three Goldstones from the three broken generators. Effectively we may write

$$G/H_I \to U(1)_{\text{gauge}} \times U(1)_{J_z''}. \tag{5.39}$$

The effective $U(1)_{J_z''}$ degeneracy of vacuum I implies an additional topological charge associated with the integer winding of a closed contour about the vortex axis. We will explore numerical solutions with this winding in the next section.

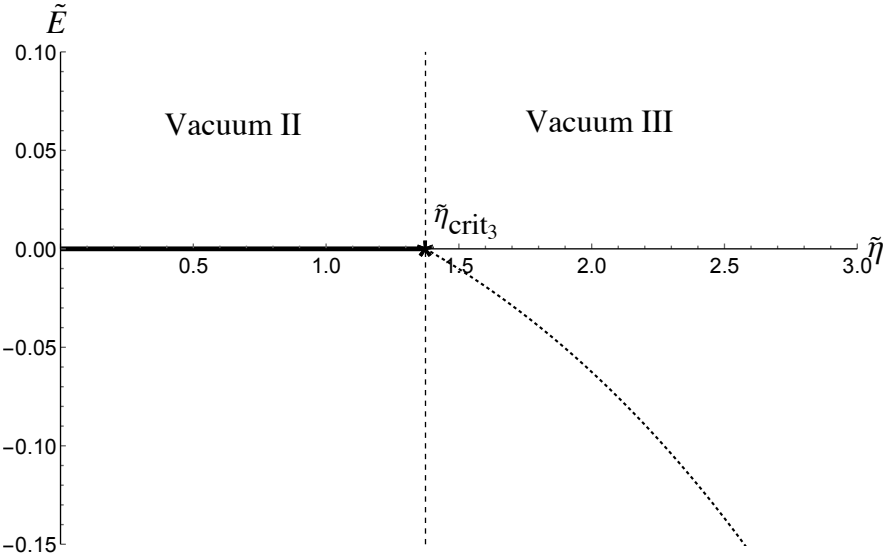

Figure 5.2: $b = 1,\ c = 1.25,\ \beta = 4$. Vacuum energy dependence on $\tilde{\eta}$ for $\beta(c-1) < bc$, the solid line corresponds to vacuum II and the dotted line to vacuum III.

5.4 Winding solutions

In [64] the full set of eight coupled second order three dimensional equations was solved with a pseudo-spectral numerical procedure (see [74] for a review of this method). The solution found, in which the spin field χ asymptotes to the vacuum at spatial infinity, describes a local $U(1)$ Abrikosov vortex with a cholesteric spiral inside its core. These vortices resemble the w vortices appearing in superfluid ^{3}He-B [70].

The degeneracy space $U(1)_{J_z''}$ allows for another class of solutions similar to the "spin-mass-vortices" (see [76, 77]) with a global $U(1)_{J_z''}$ winding, characterized by a dependence of the χ_i field on the polar angle θ at infinity. The θ dependence of χ_i at infinity is equivalent to translations of the vacuum state in the $\hat{k}$ direction. The compactified translational group allows for the topological integer winding about a closed spatial contour.

As a consequence of the global nature of these vortices the profile functions at large ρ are IR divergent and require a regularization. Nonetheless, these solutions are important in the context of superfluid ^{3}He [73]. We are interested in solutions with spontaneous breaking of gauge symmetry, hence we only consider vacua I and II below.

The geometry of our system is shown in Figure 5.3. In order to find the $U(1)_{J_z''}$ winding solutions we switch to axially symmetric coordinates and use the ansatz

$$\begin{aligned} \chi_i &= \frac{\mu}{\sqrt{2\beta}}(\chi_r(\rho,z),\tilde{\chi}_\theta(\rho,z),\chi_z(\rho,z)), \qquad (5.40)\\ A_r &= A_z = 0\,, \quad A_\theta = 1 - f(\rho)\,, \\ \phi &= v\varphi(\rho)\, e^{i\theta}\,. \qquad (5.41) \end{aligned}$$

Then extremization of the energy density gives the following equations,

$$\begin{aligned} &\frac{1}{\rho}\partial_\rho\left(\rho\partial_\rho\chi_z\right) + \partial_z^2\chi_z - \tilde{\eta}\left(\partial_\rho\tilde{\chi}_\theta + \frac{\tilde{\chi}_\theta}{\rho}\right) - \frac{b}{c-1}(c\varphi^2 + \vec{\chi}^2 - 1)\chi_z = 0,\\ &\frac{1}{\rho}\partial_\rho\left(\rho\partial_\rho\tilde{\chi}_\theta\right) + \partial_z^2\tilde{\chi}_\theta - \frac{\tilde{\chi}_\theta}{\rho^2} - \tilde{\eta}(\partial_z\chi_r - \partial_\rho\chi_z) - \frac{b}{c-1}(c\varphi^2 + \vec{\chi}^2 - 1)\tilde{\chi}_\theta = 0,\\ &\frac{1}{\rho}\partial_\rho\left(\rho\partial_\rho\chi_r\right) + \partial_z^2\chi_r - \frac{\chi_r}{\rho^2} + \tilde{\eta}\partial_z\tilde{\chi}_\theta - \frac{b}{c-1}(c\varphi^2 + \vec{\chi}^2 - 1)\chi_r = 0,\\ &\frac{1}{\rho}\partial_\rho(\rho\partial_\rho\varphi) + \partial_z^2\varphi - \left[\frac{1}{2}(\varphi^2-1) + \frac{1}{\rho^2}f^2 + \frac{b}{2\beta(c-1)}\vec{\chi}^2\right]\varphi = 0,\\ &\partial_\rho^2 f - \frac{1}{\rho}\partial_\rho f + \partial_z^2 f - a\varphi^2 f = 0. \qquad (5.42) \end{aligned}$$

We wish to solve the equations (5.42) with the following boundary conditions

$$\begin{aligned} \varphi(0) = 0, &\qquad \varphi(\infty) = \varphi_0,\\ f(0) = 1, &\qquad f(\infty) = 0,\\ \chi_z'(0,z) = 0, &\qquad \chi_z(\infty,z) = 0,\\ \chi_r(0,z) = 0, &\quad \chi_r(\infty,z) = \chi_0\cos\left(\tfrac{\eta}{2}z\right),\\ \tilde{\chi}_\theta(0,z) = 0, &\quad \tilde{\chi}_\theta(\infty,z) = \chi_0\sin\left(\tfrac{\eta}{2}z\right), \qquad (5.43) \end{aligned}$$

where χ_0 and φ are the same as the previous section and we demand continuity in the z direction. In terms of the cartesian vector this boundary condition takes the form

$$\chi_i = \chi_0\big\{\cos(kz+\theta),\ \sin(kz+\theta),\ 0\big\} \qquad (5.44)$$

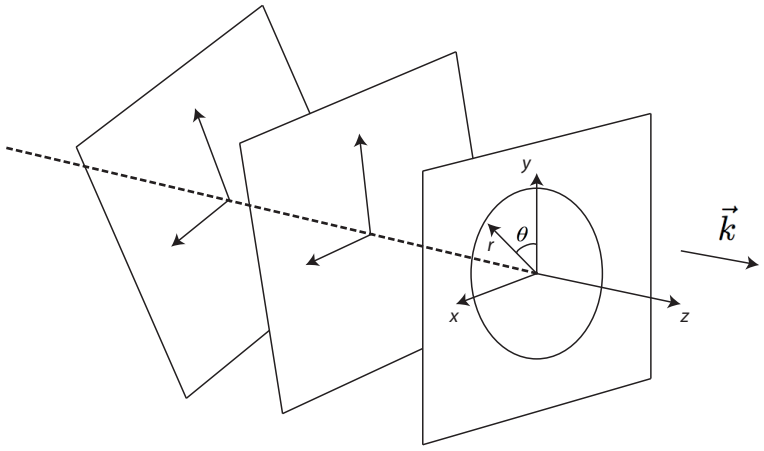

Figure 5.3: Geometric set-up of the problem. The vortex axis, in the z direction, is parallel to the wave-vector $\vec{k}$ which is normal to the cholesteric planes.

which is not to be confused with the $U(1)$ vortex solution of [64]. In fact, it is only because of this subtle difference between asymptotic conditions that the full set of three dimensional equations (5.17) becomes two dimensional. This greatly simplifies the numerical procedure.

5.4.1 Outline of numerical procedure

The reduction of the spatial dependence of the coupled system (5.42) from three to two coordinates greatly simplifies the numerical analysis by reducing the computing power needed. However, for precise numerical results, two dimensional finite difference methods are still impractical when efficiency and precision are the goals. To achieve these goals we chose instead to use a pseudospectral method on a collocated grid. In this section we will give a brief outline of our procedure. A detailed and very readable description of these methods can be found in [74].

For the z dependence of the functions defined above, we choose to expand in Fourier modes and evaluate the functions at the discrete points $z_m = 2\pi m/kM$, where M is

the total number of Fourier modes used in the decomposition. To decompose the r dependence in the functions above, we first compactify the radial direction using the transformation:

$$r = \frac{Lx}{\sqrt{1-x^2}}, \quad x \in [0,1]. \tag{5.45}$$

The parameter L determines the distribution of grid points. For this procedure we selected $L = 2$ to achieve the desired density of grid points near the origin. The radial dependence of the functions is then expanded in rational Chebyshev polynomials $T_n(x(r))$ on a collocated Radau grid:

$$x_p = \sin \frac{\pi(2p-1)}{4N-2}, \quad n \in [1,N], \tag{5.46}$$

where N is the total number of Chebyshev polynomials used in the decomposition. The Radau grid allows for boundary conditions to be imposed at spatial infinity with no conditions required at the origin. For functions required to vanish at the origin we expand in odd Chebyshevs.

The pseudospectral decomposition allows the equations (5.42) to be written as a set of algebraic equations to be solved for the coefficients in the expansion. For the five functions to be solved for above, this amounts to solving a coupled system of $5 \times N \times M$ polynomial equations. To approximate a solution the system is linearized and solved recursively. Each iteration of the procedure is repeated until convergence is achieved.

5.4.2 Vacuum I

Let us first consider solutions in which $\chi_0 \neq 0$. In this case the vacuum of the system is vacuum I, given by (5.28). Clearly in this case the solutions with boundary conditions (5.43) don't approach the vacuum at infinity and are logarithmically divergent in the IR. These solutions require an IR regularization. We restrict our solutions to a finite radial distance L. The winding of these spin-vortices ensures their topological stability. It should be pointed out that near the vortex core a non-zero value of χ_z appears due to the variation of χ_θ in the radial direction.

For parameter values $a = 1,\ b = 1,\ c = 1.25,\ \beta = 8$, and $\eta = 2.5$ we obtain the solutions shown in Figures 5.4-5.6.

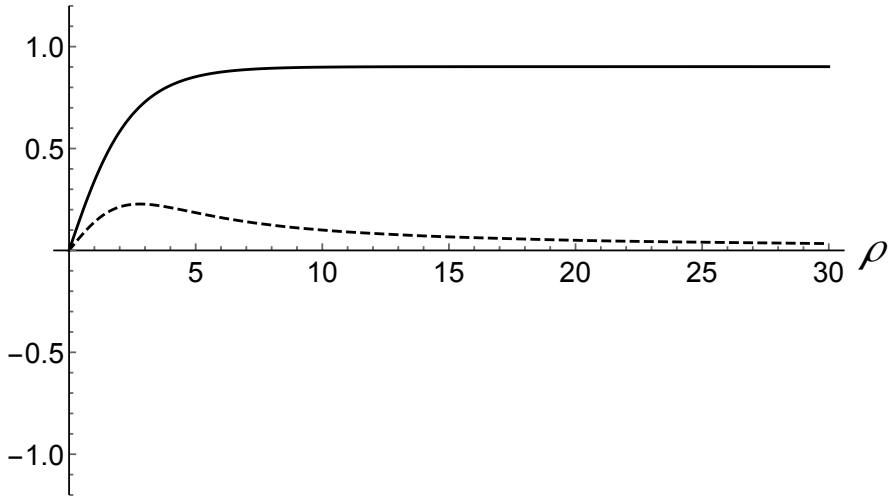

Figure 5.4: The graph shows the solutions for $\phi(r)$ (solid) and $A_\theta(r)$ (dashed) at $z = 0$, for $\eta = 2.5$. These solutions have negligable z dependence.

5.4.3 Vacuum II

When $\chi_0 = 0$ the vacuum has the structure of vacuum II (5.30). In this case, the asymptotics of the solutions (5.43) have no cholesteric structure and thus we expect finite energy solutions. However, the winding nature of these solutions is lost. These solutions lack the topological stability of the previous case in vacuum I. They are instead metastable solutions whose topological stability is only supported to finite radial distance from the core. Presumably, these solutions will decay to the zero winding state through quantum tunneling via bubble nucleation. We leave an investigation of the tunneling rate to another project. Figures 5.7-5.9 illustrate these solutions for $a = 1,\ b = 1,\ c = 1.25,\ \beta = 8$, and $\eta = 2.2$.

5.5 Low energy theory of vortex moduli

To complete the analysis of the spin vortices in vacuums I and II, we discuss the low energy dynamics of their excitations localized on the vortex core. In [64] the low energy expansion was done at least for small η for both the translational (Kelvin) and orientational moduli appearing in vacuum I and II. Here we will do an analogous treatment for the case of vacuum I spin vortices only. The moduli appearing in vacuum

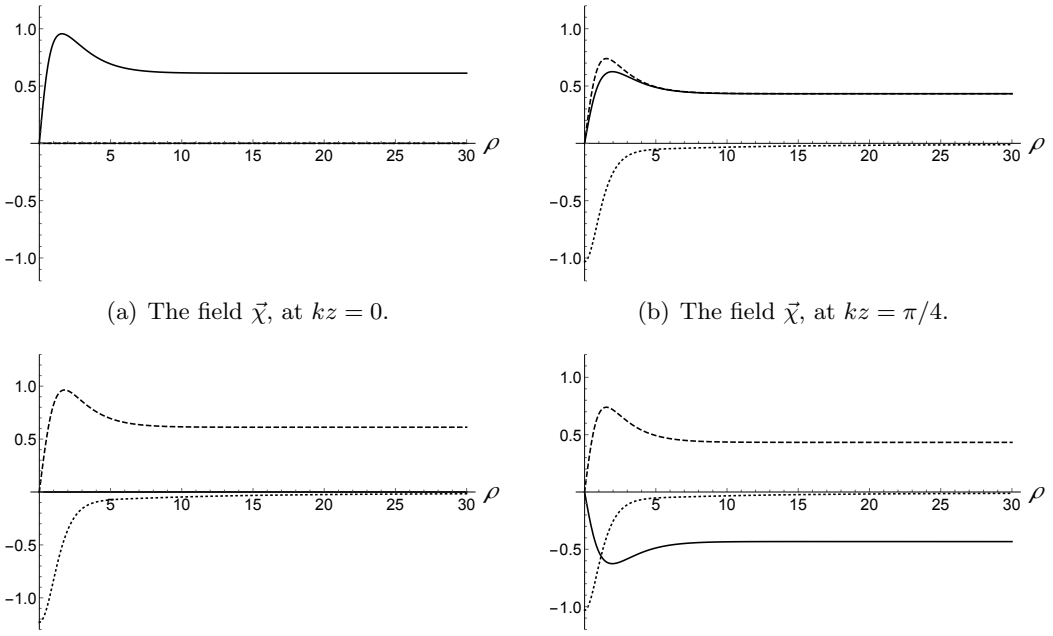

(a) The field $\vec{\chi}$, at $kz = 0$.

(b) The field $\vec{\chi}$, at $kz = \pi/4$.

(c) The field $\vec{\chi}$, at $kz = \pi/2$.

(d) The field $\vec{\chi}$, at $kz = 3\pi/4$.

Figure 5.5: The graphs show the radial dependence of χ_r (solid), χ_θ (dashed), and χ_z (dotted) at various values of kz.

II are difficult to analyze due to the coupling of all translational and orientational modes, and give little additional physical information. We will content ourselves with a brief topological analysis of the vacuum II case, leaving the details for future work.

It is best to consider topological arguments at first to provide a guide in the search for the gapless excitations appearing on the vortex core. We begin with vacuum I where the non-zero value of the spin field χ_i breaks the translation symmetry in the z direction. The global symmetry group of the lagrangian (5.6) is given by

$$G_{\text{global}} = SO(3)_J \times T \tag{5.47}$$

where T represents the three dimensional translational symmetry. In vacuum I the ground state is invariant to the symmetry group

$$H_I = U(1)_{J'_z} \times T_{xy} \subset G_{\text{global}}. \tag{5.48}$$

However, in the asymptotic limit $r \to \infty$ the vortex posseses complete axial symmetry

$$H_I' = U(1)_{J_z} \times T_{xy}. \tag{5.49}$$

Gapless excitations of the vortex must appear from generators of H_I' that are broken in the core. All other modes appearing from the generators of G_{global} would have infinite tension in the kinetic terms. They would not be normalizable.

In the previous section we found vortex solutions by assuming rotational symmetry about the z-axis. Thus, since the vortex solutions automatically break the translations in the x and y directions, our vortex solutions obey the symmetry group

$$H_{I,\text{vortex}}' = U(1)_{J_z}. \tag{5.50}$$

Thus, the degernacy space of the vortex solutions in vacuum I follow from

$$H_I'/H_{I,\text{vortex}}' = (U(1)_{J_z} \times T_{xy})/U(1)_{J_z} = T_{xy}. \tag{5.51}$$

We should thus find two moduli fields $\xi_{x,y}(t,z)$ associated with the broken translational symmetries by the vortex axis. These moduli will however acquire a mass gap $m \sim 1/R$ due to the IR cutoff imposed at large distances R from the vortex core. The details will be shown below.

For the case of vacuum II the cholesteric structure does not appear in the vacuum and thus the full symmetry group of vacuum II is given by:

$$H_{II} = G_{\text{global}} = SO(3)_J \times T. \tag{5.52}$$

As in the case of vacuum I the vortex preserves the subgroup $SO(2)_{J_z}$ thus the degeneracy space is:

$$H_{II}/H_{II,\text{vortex}} = (SO(3)_J \times T)/U(1)_{J_z} = S^2_{J_\perp} \times T. \tag{5.53}$$

In this case the cholesteric structure only appears in the vortex core and thus an additional longitudinal translational mode appears on the vortex. The expansion of the low energy Lagrangian in terms of the gapless modes introduces additional interactions between the translational and orientational modes. We have omitted this topic for sake of clarity and space.

We proceed with the analysis by expanding the lagrangian by the small adiabatic translations $\xi_{x,y}(t,z)$ of the vortex solution

$$\begin{aligned}
&\phi(\vec{x}) \to \phi(\vec{x} - \vec{\xi}(t,z)) \\
&A_\mu(\vec{x}) \to A_\mu(\vec{x} - \vec{\xi}(t,z)) \\
&\vec{\chi}(\vec{x}) \to \vec{\chi}(\vec{x} - \vec{\xi}(t,z)).
\end{aligned} \tag{5.54}$$

Here $\vec{\xi}(t,z)$ only oscillates along the directions x and y perpendicular to the vortex axis. Proceding with the expansion of (5.11) we arrive at the low energy theory

$$\delta^2 E = S_{ab}\partial_z\xi_a\partial_z\xi_b + A\epsilon_{ab}\xi_a\partial_z\xi_b, \tag{5.55}$$

where a and b are indices for the x and y directions. The symbol $\epsilon_{ab} = -\epsilon_{ba}$ is the two dimensional antisymmetric symbol. The parameters S_{ab} and A are given by

$$\begin{aligned}
S_{ab} &= \int d^2x_\perp \partial_a\chi_i\partial_b\chi_i, \\
A &= \frac{1}{2}\epsilon_{ab}\int d^2x_\perp \left(2\partial_z\partial_a\chi_i\partial_b\chi_i + \eta\epsilon_{nm}\partial_a\chi_n\partial_b\chi_m\right).
\end{aligned} \tag{5.56}$$

Here m and n run over the x and y indices. We point out that S and A are in general functions of the z coordinate, owing to the dependence of the spin field χ^i on z.

The expansion in (5.55) considered only the kinetic terms in $\xi_a(t,z)$. We hasten to point out that this expansion is only valid up to the infrared regularization of our vortex solution far from the core. However, due to the global nature of the spin vortex, the hard cutoff of the vortex solution in the infrared leads to a non-local boundary contribution to the low energy theory. The infrared cutoff explicitly breaks the translational symmetry in the x and y directions and thus our low energy theory should include mass terms proportional to the inverse cutoff $m \sim 1/R$:

$$\delta^2\mathcal{L}_{\rm IR} = S_{ab}\dot{\xi}_a\dot{\xi}_b - S_{ab}\partial_z\xi_a\partial_z\xi_b - A\epsilon_{ab}\xi_a\partial_z\xi_b - m^2\xi_a\xi_a. \tag{5.57}$$

The details of the calculation of m^2 are given in the appendix. For a cylindrical boundary find that

$$m^2 = -\pi\frac{\chi_0^2}{R^2}, \tag{5.58}$$

and hence the mass term is negative implying an instability of the vortex solution. We should point out however, that this value for m^2 is dependent on the shape of the

boundary. For non-rotationally symmetric boundaries, the mass term will in fact be tensorial:

$$m^2 \to m^2_{ab}. \tag{5.59}$$

We consider only the rotationally symmetric boundary.

For relativistic lagrangians this instability means the vortex wants to escape the finite volume. For non-relativistic cases, the negative mass implies a threshold for the dispersion relations where the Kelvin modes change their direction of propagation [55].

For the equation (5.57) the more appropriate context to consider is the relativistic case - although this is not strictly a relativistic system because the third term in (5.57) is not Lorentz invariant. There are two important limits in this system characterised by the wavelength of the modes λ compared to that of the cholesteric structure k^{-1}. In the limit in which $\lambda \gg 1/k$ the asymptotic values of the χ^i field dominates the integral appearing in (5.56), the z dependence of S_{ab} disappears and we have that $A = 0$ identically. The long wavelength modes effectively ignore the "high" k structure of the vortex. As $\lambda \sim 1/k$ the wavelengths become comparable and we may no longer ignore the z dependence of S_{ab}. Clearly, $A \neq 0$ in this limit. This region becomes difficult to tackle analytically and we won't consider it further. We may however approximate an intermediate region in which $\lambda > 1/k$ where the z dependence of S_{ab} and A is small but $A \neq 0$. Then, varying (5.57) and using the isotropicity of the matrix S ($S_{xx} = S_{yy}$ and $S_{xy} = S_{yx}$) we obtain the equation

$$S_{ac}\left(\xi''_a - \ddot{\xi}_a\right) + A\epsilon_{ac}\xi'_a - m^2\delta_{ac}\xi_a = 0. \tag{5.60}$$

Taking the ansatz

$$\xi_a = C_1 e^{i(kz+\omega t)}\tilde{\xi}_a, \tag{5.61}$$

where $\tilde{\xi}_a$ is a constant vector, we may reduce this to

$$M_{ab}\tilde{\xi}_b = 0, \tag{5.62}$$

with

$$M_{ab} = \left(S_{ab}(\omega^2 - k^2) + Ai\epsilon_{ab}k - m^2\delta_{ab}\right), \tag{5.63}$$

for the vector components of $\tilde{\xi}_a$. Finding the corresponding modes is therefore equivalent to finding the zero eigenvalues of the matrix M_{ab}. The eigenvalues are

$$\omega^2_{\pm} = (\omega^2 - k^2)S_{yy} - m^2 \pm \sqrt{(Ak)^2 + ((k^2 - \omega^2)S_{yx})^2}, \tag{5.64}$$

setting these to zero gives four solutions for ω,

$$\omega_1^2 = \frac{k^2\left(S_{yx}^2 - S_{yy}^2\right) - m^2 S_{yy} + \sqrt{(AkS_{yy})^2 + S_{yx}^2\left(m^4 - (Ak)^2\right)}}{S_{yx}^2 - S_{yy}^2} \tag{5.65}$$

$$\omega_2^2 = \frac{k^2\left(S_{yx}^2 - S_{yy}^2\right) - m^2 S_{yy} - \sqrt{(AkS_{yy})^2 + S_{yx}^2\left(m^4 - (Ak)^2\right)}}{S_{yx}^2 - S_{yy}^2}. \tag{5.66}$$

In order to describe stable non-dissipating modes the solutions for ω must be real. These relations thus give inequalities required for the particular ω mode to be stable.

The (un-normalized) eigenvectors are

$$\xi_\pm = \begin{pmatrix} \pm\dfrac{i\sqrt{(Ak)^2 + ((k^2-\omega^2)S_{yx})^2}}{Ak - i(k^2-\omega^2)S_{yx}} \end{pmatrix} \tag{5.67}$$

which define the diagonal basis as

$$\xi_{\text{diag}} = \left(-\frac{Ak - (k^2-\omega^2)S_{yx}}{\sqrt{-(Ak)^2 + (k^2-\omega^2)^2 S_{yx}^2}}(\tilde{\xi}_x - \tilde{\xi}_y),\ \ \tilde{\xi}_x + \tilde{\xi}_y \right). \tag{5.68}$$

The limit $\lambda \gg 1/k$ corresponds to

$$S_{ab} \to \pi\chi_0^2 \log\frac{R}{r_0}\delta_{ab}, \text{ and } A \to 0. \tag{5.69}$$

where r_0 represents the coherence length of the vortex core. In this limit the system is Lorentz invariant and we find the dispersion relation:

$$\omega = \pm\sqrt{k^2 - \Delta^2}, \text{ where } \Delta^2 = \frac{1}{R^2 \log R/r_0}. \tag{5.70}$$

Here $2\pi/\Delta \equiv \lambda_c$ is the critical wavelength of stability. Modes with wavelengths longer than λ_c have purely imaginary ω and are thus tachyonic. For the specific case $k = 0$ the mode represents a complete transverse translation of the vortex solution. Thus the vortex tends to escape from the finite volume. On the other hand wavelengths shorter than λ_c are real and thus represent stable solutions for the vortex [55].

In the proximicity of the long wavelength limit, where we may still consider equation (5.60) as a good approximation for the low energy modes, higher order terms in the S_{ab}

and A calculation need to be included. Even though we don't perform this computation explicitly we note the main important feature of having a non-zero A: it introduces terms in the dispersion relation of the form $\omega \propto \sqrt{k}$, which is characteristic of surface waves in deep water. Finally, leaving the long-wavelength limit entirely equation (5.60) can no longer be trusted and one is forced to resort to numerics. We leave this treatment to a future publication.

5.6 Conclusions

The goal of this chapter was to consider an extension of the analysis presented in [64] where mass vortices with a $U(1)_{\text{gauge}}$ charge were considered in systems with cholesteric vacuum structure. Such vortices play a role in many contexts including supersymmetric solitons [66], type II superconductors [66], and superfluid ^{3}He [70]. In the current chapter, we extended the analysis to include a different type of vortex, which supported a global topological $U(1)_{J_z''}$ charge in addition to the $U(1)_{\text{gauge}}$ charge. Spin vortices of a similar description were first observed in superfluid ^{3}He [76, 77]. However, for the cholesteric vacuum state we have discussed above, the equivalence of rotations and translations along the z direction in the vacuum leads to a reduction of the degeneracy space $SO(3)_J \to U(1)_{J_z''}$.

Due to the cholesteric behavior of the vacuum I solution, the $U(1)_{J_z''}$ vortices are stable to deformation [71]. The low energy effective field theory of these vortices thus gives rise to a $1+1$ dimensional field theory of translational excitations. A similar result is true in vacuum II, however the solutions here are free to tunnel to solutions with no $U(1)_{J_z''}$ charge since the asymptotic form of the vacuum has no cholesteric structure. We have left a calculation of the tunneling process to future work.

We have focused our attention on the classical description of the $1+1$ dimensional effective field theory of gapless excitations. Specifically, we've calculated the low energy Lagrangan for Kelvin modes of vortices in vacuum I in the long-wavelength limit. For a relativistic dispersion relation a classical analysis is all that is necessary to count Goldstone modes appearing on the vortex. However, for the non-relativistic despersion relation, the quantization of modes becomes more complicated. Some general results for non-Lorentz invariant systems are discussed in [35, 78], and to systems with broken

spacetime symmetries in [50, 51, 61, 79], however we have omitted a detailed analysis here. We have however explored the effects of a finite volume on the gapless excitations appearing on the vortex as was first pointed out in [55]. In particular, the global behavior of the vortex solution in vacuum I lifts the translational degeneracy, and mass gaps are generated for the Kelvin excitations.

For vacuum II additional orientational modes appear on the vortex, however the details of these modes have added complications and we have left their analysis to future projects.

5.6.1 Appendix

In this appendix we wish to show the details of the calculation of the boundary terms leading to the mass term appearing for the translational moduli in (5.57). We will first show that the linear term in ξ_i vanishes, confirming that no instabilities appear on the vortex. Following this calculation we will expand to second order in ξ_i and determine the mass term for the particular vortex configuration.

We begin with a calculation of the linear term for the expansion parameter ξ, which we may take to be constant. The t and z dependence is accounted for in the kinetic terms shown in (5.55). To first order in $\delta\chi_i = -\xi_a \partial_a \chi_i$

$$\begin{aligned}
\delta E &= 2\partial_i(\delta\chi_j \partial_i \chi_j) + \eta\varepsilon_{ijk}(\delta\chi_i \partial_j \chi_k + \chi_i \partial_j \delta\chi_k) + \delta\chi_i \frac{\partial V}{\partial \chi_i} \\
&= 2\partial_i \left(\delta\chi_j \partial_i \chi_j - \frac{\eta}{2}\varepsilon_{ijk}\chi_j \delta\chi_k\right) \\
&\quad +2\delta\chi_i \left(-\partial^2 \chi_i + \eta\varepsilon_{ijk}\partial_j \chi_k + \frac{1}{2}\frac{\partial V}{\partial \chi_i}\right) \\
&= -2\xi_a \partial_i \left(\partial_a \chi_j \partial_i \chi_j + \frac{\eta}{2}\varepsilon_{ijk}\partial_a \chi_j \chi_k\right), \qquad (5.71)
\end{aligned}$$

where the second line in the second equality vanished by the equations of motion for χ_i. To obtain the contribution of the linear term to the low energy theory, we integrate over the perpendicular directions x and y:

$$\begin{aligned}
\delta E &\rightarrow -2\xi_a \int d^2 x_\perp \partial_i \left(\partial_a \chi_j \partial_i \chi_j + \frac{\eta}{2}\varepsilon_{ijk}\partial_a \chi_j \chi_k\right) \\
&= -2\xi_a \int d\theta\, R\, \hat{r}_i \left(\partial_a \chi_j \partial_i \chi_j + \frac{\eta}{2}\varepsilon_{ijk}\partial_a \chi_j \chi_k\right), \qquad (5.72)
\end{aligned}$$

where we have used Greens theorem, and $\hat{r}$ is the unit vector in the radial direction.

At this point we may substitute the asymptotic form of χ_i. Ignoring the z dependence

$$\chi_i \to \chi_0 \frac{x_i}{r} \text{ and } \partial_j \chi_i \to \left(\frac{\delta_{ij}}{r} - \frac{x_i x_j}{r^3} \right) \tag{5.73}$$

Inserting this into the equation above we find that the linear term identically vanishes as required.

We now proceed to calculate the second order contribution to the energy density

$$\begin{aligned} \delta^2 E &= \partial_j \delta\chi_i \partial_j \delta\chi_i + \eta \varepsilon_{ijk} \delta\chi_i \partial_j \delta\chi_k + \frac{1}{2} \frac{\partial^2 V}{\partial\chi_i \partial\chi_j} \delta\chi_i \delta\chi_j \\ &= \partial_j \left(\delta\chi_i \partial_j \delta\chi_i \right) + \delta\chi_i \left(-\partial^2 \delta\chi_i + \eta \varepsilon_{ijk} \partial_j \delta\chi_k + \frac{1}{2} \frac{\partial^2 V}{\partial\chi_i \partial\chi_j} \delta\chi_j \right). \end{aligned} \tag{5.74}$$

Inserting $\delta\chi_i = -\xi_a \partial_a \chi_i$

$$\begin{aligned} \delta^2 E &= \xi_a \xi_b \partial_i \left(\partial_a \chi_j \partial_i \partial_b \chi_j \right) \\ &\quad + \xi_a \xi_b \partial_a \chi_i \partial_b \left(-\partial^2 \chi_i + \eta \varepsilon_{ijk} \partial_j \chi_k + \frac{1}{2} \frac{\partial V}{\partial \chi_i} \right) \\ &= \xi_a \xi_b \partial_i \left(\partial_a \chi_j \partial_i \partial_b \chi_j \right), \end{aligned} \tag{5.75}$$

where we have used the equation of motion in the last line.

We may now integrate over the perpendicular coordinates and use Green's theorem:

$$\delta^2 E \to \xi_a \xi_b \int d^2 x_\perp \partial_i \left(\partial_a \chi_j \partial_i \partial_b \chi_j \right) = \xi_a \xi_b \int d\theta R \, \hat{r}_i \partial_a \chi_j \partial_i \partial_b \chi_j \tag{5.76}$$

Finally, we insert the asymptotic form of χ_i in (5.73) and find

$$\delta^2 E = -\frac{\pi \chi_0^2}{R^2} \xi_a \xi_a. \tag{5.77}$$

This particular value of m^2 was determined from our particular choice of boundary contour. Depending on the boundary conditions, this term may be modified and may even be tensorial depending on the symmetries of the contour choice. However, by dimensional analysis we are guaranteed to have

$$m_{ab}^2 \sim -\frac{\chi_0^2}{R^2}. \tag{5.78}$$

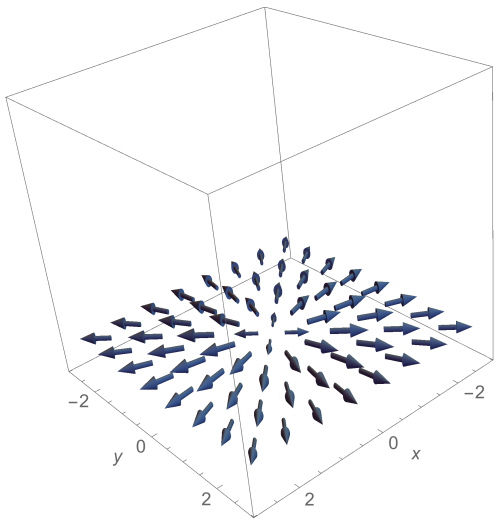

(a) The field $\vec{\chi}$, at $kz = 0$.

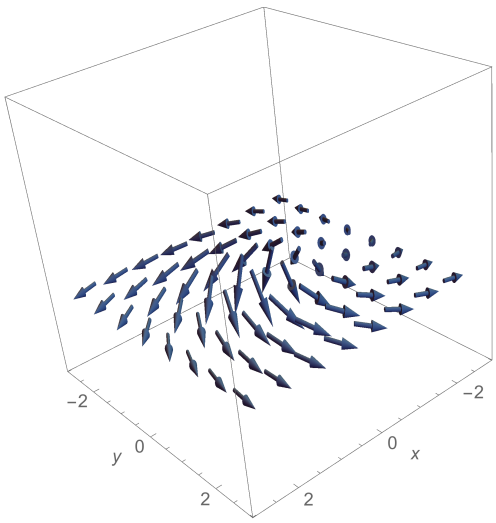

(b) The field $\vec{\chi}$, at $kz = \pi/4$.

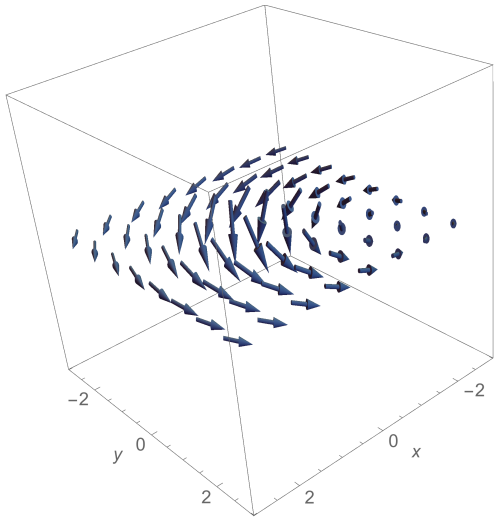

(c) The field $\vec{\chi}$, at $kz = \pi/2$.

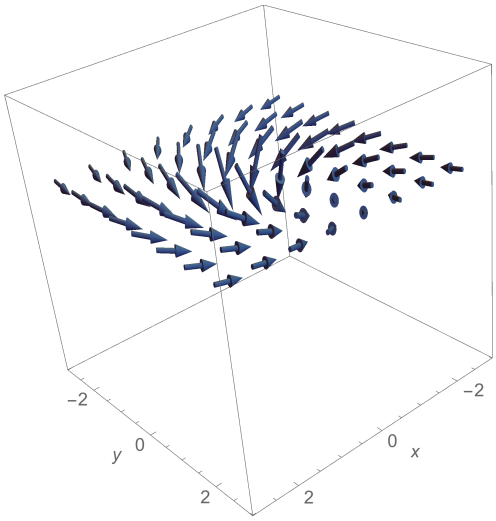

(d) The field $\vec{\chi}$, at $kz = 3\pi/4$.

Figure 5.6: Shown are the vector fields $\vec{\chi}$ at various values of the coordinate $z \in [0, 3\pi/4k]$ for $\eta = 2.5$. We note that as the vortex core is approached a non-zero value of χ_z appears. This is expected from the equations of motion when χ_θ has an r-dependence near the core.

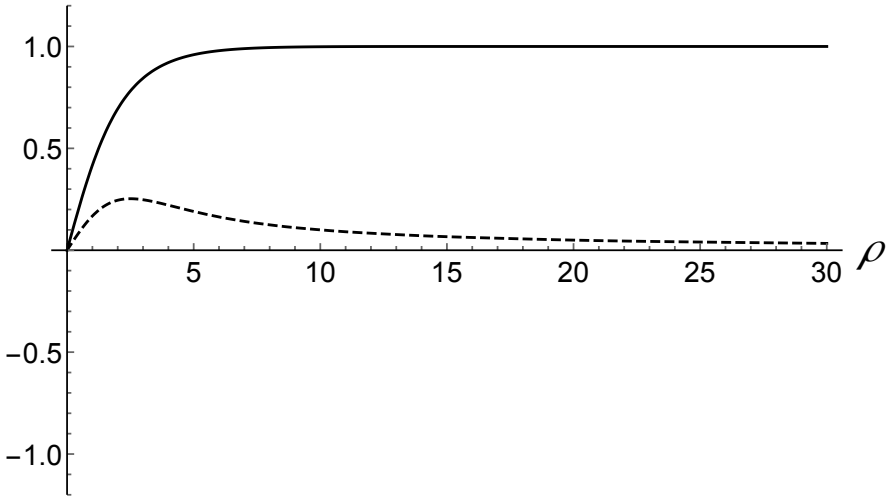

Figure 5.7: The graph shows the solutions for $\phi(r)$ (solid) and $A_\theta(r)$ (dashed) at $z = 0$, for $\eta = 2.2$. These solutions have negligable z dependence.

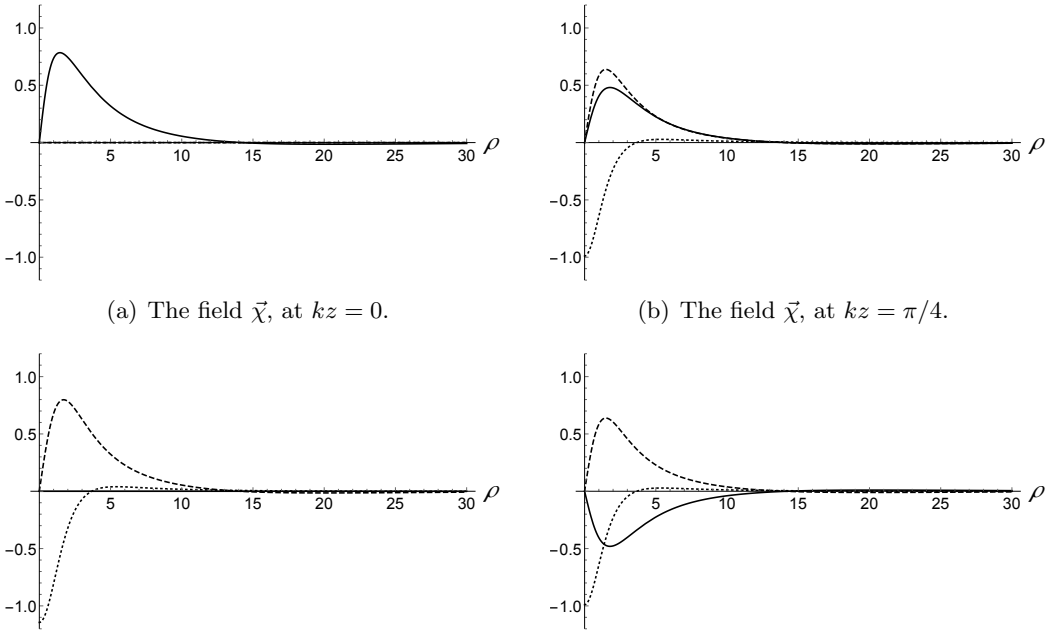

(a) The field $\vec{\chi}$, at $kz = 0$.

(b) The field $\vec{\chi}$, at $kz = \pi/4$.

(c) The field $\vec{\chi}$, at $kz = \pi/2$.

(d) The field $\vec{\chi}$, at $kz = 3\pi/4$.

Figure 5.8: The graphs show the radial dependence of χ_r (solid), χ_θ (dashed), and χ_z (dotted) at various values of kz.

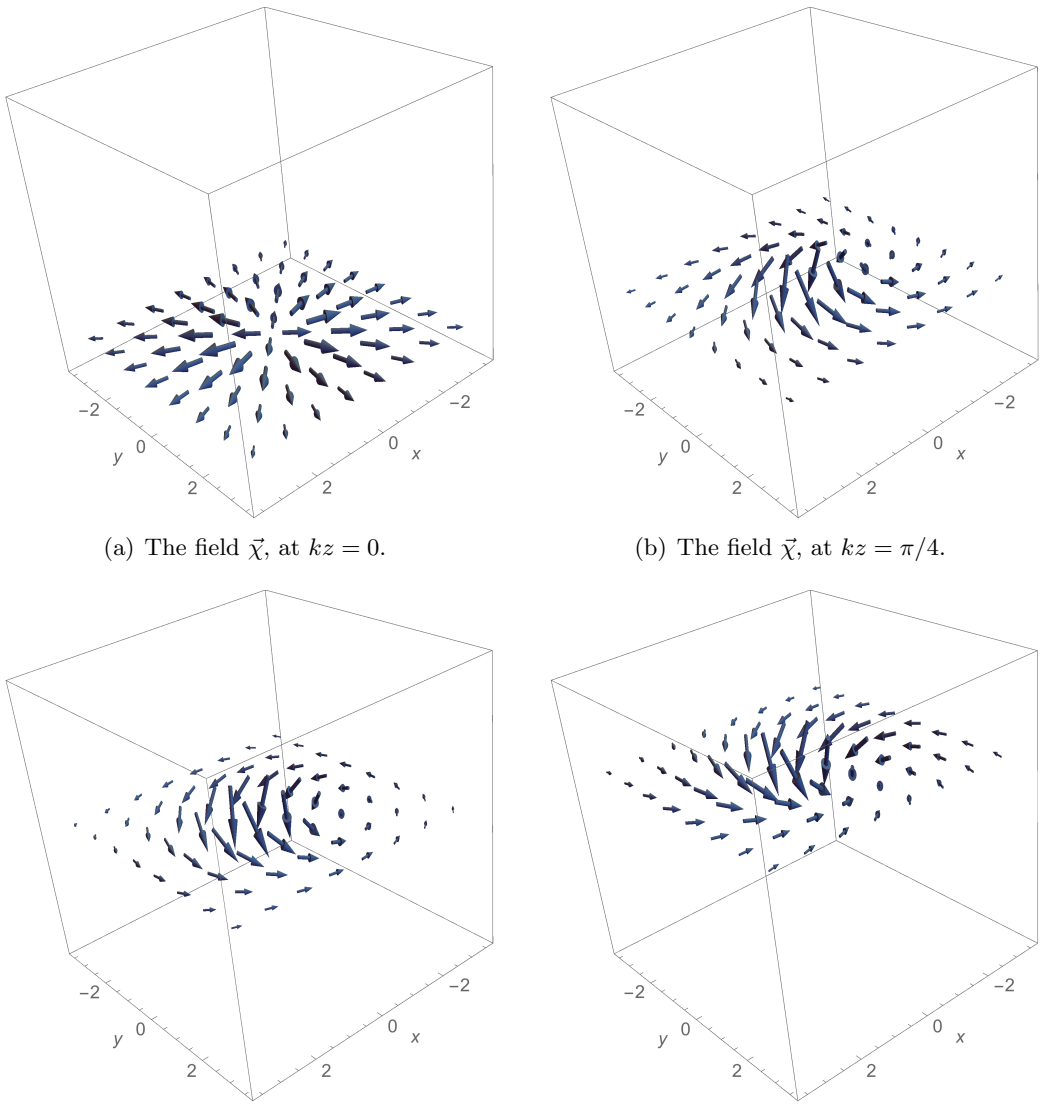

(a) The field $\vec{\chi}$, at $kz = 0$.

(b) The field $\vec{\chi}$, at $kz = \pi/4$.

(c) The field $\vec{\chi}$, at $kz = \pi/2$.

(d) The field $\vec{\chi}$, at $kz = 3\pi/4$.

Figure 5.9: Shown are the vector fields $\vec{\chi}$ at various values of the coordinate $z \in [0, 3\pi/4k]$ for the critical point $\eta = 2$. We note that as the vortex core is approached a non-zero value of χ_z appears. This is expected from the equations of motion when χ_θ has an r-dependence near the core.

Chapter 6

Conclusion and Discussion

The goal of this dissertation has been to illustrate the process of exploring the low energy dynamics of $1+1$ dimensional models. In the cases considered in this work, the $1+1$ dimensional models emerged from a $3+1$ dimensional bulk theory that was inspired by a particular model appearing in condensed matter physics, or examples constructed from superconductivity, superfluidity, or materials sciences. This method of understanding the low energy excitations of a bulk theory is not new from the perspective of high energy theory. Vortices are ubiquitous in models such as $U(1) \times SU(N)$ gauge theories in four dimensions, where they are presented as flux tube strings [8, 9, 10, 11, 12, 13]. It is well known that the dynamics of these flux tubes contain non-Abelian gapless excitations in addition to the well known Kelvin excitations due to the broken translational symmetry of the vortex axis. More recently it was also shown how a low energy analysics of supersymmetric $1+1$ dimensional models with connected $SU(N)$ or $O(N)$ symmetries at large N can explain the non-breaking of supersymmetry in those models where the Witten index vanishes [82, 83]. However, these techniques have not appeared within the condensed matter or materials science community to the best of our knowledge. It is thus interesting to see whether new predictions about well known condensed matter systems can be made by applying methods of high energy theory.

We have made an effort to show how similar dynamics may appear in systems similar to the vortices emerging in the B phase of superfluid ^{3}He. In this case, we have shown that non-Abelian excitations of $1+1$ dimensional vortices may only appear due to the enhanced rotational symmetries $SO(3)_{L_{\text{ext}}} \times SO(3)_{L_{\text{int}}} \times SO(3)_S$, where the internal

(spin) degrees of freedom are independent of the external symmetries that rotate the vortex profile non-locally. In the specific case of superfluid ^{3}He-B this enhancement is not observed at any point in the phase diagram to our knowledge, and thus non-Abelian gapless excitations of the vortex string are not observed. At this point, it is not clear how this enhanced symmetry could be experimentally enforced within the context of superfluid ^{3}He-B, however other systems have been shown to produce similar enhancements of rotational symmetries such as ultra cold fermi gases, or theories of elasticity under certain conditions involving conformal and scale symmetries [22].

If such a system with the correct enhancement of rotational symmetries could be constructed experimentally, it will be interesting to determine how non-Abelian excitations could be detected in the laboratory. We have made no attempt to make an experimentally testable prediction from our results, however our findings suggest approaches for future investigations. In particular, the quantization of the non-Abelian vortex excitations presents a specific form for the dispersion relations and number of independent gapless modes that should be localized on the vortex axis. This signiture of excitation number and dispersion is required from the analysis of collective coordinates when there is no Lorentz symmetry [34, 35, 36]. It is conceivable that the dispersion relation could be investigated from X-ray scattering experiments. On the other hand, finite temperature investigations of specific heat of vortex lattices should reveal the number of gapless degrees of freedom localized on the vortices in addition to the translational degrees of freedom, and excitations of the bulk. A finite temperature analysis of such systems is left for future research projects.

We have also discussed the behaviour of two types of vortices appearing in the hypothetical models with cholesteric vacua in chapters 4 and 5. These discussions lead to interesting results about the behavior of vortices due to the cholesteric behavior of their cores. However, on our way to determining the low energy effective theory of the vortex excitations, we have left a thorough investigation of the stability of the vortices in the cholesteric vacuum. In particular, it remains an open question on the conditions that a stable vortex exists in the vacuum with axis oriented along the wave vector $\vec{k}$ of the cholesteric vacuum. A purely analytical answer to this question has proven to be difficult to achieve, and a numerical analysis is only useful for determining local stability of the vortex core. At present it is unclear what configuration of the vortex is the most

stable, and future work could be devoted to this topic.

Our discussion of numerical techniques for the case of vortices in the Abelian-Higgs model has also lead to an investigation of vortex lattices in similar models. It has become apparent that the power of the numerical methods used in this dissertation could be used to understand how vortex lattices are formed, and the discrete symmetries they contain. A current analysis of these topics is currently underway by the author and collaborators.

References

[1] G. t Hooft, C. Itzykson, A. Jaffe, H. Lehmann, P. K. Mitter, I. M. Singer, R. Stora, and K. Cahill. Physics Today **34**, 83 (1981).

[2] M. Shifman, *Advanced topics in quantum field theory. : A lecture course*, Cambridge: Cambridge University Press (2012).

[3] G. E. Volovik, Int. Ser. Monogr. Phys. **117**, 1 (2006).

[4] D. Vollhardt and P. Wolfle, *The superfluid phases of helium 3*, Courier Corporation (2013).

[5] M. Tinkham, *Introduction to superconductivity*, Courier Corporation (1996).

[6] A.J. Peterson, M. Shifman, J. Phys.: Condens. Matter **26**, 075102 (2014).

[7] E. Babaev, L. D. Faddeev and A. J. Niemi, Phys. Rev. B **65**, 100512 (2002).

[8] A. Gorsky, M. Shifman and A. Yung, Phys. Rev. D **71**, 045010 (2005).

[9] A. Hanany and D. Tong, JHEP **0307**, 037 (2003).

[10] R. Auzzi, S. Bolognesi, J. Evslin, K. Konishi and A. Yung, Nucl. Phys. B **673**, 187 (2003).

[11] M. Shifman and A. Yung, Phys. Rev. D **70**, 045004 (2004).

[12] A. Hanany and D. Tong, JHEP **0404**, 066 (2004).

[13] M. Eto, Y. Isozumi, M. Nitta, K. Ohashi and N. Sakai, Phys. Rev. Lett. **96**, 161601 (2006).

[14] M. Nitta, M. Shifman and W. Vinci, Phys. Rev. D **87**, 081702 (2013).

[15] W. Thomson Phil. Mag. **10** 155 (1880).

[16] E. B. Sonin, Rev. Mod. Phys. **59**, 87 (1987).

[17] T. Simula, T. Mizushima and K. Machida, Phys. Rev. Lett. **101**, 020402 (2008).

[18] E. Fonda, D. Meichle, N. Ouellette, S. Hormoz, K. Sreenivasan and D. Lathrop, *preprint* arXiv:1210.5194.

[19] M. Krusius, Physica **B126**, 22 (1984).

[20] J. Pekola and J. Simola, J. Low. Temp. Phys. bf 58, 555 (1985).

[21] P. Hakonen,M. Krusius, M. Salomaa,J. Simola,Y. Bunkov, V. Mineev and G. Volovik, Phys. Rev. Lett. **51**, 1362 (1983).

[22] V. Riva and J. L. Cardy, Phys. Lett. B **622**, 339 (2005).

[23] M. Shifman and A. Yung, Phys. Rev. Lett. **110**, 201602 (2013).

[24] A. Leggett, Phys. Rev. Lett. **29**, 1227 (1972).

[25] A. J. Leggett, Rev. Mod. Phys. **47**, 331 (1975).

[26] E. Thuneberg, Phys. Rev. B bf 36, 3583 (1987).

[27] J. Sauls and J. Serene, Phys. Rev. B **24**, 183 (1981).

[28] M. G. Alford, A. Schmitt, K. Rajagopal and T. Schfer, Rev. Mod. Phys. **80**, 1455 (2008).

[29] N. Lepora and T. Kibble, Phys. Rev. D **59**, 125019 (1999).

[30] E. Thuneberg, Phys. Rev. Lett. bf 56, 359 (1986).

[31] M. Salomaa and G. Volovik, Phys. Rev. Lett. bf 56, 363 (1986).

[32] J. Goldstone, Nuovo Cim. bf 19, 154 (1961).

[33] J. Goldstone,A. Salam and S. Weinberg, Phys. Rev. **127**, 965 (1962).

[34] H. Nielsen and S. Chadha, Nucl. Phys. B **105**, 445 (1976).

[35] H. Watanabe and H. Murayama, Phys. Rev. Lett. bf 108, 251602 (2012).

[36] Y. Hidaka, Phys. Rev. Lett. **110**, 091601 (2013).

[37] V. Mineev, *Topologically Stable Defects and Solitons in Ordered Media*, New York: Harwood Academic (1998).

[38] D. Mermin and G. Stare, Phys. Rev. Lett. **30**, 1135 (1973).

[39] L. Buchholtz, Phys. Rev. B **15**, 5225 (1977).

[40] A. Leggett, *Quantum Liquids*, Oxford: Oxford University Press, (2006).

[41] H. Choi, J. Davis, J. Pollanen, T. Haard and W. Halperin, Phys. Rev. B **75**, 174503 (2007).

[42] N. Kopnin, Phys. Rev. B bf 45, 5491 (1992).

[43] Q. Tang and S. Wang, Physica D **88**, 139 (1995).

[44] E. Witten, Nucl. Phys. B bf 249, 557 (1985).

[45] S. Monin, M. Shifman and A. Yung, Phys. Rev. D **88**, 025011 (2013).

[46] A. Abrikosov, Sov. Phys. JETP bf 32, 1442 (1957).

[47] H. Nielsen and P. Olesen, Nucl. Phys. B bf 61, 45 (1973).

[48] M. Salomaa and G. Volovik, Phys. Rev. B bf 31, 203 (1985).

[49] E. Ivanov and V. Ogievetsky, Lett. Math. Phys. **1**, 309 (1976).

[50] T. Clark, M. Nitta and T. Veldhuis, Phys. Rev. D **67**, 085026 (2003).

[51] I. Low and A. Manohar, Phys. Rev. Lett **88**, 101602 (2002).

[52] L. Alvarez-Gaume and D. Freedman, Commun. Math. Phys. **91**, 87 (1983).

[53] J. Gates, C. Hull and M. Rocek, Nucl. Phys. B **248**, 157 (1984).

[54] A. J. Peterson and M. Shifman, Annals Phys. **348**, 84 (2014).

[55] M. Kobayashi and M. Nitta, Prog. Theor. Exp. Phys. 2014 (2), 021B01 (2014).

[56] P. F. Bedaque, G. Rupak, and M. J. Savage, Phys. Rev. C **68**, 065802 (2003).

[57] M. Eto, Y. Hirono, M. Nitta and S. Yasui, Prog. Theor. Exp. Phys. 2014 **1**, (2013).

[58] S. P. Novikov, Russian Math. Surveys **37**, 5 (1982).

[59] G. E. Volovik and M. V. Khazan, J. Exp. Theor. Phys. **55**, 867 (1982).

[60] G. E. Volovik and M. V. Khazan, J. Exp. Theor. Phys. **58**, 551 (1983).

[61] E. Ivanov and V. Ogievetskii, Theoret. Math. Phys. **25**, 1050 (1975).

[62] M. Nitta, S. Uchino and W. Vinci, JHEP **1409**, 098 (2014).

[63] G. Volovik and M. Salomaa, JETP Lett. **42**, 10 (1985).

[64] A. Peterson, M. Shifman and G. Tallarita, Ann. Physics **353**, 48 (2014).

[65] M. Shifman and A. Yung, *Supersymmetric Solitons*, Cambridge University Press, (2009).

[66] E. W. Carlson, A. H. Castro Neto and D. K. Campbell, Phys. Rev. Lett. **90**, 087001 (2003).

[67] M. Shifman, G. Tallarita and A. Yung, J. Modern Phys. A **29**, 1450062 (2014).

[68] M. Shifman, Phys. Rev. D **87**, 025025 (2013).

[69] P. de Gennes and J. Prost, *The Physics of Liquid Crystals*, Oxford Clarendon Press (1993).

[70] M.M. Salomaa and G. E. Volovik, Rev. Modern Phys. **59**, 533 (1987).

[71] L. Radzihovsky and T. C. Lubensky, Phys. Rev. E **83**, 051701 (2011).

[72] H. Watanabe and A. Vishwanath, Proc. Natl. Acad. Sci. **111**, 16314 (2014).

[73] G. E. Volovik and V. P. Mineev, Sov. Phys. JETP **45** (6), 1186 (1977).

[74] J. P. Boyd, *Chebyshev and Fourier Spectral Methods*, Courier Dover Publications (2001).

[75] A. Galantai, J. Comput. Appl. Math. **124** (1), (2000).

[76] Y. Kondo, J. S. Korhonen, M. Krusius, V. V. Dmitriev, E. V. Thuneberg and G. E. Volovik, Phys. Rev. Lett. **68**, 3331 (1992).

[77] J. S. Korhonen, Y. Kondo, M. Krusius, E. V. Thuneberg and G. E. Volovik, Phys. Rev. B **47**, 8868 (1993).

[78] H. Leutwyler, Phys. Rev. D **49**, 3033 (1994).

[79] H. Leutwyler, Helv. Phys. Acta **70**, 275 (1997).

[80] A. J. Peterson, M. Shifman and G. Tallarita, Annals Phys. **363**, 515 (2015).

[81] N. D. Mermin, Rev. Modern Phys. **51**, 591 (1979).

[82] M. Shifman, A. Vainshtein and A. Yung, Phys. Rev. D **91**, 045010 (2015).

[83] A. J. Peterson, E. Kurianovych and M. Shifman, Phys. Rev. D **93**, 065016 (2016).